

1979

Phosphorus-31 NMR of some bicyclic phosphorus compounds

Phil Marvin Stricklen
Iowa State University

Follow this and additional works at: <https://lib.dr.iastate.edu/rtd>

 Part of the [Inorganic Chemistry Commons](#)

Recommended Citation

Stricklen, Phil Marvin, "Phosphorus-31 NMR of some bicyclic phosphorus compounds " (1979). *Retrospective Theses and Dissertations*. 7312.
<https://lib.dr.iastate.edu/rtd/7312>

This Dissertation is brought to you for free and open access by the Iowa State University Capstones, Theses and Dissertations at Iowa State University Digital Repository. It has been accepted for inclusion in Retrospective Theses and Dissertations by an authorized administrator of Iowa State University Digital Repository. For more information, please contact digirep@iastate.edu.

INFORMATION TO USERS

This was produced from a copy of a document sent to us for microfilming. While the most advanced technological means to photograph and reproduce this document have been used, the quality is heavily dependent upon the quality of the material submitted.

The following explanation of techniques is provided to help you understand markings or notations which may appear on this reproduction.

1. The sign or "target" for pages apparently lacking from the document photographed is "Missing Page(s)". If it was possible to obtain the missing page(s) or section, they are spliced into the film along with adjacent pages. This may have necessitated cutting through an image and duplicating adjacent pages to assure you of complete continuity.
2. When an image on the film is obliterated with a round black mark it is an indication that the film inspector noticed either blurred copy because of movement during exposure, or duplicate copy. Unless we meant to delete copyrighted materials that should not have been filmed, you will find a good image of the page in the adjacent frame.
3. When a map, drawing or chart, etc., is part of the material being photographed the photographer has followed a definite method in "sectioning" the material. It is customary to begin filming at the upper left hand corner of a large sheet and to continue from left to right in equal sections with small overlaps. If necessary, sectioning is continued again—beginning below the first row and continuing on until complete.
4. For any illustrations that cannot be reproduced satisfactorily by xerography, photographic prints can be purchased at additional cost and tipped into your xerographic copy. Requests can be made to our Dissertations Customer Services Department.
5. Some pages in any document may have indistinct print. In all cases we have filmed the best available copy.

University
Microfilms
International

300 N. ZEEB ROAD, ANN ARBOR, MI 48106
18 BEDFORD ROW, LONDON WC1R 4EJ, ENGLAND

STRICKLEN, Phil Marvin

31

P NMR OF SOME BICYCLIC PHOSPHORUS COMPOUNDS.

Iowa State University, Ph.D., 1979

University

Microfilms

International

300 N. Zeeb Road, Ann Arbor, MI 48106

18 Bedford Row, London WC1R 4EJ, England

^{31}P NMR of some bicyclic
phosphorus compounds

by

Phil Marvin Stricklen

A Dissertation Submitted to the
Graduate Faculty in Partial Fulfillment of the
Requirements for the Degree of
DOCTOR OF PHILOSOPHY

Department: Chemistry
Major: Inorganic Chemistry

Approved:

Signature was redacted for privacy.

In/Charge of Major Work

Signature was redacted for privacy.

For /the/Major Department

Signature was redacted for privacy.

For the Graduate College

Iowa State University
Ames, Iowa

1979

TABLE OF CONTENTS

	Page
PREFACE	1
PART I. A NEW 1,4-DIPHOSPHABICYCLO[2.2.2]OCTANE SYSTEM	10
INTRODUCTION	11
EXPERIMENTAL	13
Techniques	13
Materials	13
NMR spectroscopy	13
Infrared spectroscopy	15
Mass spectrometry	15
Preparation of compounds	15
RESULTS AND DISCUSSION	25
Synthesis	25
Mass Spectra	30
NMR Spectra	36
¹ H NMR	36
¹³ C NMR	46
³¹ P NMR	47
Determination of coupling constant signs	52
Quadrupolar effects	66
Infrared Spectra	74
Crystal and Molecular Structure of P(CH ₂ NPh) ₃ P	76
PART II. ³¹ P NMR OF POLYCYCLIC PHOSPHORUS COMPOUNDS	98
INTRODUCTION	99
Theory of ³¹ P NMR Chemical Shifts	99
Orbital Interactions of Cage Compounds	109

	Page
Electronegativity Considerations	118
EXPERIMENTAL	123
Techniques	123
Materials	123
NMR spectroscopy	123
Mass spectrometry	124
Preparation of compounds	125
RESULTS AND DISCUSSION	130
Cage Compounds	130
Bicyclic systems	131
Tricyclic systems	142
Electronegativity Considerations	143
PART III. $P(CH_2O)_3$ -BRIDGED SQUARE COORDINATION COMPLEXES	151
INTRODUCTION	152
EXPERIMENTAL	154
Techniques	154
Materials	154
NMR spectra	154
Infrared spectra	155
Preparation of compounds	155
RESULTS AND DISCUSSION	158
CONCLUSIONS	170
SUGGESTIONS FOR FUTURE RESEARCH	171
REFERENCES	172
ACKNOWLEDGEMENTS	180

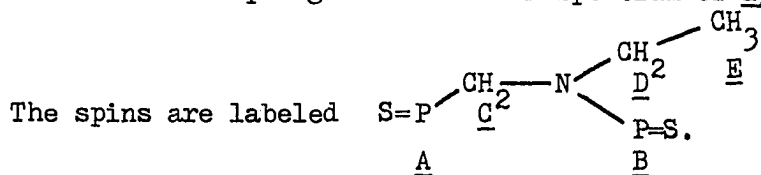
	Page
APPENDIX 1. CALCULATED AND OBSERVED STRUCTURE FACTORS FOR <u>14</u>	181
APPENDIX 2. SAMPLE CALCULATION OF GROUP ELECTRONEGATIVITY	190

LIST OF TABLES

Table	Page
1. Compounds discussed in this dissertation	2
1.1. ^{31}P NMR data for precursors and derivatives of <u>12</u> , <u>13</u> , and <u>14</u>	48
1.2. ^{31}P NMR data for metal carbonyl complexes	49
1.3. A representation of the origin and connectedness of the ^1H and ^{31}P NMR resonances of the system consisting of the methyl group and two phosphorus atoms of $\text{S}=\text{P}(\text{CH}_2\text{NMe})_3\text{P}=\text{S}$, <u>17</u>	55
1.4. Spin-spin coupling constants for some cage compounds	65
1.5. CO stretching frequencies of metal complexes	75
1.6. Final fractional coordinates of <u>14</u>	79
1.7. Final thermal parameters for <u>14</u>	81
1.8. Bond lengths between all nonhydrogen atoms of <u>14</u>	83
1.9. Bond angles between nonhydrogen atoms of <u>14</u>	85
1.10. P-P separation of compounds for which structural data are available	95
2.1. Remote substituent effect on δ ^{19}F of 1-fluoro bicyclo[2.2.2]octanes	115
2.2. Phosphorus cage compounds	132
2.3. Group electronegativities and δ ^{31}P for aminomethylphosphines $\text{P}(\text{CH}_2\text{NR}_1\text{R}_2)_3$	144
3.1. Infrared frequency assignments for the carbonyl region	162
3.2. ^{31}P NMR chemical shifts for the compounds of Part III	163

LIST OF FIGURES

Figure		Page
1.1.	Parent ion region of the mass spectrum of $\text{Se}=\text{P}(\text{CH}_2\text{NEt})_3\text{P}=\text{Se}$, <u>21</u>	32
1.2.	Mass spectral fragmentation pattern for $\text{Se}=\text{P}(\text{CH}_2\text{NEt})_3\text{P}=\text{Se}$, <u>21</u>	34
1.3.	Fragmentation mechanism for mass spectrum of cage compounds. $\text{Se}=\text{P}(\text{CH}_2\text{NEt})_3\text{P}=\text{Se}$, <u>21</u> is used as an example	35
1.4.	^1H NMR spectrum of $\text{P}(\text{CH}_2\text{NMe})_3\text{P}$, <u>12</u>	38
1.5.	^1H NMR spectrum of $\text{S}=\text{P}(\text{CH}_2\text{NMe})_3\text{P}=\text{S}$, <u>17</u> The CH_2 protons couple to both phosphorus atoms equally, resulting in an apparent triplet	41
1.6.	^1H NMR spectrum of $\text{S}=\text{P}(\text{CH}_2\text{NEt})_3\text{P}=\text{S}$, <u>19</u> The triplet for the methyl protons of the ethyl group has been omitted	43
1.7.	Selective decoupling of the ^1H NMR spectrum of <u>19</u> .	45



No decoupling is present in (a). Both phosphorus atoms (A and B) are decoupled in (b). Only A is decoupled in (c) while B is decoupled in (d). The methyl protons E are decoupled in (e)

Figure		Page
1.8.	Effects of the spin tickling experiment on the ^1H NMR spectrum of the methyl protons of $\text{S}=\text{P}(\text{CH}_2\text{NMe})_3\text{P}=\text{S}$, <u>17</u> . (a) No second irradiating frequency (b) Spin tickling line 5 of Figure 1.7 (c) Spin tickling of line 6 (d) Spin tickling of line 7 (e) Spin tickling of line 8	57
1.9	The connectedness of the four proton resonances of the methyl protons in $\text{S}=\text{P}(\text{CH}_2\text{NMe})_3\text{P}=\text{S}$ (lines 1-4) to the aminophosphine sulfide (lines 5 and 6) and the phosphine sulfide (lines 7 and 8)	62
1.10.	The effect of temperature on the ^{31}P NMR line shape of the aminophosphine phosphorus, PN_3 , of $\text{P}(\text{CH}_2\text{NMe})_3\text{P}$, <u>12</u> . Impurities are labeled x	69
1.11.	^{31}P NMR spectrum of $\text{S}=\text{P}(\text{CH}_2\text{NMe})_3\text{P}=\text{S}$, <u>17</u>	71
1.12.	^{31}P NMR spectrum of $\text{P}(\text{CH}_2\text{NMe})_3\text{P}$, <u>12</u> at room temperature. Note the quadrupolar broadening of the aminophosphine doublet ($\delta = 80.0$ ppm)	73
1.13.	Perspective of <u>14</u> showing all atoms and indicating the numbering scheme	89

Figure		Page
1.14.	Perspective drawing of <u>14</u> excluding the phenyl carbons for clarity	91
1.15.	View of <u>14</u> down the P-P vector. Note the twist of the bridging groups	93
2.1.	Uncertainty of θ	103
2.2.	Steric γ effect	107
2.3.	Interaction of N lone pairs of <u>67</u>	110
2.4.	Energy diagram for the interaction of nitrogen lone pairs in <u>67</u>	112
2.5.	γ interactions of norbornyl systems	114
2.6.	Hyperconjugative interaction of lone pair electrons with the γ carbon	115
2.7.	MO interaction as a function of energy of combining orbitals	138
2.8.	Vertical ionization potentials from photoelectron spectra of selected compounds	140
2.9.	A plot of the relationship between electronegativity and ^{31}P NMR chemical shift for Group I compounds	147

Figure		Page
2.10.	A plot of the relationship between electro- negativity and ^{31}P NMR chemical shift for Group II compounds	149
3.1.	$\text{P}(\text{CH}_2\text{O})_3\text{P}$ -bridged square tetramer	152
3.2.	Proton NMR spectrum of <u>80</u> . The central peaks of the apparent triplets are due to virtual coupling	161
3.3.	^1H NMR spectrum of <u>85</u>	168

PREFACE

When the three substituents of trivalent phosphorus are constrained into a bicyclo[2.2.2]octane structure, the steric and electronic interactions of the substituents with each other and the phosphorus atom differ from the interactions in analogous acyclic compounds. The research reported in this dissertation involves the synthesis of some phosphorus compounds having the bicyclo[2.2.2]octane geometry and the comparison of the reactivity of these compounds to acyclic analogues. The effect of molecular orbital interactions within the bicyclic structure on the ^{31}P NMR chemical shift of the phosphorus atom are investigated. Finally, the rigid nature of the bicyclic structure is utilized in preparing cyclic transition metal complexes using $\text{P}(\text{OCH}_2)_3\text{P}$ as a bridging ligand.

A list of all compounds discussed in this dissertation is included in Table 1.

Table 1. Compounds discussed in this dissertation

-
- 1 $P(CH_2O)_3P$
- 2 $(OC)_4FeP(CH_2O)_3PFe(CO)_4$
- 3 $P(NMeNMe)_3P$
- 4 $O=P(NMeNMe)_3P=O$
- 5 $PhN=P(NMeNMe)_3P=NPh$
- 6 $P(NMeCH_2)_3CMe$
- 7 $O=P(NMeCH_2)_3CMe$
- 8 $H_3B-P(NMeCH_2)_3CMe$
- 9 $P(CH_2N(H)Me)_3$
- 10 $P(CH_2N(H)Et)_3$
- 11 $P(CH_2N(H)Ph)_3$
- 12 $P(CH_2NMe)_3P$
- 13 $P(CH_2NEt)_3P$
- 14 $P(CH_2NPh)_3P$
- 15 $O=P(CH_2NMe)_3P$

Table 1. (Continued)

-
- 16 $O=P(CH_2NPh)_3P=O$
- 17 $S=P(CH_2NMe)_3P=S$
- 18 $S=P(CH_2NEt)_3P$
- 19 $S=P(CH_2NEt)_3P=S$
- 20 $Se=P(CH_2NMe)_3P=Se$
- 21 $Se=P(CH_2NEt)_3P=Se$
- 22 $O=P(CH_2NMe)_3P=Se$
- 23 $(OC)_5WP(CH_2NMe)_3PW(CO)_5$
- 24 $(OC)_5WP(CH_2NEt)_3PW(CO)_5$
- 25 $(OC)_5WP(CH_2NPh)_3P$
- 26 $(OC)_5WP(CH_2NPh)_3PW(CO)_5$
- 27 $(OC)_5CrP(CH_2NPh)_3P$
- 28 $(OC)_5CrP(CH_2NPh)_3PCr(CO)_5$
- 29 $S=P(OCH_2)_3P$
- 30 $Cl-P(NMeNMe)_2P-Cl$

Table 1. (Continued)

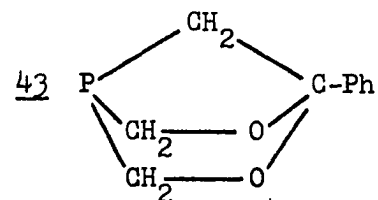
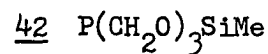
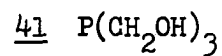
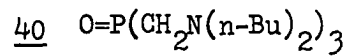
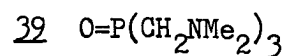
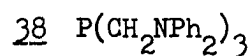
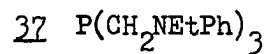
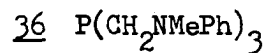
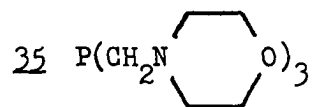
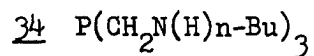
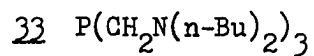
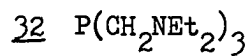
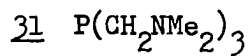


Table 1. (Continued)

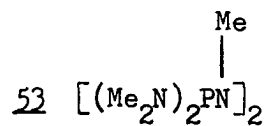
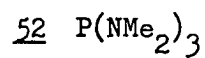
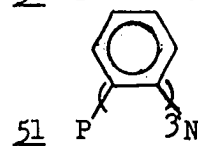
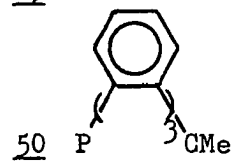
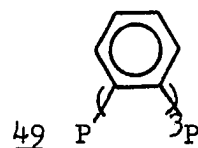
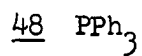
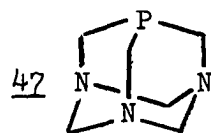
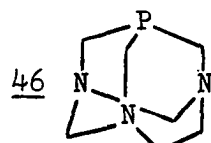
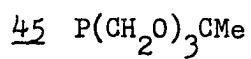
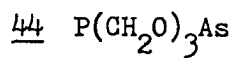


Table 1. (Continued)

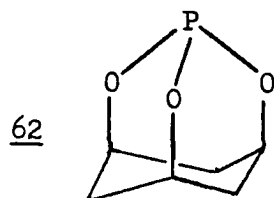
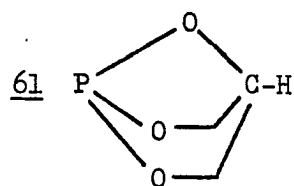
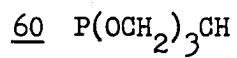
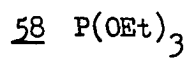
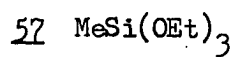
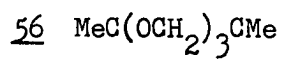
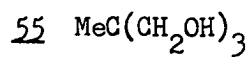
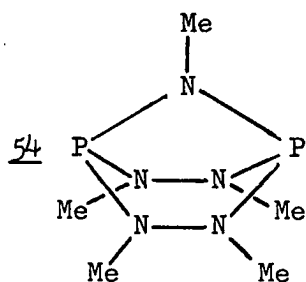


Table 1. (Continued)

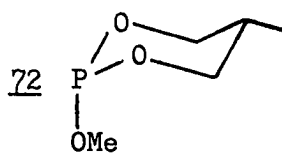
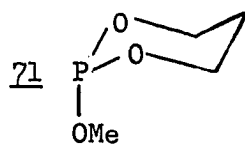
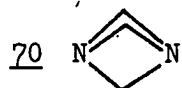
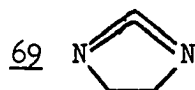
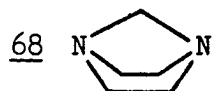
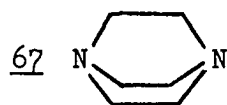
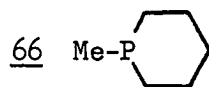
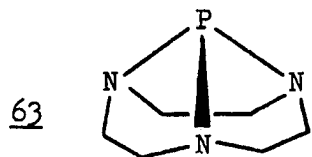


Table 1. (Continued)

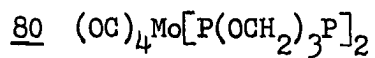
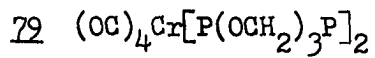
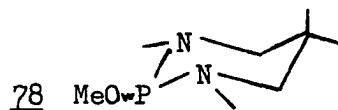
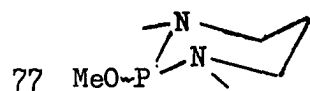
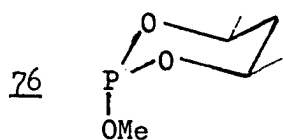
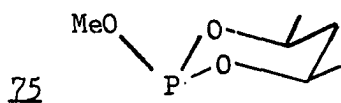
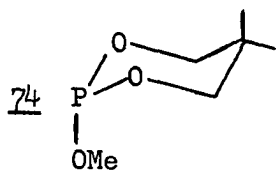
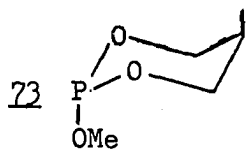
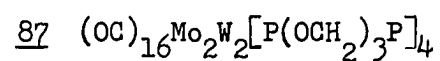
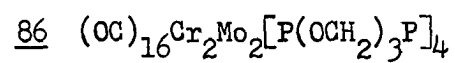
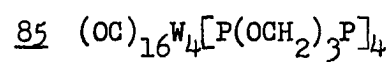
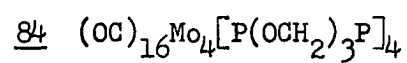
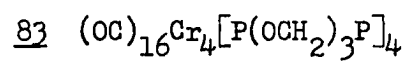
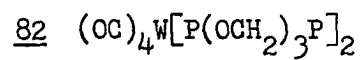
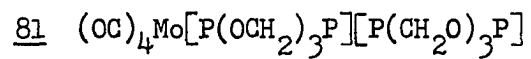


Table 1. (Continued)



PART I. A NEW 1,4-DIPHOSPHABICYCLO[2.2.2]OCTANE SYSTEM

INTRODUCTION

When trivalent phosphorus occupies the bridgehead position of a bicyclo[2.2.2]octane structure, the steric as well as electronic properties associated with the phosphorus lone pair of electrons differ from those of analogous acyclic compounds. Changes have been noted in spectral properties such as ^{31}P NMR chemical shifts (see Part II of this dissertation), metal carbonyl IR stretching frequencies, UV parameters of transition metal complexes (1), and $^1\text{J}_{\text{PH}}$ values of protonated compounds (2). Compound 1 (Table 1) is a "cage" compound which is of special interest because of the simultaneous presence of a phosphine and a phosphite moiety in the same compound. Although phosphines are usually considered to be more basic ligands than phosphites, the phosphite end of 1 reacts in preference to the phosphine end with transition metals and chalcogens (3,4). This unexpected behavior of the cage compound may be due to the strong molecular dipole moment of 3.10 D for this ligand, in which the phosphite end of the molecule comprises the negative end of the molecular dipole (4). The rigid cage structure of 1 prevents it from acting as a chelating ligand, but it can serve as a bridging group connecting two metal centers as in 2.

The two magnetically active phosphorus atoms of 1 interact with each other as well as the protons of the methylene groups to form an interesting system from the viewpoint of nuclear magnetic resonance.

A detailed study of the NMR parameters, including the determination of the signs of coupling constants, provided a probe for the bonding in 1 (5).

The new compounds 12, 13, and 14, like 1, incorporate two dissimilar phosphorus atoms into the same molecule. One of these phosphorus atoms, as in 1, is a phosphine, but an aminophosphine now occupies the second bridgehead position. Two other bicyclic cage compounds having aminophosphine bridgeheads which have been reported are 3 (6) and 6 (7). Structural data for 3 (8), its dioxide 4 (9), and its bis(phenylimide)derivative 5 (10), reveal a geometry for nitrogen which is intermediate between pyramidal and planar while 7 and 8 contain nitrogens having the planar geometry observed in the majority of aminophosphines (11).

The synthesis and characterization of 12, 13, and 14 as well as some of their derivatives will be described herein. Special attention will be given to ^1H and ^{31}P NMR parameters as they may apply to the bonding in cage compounds. The crystal structure of 14 was undertaken to determine the geometry of the nitrogen atoms and to better understand the steric and electronic interactions of the cage molecules.

EXPERIMENTAL

Techniques

Materials

All solvents were reagent grade or better. Cyclohexane and ethyl acetate were stored over 4A molecular sieves while the following solvents were further purified by distillation from an appropriate drying agent: acetone (molecular sieves); acetonitrile (P_4O_{10}); benzene and ether (NaK alloy); methylcyclohexane and toluene (Na).

Sulfur, H_2O_2 (10%), and aniline were obtained from Fisher Scientific Co. The aniline was distilled from a pinch of zinc immediately prior to use. Tris(dimethylamino)phosphine (90+%) Aldrich Chemical Co.), tetrakis(hydroxymethyl)phosphonium chloride (85% in H_2O , ROC/RIC), methylamine (40% in H_2O , Eastman Chemical Co.), ethylamine (70% in H_2O , J. T. Baker Chemical Co.), and activated manganese dioxide (Alpha Chemical Co.) were used as received. Deuterated solvents for NMR spectroscopy were dried over 4A molecular sieves before use.

NMR spectroscopy

Proton NMR spectra were obtained on either a Varian HA-100 or an A-60 spectrometer using appropriate deuterated compounds as solvents. Me_4Si was used as an internal standard and it served as the internal lock for the HA-100 instrument. The double resonance experiments necessary for determining the relative signs of spin-spin coupling

constants were performed on a Bruker HX-90 spectrometer operating at 90.0 MHz in the Fourier transform (FT) mode while locked on the ^2H resonance of the deuterated solvent. Single frequency irradiation of the phosphorus resonances was accomplished using the decoupling mechanism of the instrument operating at power levels of less than 0.1 watt. The frequency of the phosphorus resonance of $\text{P}(\text{OMe})_3$ was first located by monitoring the free induction decay (FID) of the ^1H spectrum while varying the irradiation frequency. Using an irradiating power of 0.5 watt, a dramatic change is observed in the FID when the irradiating frequency approaches the resonance frequency of $\text{P}(\text{OMe})_3$. The frequencies of the phosphorus atoms in the compound of interest can then be estimated using the $\text{P}(\text{OMe})_3$ frequency as a reference. Difficulties were encountered in the irradiation of some aminophosphine resonances due to broad lines resulting from quadrupolar effects.

^{31}P NMR spectra were obtained on solutions in 10 mm tubes with a Bruker HX-90 spectrometer operating at 36.434 MHz in the FT mode while locked on the ^2H resonance of the deuterated solvent. The external standard was 85% H_3PO_4 sealed in a 1 mm capillary tube held coaxially in the sample tube by a Teflon vortex plug. The spectrometer was interfaced with a Nicolet Instruments 1080 minicomputer system.

^{13}C NMR spectra were obtained on a JEOL FX90Q spectrometer operating at 22.50 MHz in the FT mode while locked on the ^2H resonance of the deuterated solvents. The carbon atoms of the solvent were used as references.

Infrared spectroscopy

Carbonyl stretching frequencies were measured on a Beckman IR4250 double beam spectrometer using NaCl optics. Absorption bands for the solutions were referenced to the 1601.8 cm^{-1} band of polystyrene.

Mass spectrometry

High resolution mass spectra were obtained on an AEI MS-902 high-resolution mass spectrometer. Exact masses were determined by peak matching.

Low resolution and chemical ionization mass spectra were obtained on a Finnigan 4000 mass spectrometer. The interfaced gas chromatograph utilized a temperature-programmed six foot, 3% OV-101 column. Isotopic abundances of the parent ion regions of selenium-containing compounds are the average values of ten spectra. The computer program MASP (12) was used to calculate the expected isotopic abundances of the selenium compounds.

Preparation of compounds

KSeCN This compound was prepared by the method of Watkins and Shutt (13).

$\text{CH}_3\text{CNM}(\text{CO})_5$; M = Cr, W These compounds were prepared using the method of Connor et al. (14).

$P(CH_2NHMe)_3$, 9 Reaction of $P(CH_2OH)_4Cl$ with four moles of methyl amine in a manner analogous to the procedure of Coates and Wilson (15) for the reaction of $P(CH_2OH)_4Cl$ with secondary amines gave 9 in quantitative yield. The compound decomposed when a vacuum distillation was attempted. (1H NMR (CDCl₃) 2.26 (s, 3H, Me), 2.62 (d, 2H, $^2J_{PH} = 12.0$ Hz, CH₂), 3.20 (br s, 1H, NH)).

$P(CH_2NHEt)_3$, 10 Four moles of ethyl amine react with $P(CH_2OH)_4Cl$, as in the preparation of 9, to form 10 in quantitative yield. As with 9, vacuum distillation was unsuccessful. (1H NMR (CDCl₃) 1.05 (t, 3H, CH₃), 2.20-3.50 (m, 5H, CH₂NHCH₂)).

$P(CH_2NHPH)_3$, 11 This triamine was prepared from $P(CH_2OH)_4Cl$ and aniline by the method of Frank and Drake (16). Recrystallization from boiling benzene provided 11 in 39% yield (mp = 84-86°; (lit. (16), 74% yield, mp = 85-86°); 1H NMR (CDCl₃) 3.52 (d, 2H, $^2J_{PH} = 5$ Hz, CH₂), 3.64 (br s, 1H, NH), 6.5-7.4 (m, 5H, Ph)).

$P(CH_2NMe)_3P$, 12 A 10.0 g (61.3 mMol) sample of 9 was charged into a 50 ml flask under a blanket of dry nitrogen. The flask was heated, while being stirred magnetically, to 95° at which time 10.0 g (61.3 mMol) of tris(dimethylamino)phosphine was added dropwise over a period of one hour. Evolution of dimethylamine began less than ten minutes after starting the addition. When the addition was complete, the temperature was raised to 130° for a twenty-one hour period. The dimethylamine evolution had then ceased and the reaction mixture was

allowed to cool to room temperature. The 16.9 g of distilled product ($b_{0.05} = 68^\circ$) was estimated by integration of the ^1H NMR spectrum and by gas chromatography to contain approximately 40% of 12. On this basis the yield of 12 was approximately 55-60%. A pure sample of 12 for spectral analysis was obtained by dropwise addition of 10% H_2O_2 to a cyclohexane solution of the distilled product while monitoring the reaction by ^{31}P NMR spectroscopy. When the impurities were completely oxidized, the H_2O_2 addition was ceased, since reaction of 12 with H_2O_2 destroyed the cage structure. The oxidized impurities were extracted into the water layer. The cyclohexane layer was dried over sodium sulfate and the solvent removed under reduced pressure leaving pure 12 as a colorless liquid. (^1H NMR ($(\text{CD}_3)_2\text{CO}$) 2.25 (d, 3H, $^3\text{J}_{\text{PH}} = 15.8$ Hz, Me), 2.90 (dd, 2H, $^2\text{J}_{\text{PH}} = 6.8$ Hz, $^3\text{J}_{\text{PH}} = 3.2$ Hz, CH_2); ^{13}C NMR ($(\text{CD}_3)_2\text{CO}$) 42.7 (d, 1C, $^2\text{J}_{\text{PC}} = 35.4$ Hz, Me), 44.8 (dd, 1C, $^1\text{J}_{\text{PC}} = 14.6$ Hz, $^2\text{J}_{\text{PC}} = 4.9$ Hz, CH_2); mass spectrum m/e for P^+ 191.07390 measured, 191.07413 calculated).

$\text{P}(\text{CH}_2\text{NEt})_3$, 13 This compound was prepared from the triamine 10 and tris(dimethylamino)phosphine in a manner analogous to the preparation of 12. The distillate contained approximately 40% of 13 representing a yield of approximately 45% for the reaction. The selective oxidation of impurities, as performed in the case of 12, was unsuccessful for 13, but the mixture was suitable for spectral analysis. ($b_{0.05} = 72^\circ$; ^1H NMR ($(\text{CD}_3)_2\text{CO}$) 1.08 (t, 3H, $^3\text{J}_{\text{HH}} = 7.0$ Hz, CH_3), 2.78 (m, 2H, CH_2CH_2), 3.05 (dd, 2H, $^2\text{J}_{\text{PH}} = 6.2$ Hz, $^3\text{J}_{\text{PH}} = 2.5$ Hz,

PCH_2); mass spectrum (low resolution) molecular ion $m/e = 233$ as calculated for $\text{C}_9\text{H}_{21}\text{N}_3\text{P}_2$).

$\text{P}(\text{CH}_2\text{NPh})_3\text{P}$, 14 The triamine 11, 5.00 g (14.3 mMol) was charged into a flask and heated to 90° . To this stirred melt was added 2.43 g (14.3 mMol) of tris(dimethylamino)phosphine all at once. After seventy-two hours at 90° the resultant dark oil was cooled and subjected to chromatographic purification on a Florisil column (benzene eluent). Removal of the benzene under reduced pressure left an oil which was recrystallized from ethyl acetate to give 0.96 g (17.8% yield) of 14 as diamond shaped crystals (mp = $194\text{--}196^\circ$; ^1H NMR (CDCl_3) 3.62 (dd, 2H, $^2J_{\text{PH}} = 7.0$ Hz, $^3J_{\text{PH}} = 1.5$ Hz, CH_2), 6.8–7.4 (m, 5H, C_6H_5 ; ^{13}C NMR (CDCl_3) 148.5 (d, 1C, $^2J_{\text{PC}} = 28.1$ Hz, C_{11}), (see Figure 1.13 for numbering system for carbon atoms), 129.2 (2C, C_{13} , C_{15}), 120.2 (1C, C_{14}), 115.9 (d, 2C, $^3J_{\text{PC}} = 18.3$ Hz, C_{12} , C_{16}), 40.4 (dd, 1C, $^1J_{\text{PC}} = 17.70$ Hz, $^2J_{\text{PC}} = 3.1$ Hz, C_1); mass spectrum (chemical ionization spectrum (17) using CH_4 as the ionizing gas showed peaks at $m/e = 378$ and 406 for $(\text{P} + 1)^+$ and $(\text{P} + 29)^+$ due to reaction of 14 with H^+ and C_2H_5^+ present in the ionized methane)).

$\text{O}=\text{P}(\text{CH}_2\text{NMe})_3\text{P}$, 15 To a solution of 4.0 g (21 mMol) of 12 in 75 mL of toluene were added 11.0 g (125 mMol) of activated MnO_2 . The flask became slightly warm and it was then heated at 100° for two hours. After the solution had cooled it was filtered and the toluene removed under reduced pressure leaving a colorless oil. Upon standing

overnight, 0.96 g (55%; based on the purity of 12) of 15 was deposited as hexagonal crystals (mp = 114-116°; $^1\text{H NMR}$ (CDCl_3) 2.68 (dd, 3H, $^3\text{J}_{\text{PH}} = 16.25$ Hz, $^4\text{J}_{\text{PH}} = 2.38$ Hz, Me), 3.19 (dd, 2H, $^2\text{J}_{\text{PH}} = 13.0$, $^3\text{J}_{\text{PH}} = 2.75$, CH_2); low resolution mass spectrum contained the parent ion $\underline{m/e}$ 207 plus strong peaks at $\underline{m/e}$ 164 and 121 indicative of successive loss of two $\text{CH}_2=\text{NCH}_3$ groups.

$\text{O}=\text{P}(\text{CH}_2\text{NPh})_3\text{P}=\text{O}$, 16 Gaseous N_2O_4 was passed through a solution of 0.30 g (0.80 mMol) of 14 in 100 mL of toluene at -78° . When the solution became slightly green, N_2O_4 addition was stopped and the solution allowed to gradually warm to room temperature. The solution was filtered and the toluene removed under reduced pressure leaving 0.02 g (6%) of pure 16 as a white solid (mp = 250° (decomposition); $^1\text{H NMR}$ (CD_3CN) 4.20 (dd, 2H, $^2\text{J}_{\text{PH}} = 10.0$ Hz, $^3\text{J}_{\text{PH}} = 8.0$ Hz, CH_2), 7.1-7.5 (m, 5H, Ph); mass spectrum, $\underline{m/e}$ for P^+ 409.10976 measured, 409.11909 calculated).

$\text{S}=\text{P}(\text{CH}_2\text{NMe})_3\text{P}=\text{S}$, 17 To a benzene solution of 12 (4.80 g, 25.1 mMol) was added sulfur (1.60 g, 50.2 mMol) in small portions over a 30 minute period. After the exothermic reaction had subsided, the solution was refluxed for one hour. After evaporation of the benzene, the impurities were extracted from the residue remaining with boiling cyclohexane. Further extraction with hot acetone gave, upon cooling to -20° , 0.77 g of 17 which, based on the 40% purity of 12, would be a 90% yield (mp = 224.0-224.5°; $^1\text{H NMR}$ (CDCl_3) 2.90 (dd, 3H, $^3\text{J}_{\text{PH}} = 12.0$

Hz, ${}^4J_{\text{PH}} = 3.0$ Hz, Me), 3.64 (apparent t, 2H, ${}^2J_{\text{PH}} = {}^3J_{\text{PH}} = 7.5$ Hz, CH_2); mass spectrum, m/e for P^+ 255.01771 measured, 255.01827 calculated).

$\text{S}=\text{P}(\text{CH}_2\text{NEt})_3\text{P}$, 18 and $\text{S}=\text{P}(\text{CH}_2\text{NEt})_3\text{P}=\text{S}$, 19 Sulfur

(5.50 g, 172 mMol), was added in small portions over a period of one hour to a solution of 20.0 g (34.0 mMol) of 13 in 150 mL of benzene. After the exothermic reaction had subsided the solution was refluxed for two hours. After cooling, the benzene was removed under reduced pressure leaving a yellow residue. This residue was extracted with 3 x 50 mL of hot cyclohexane which, upon cooling to room temperature, deposited 3.0 g of colorless needle-like crystals of 19 representing a yield of 30% based on the 40% purity of the 13 (mp = 169-170 $^\circ$; ${}^1\text{H}$ NMR (CDCl_3) 1.13 (t, 3H, ${}^3J_{\text{HH}} = 7.1$ Hz, CH_3), 3.22 (m, 2H, ${}^3J_{\text{HH}} = 7.1$ Hz, ${}^3J_{\text{PH}} = 7.1$ Hz, ${}^4J_{\text{PH}} = 2.1$ Hz, CH_2CH_3), 3.58 (apparent t, 2H, ${}^2J_{\text{PH}} = {}^3J_{\text{PH}} = 7.1$ Hz, PCH_2); mass spectrum, m/e for P^+ 297.06508 measured, 297.06523 calculated).

Further extraction of the yellow residue with 3 x 50 mL of hot benzene removed the excess sulfur and other impurities while leaving 0.5 g (6%) of 18 as a pure, white solid (mp = 226-227 $^\circ$; ${}^1\text{H}$ NMR ($\text{DMSO}-d_6$) 1.19 (t, 3H, ${}^3J_{\text{HH}} = 7.0$ Hz, CH_3), 3.37 (m, 2H, CH_3CH_2), 3.65 (d, 2H, ${}^2J_{\text{PH}} = 7.0$ Hz, PCH_2); mass spectrum m/e for P^+ 265.09354 measured, 265.09315 calculated).

Se=P(CH₂NMe)₃P=Se, 20 A solution of 4.88 g (10.2 mMol) of 12 in 25 mL of warm acetonitrile was added to a solution of 7.36 g (51.1 mMol) of KSeCN in 50 mL of acetonitrile. A white precipitate formed immediately. After two hours of magnetic stirring, the solvent was removed under reduced pressure leaving a white solid residue. Extraction of this residue with 3 X 50 mL of hot cyclohexane removed the nonpolar impurities while 3 X 25 mL of hot ethyl acetate extracted 2.31 g (6%) of 20 which remained after removal of the ethyl acetate under reduced pressure (mp = 124-126°; ¹H NMR (CDCl₃) 2.98 (dd, 3H, ³J_{PH} = 12.3 Hz, ⁴J_{PH} = 2.9 Hz, CH₃), 3.73 (dd, 2H, ²J_{PH} = 7.2 Hz, ³J_{PH} = 5.9 Hz, CH₂); mass spectrum: Isotopic abundance for parent ion region is shown below).

<u>m/e</u>	343	344	345	346	347	348	349	350	351	352	353
Calc.	4.21	4.99	19.76	13.70	51.07	29.73	87.74	11.55	100	7.83	31.50
Meas.	3.74	4.49	20.92	13.62	53.63	29.87	89.42	10.80	100	6.74	29.16

<u>m/e</u>	354	355
Calc.	2.46	2.97
Meas.	1.28	1.81

Se=P(CH₂NEt)₃P=Se, 21 To a solution of 2.57 g (17.2 mMol) of KSeCN in 25 mL of acetonitrile was added a solution of 2.00 g (3.40 mMol) of 13 in 25 mL of acetonitrile. After 30 minutes of stirring the solution was filtered and the solvent removed under reduced pressure. The resultant oil was subjected to chromatographic purification on a Florisil column (cyclohexane eluent) with 21 being eluted first. Evaporation of the cyclohexane at reduced pressure provided

0.77 g (58%) of 21 as a white solid (mp = 118-119°; ^1H NMR (CDCl_3) 1.36 (t, 3H, $^3\text{J}_{\text{HH}} = 7.0$ Hz, CH_3), 3.29 (m, 2H, CH_3CH_2), 3.66 (dd, 2H, $^2\text{J}_{\text{PH}} = 7.1$ Hz, $^3\text{J}_{\text{PH}} = 5.8$ Hz, PCH_2); mass spectrum: Isotopic abundance for the parent ion region is shown below).

m/e	385	386	387	388	389	390	391	392	393	394	395
Calc.	4.21	5.11	19.85	14.30	51.32	31.30	88.38	14.43	100	11.12	31.67
Meas.	3.45	4.64	20.75	14.12	53.72	31.68	91.40	13.34	100	9.94	29.32

m/e	396	397
Calc.	3.50	3.05
Meas.	2.13	1.47

$\text{O}=\text{P}(\text{CH}_2\text{NMe})_3\text{P}=\text{Se}$, 22 A solution of 20 in $(\text{CD}_3)_2\text{CO}$ was treated with 30% H_2O_2 while being monitored by ^{31}P NMR. As the solution turned red, the two doublets associated with 20 decreased in intensity while two new doublets for 22 grew in intensity. The conversion appeared to be quantitative but attempts to isolate 22 resulted in decomposition of the product. A mass spectrum was obtained on a freshly prepared solution by means of GC-mass spectrometry (^1H NMR ($(\text{CD}_3)_2\text{CO}$) 2.94 (dd, 3H, $^3\text{J}_{\text{PH}} = 12.7$ Hz, $^4\text{J}_{\text{PH}} = 2.8$ Hz, CH_3), 3.83 (dd, 2H, $^2\text{J}_{\text{PH}} = 7.0$ Hz, $^3\text{J}_{\text{PH}} = 6.0$ Hz, CH_2); mass spectrum: Isotopic abundance of parent ion region is shown below).

m/e	281	282	283	284	285	286	287	288	289	290
Calc.	1.75	0.14	18.07	16.61	48.39	3.79	100	7.89	18.88	1.47
Meas.	3.77	0.14	17.91	14.50	47.23	2.19	100	5.70	16.55	0.14

(OC)₅WP(CH₂NMe)₃PW(CO)₅, 23 A solution of 1.00 g (2.72 mMol) of CH₃CNW(CO)₅ and 0.40 g (1.4 mMol) of 12 in methylcyclohexane (50 mL) was heated for twenty hours at 85°. After cooling to room temperature, the solvent was removed under reduced pressure and the residue purified on a Florisil column using cyclohexane as eluent. Evaporation of solvent provided 0.21 g (20%) of 23 as colorless crystals (mp = 109° (decomposition); ¹H NMR ((CD₃)₂CO) 3.05 (dd, 3H, ³J_{PH} = 14.0 Hz, ⁴J_{PH} = 1.5 Hz, CH₃), 3.77 (d, 2H, ³J_{PH} = 4.5 Hz, CH₂)).

(OC)₅WP(CH₂NEt)₃PW(CO)₅, 24 This compound was prepared from 13 and CH₃CNW(CO)₅ in 23% yield using a procedure analogous to that just described for 23, except that benzene was used to elute the Florisil column (mp = 143-145°; ¹H NMR ((CD₃)₂CO) 1.22 (t, 3H, ³J_{HH} = 7.0 Hz, CH₃), 3.35 (m, 2H, CH₃CH₂), 3.78 (d, 2H, ³J_{PH} = 4.5 Hz, PCH₂)).

(OC)₅WP(CH₂NPh)₃P, 25 A solution of 0.2 g (0.5 mMol) of 14 and 0.2 g (0.5 mMol) of CH₃CNW(CO)₅ in 10 mL of methylcyclohexane was heated at 85° for twenty hours. The solution was allowed to cool to room temperature at which time the solvent was removed and the residue extracted with acetone. Evaporation of the acetone gave 0.16 g (42%) of 25 as a white powder (mp = 154° (decomposition); ¹H NMR ((CD₃)₂CO) 4.42 (d, 2H, ³J_{PH} = 4.0 Hz, CH₂), 7.1-7.7 (m, 5H, Ph)).

(OC)₅WP(CH₂NPh)₃PW(CO)₅, 26 This compound was prepared and purified in the same manner as 25, except that a 4:1 ratio of

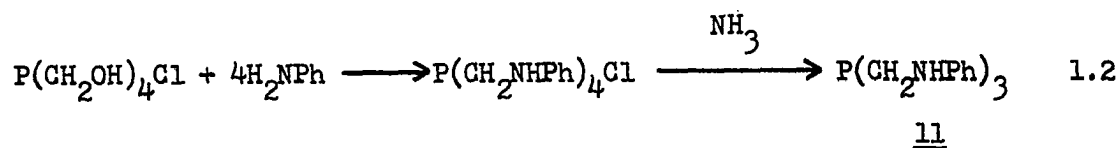
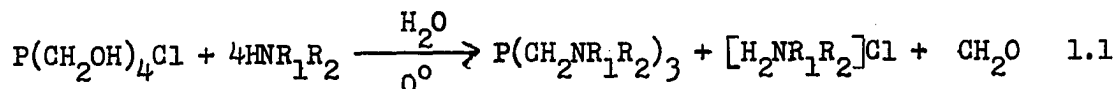
$\text{CH}_3\text{CNW}(\text{CO})_5$ to 14 was used. A 20% yield of 26 was obtained as a white powder (mp = 163-165°; ^1H NMR ($(\text{CD}_3)_2\text{CO}$) 4.15 (dd, 2H, $^3\text{J}_{\text{PH}} = 6.5$ Hz, $^2\text{J}_{\text{PH}} = 1.0$ Hz, CH_2), 6.6-7.4 (m, 5H, Ph)).

$(\text{OC})_5\text{CrP}(\text{CH}_2\text{NPh})_3\text{P}$, 27 and $(\text{OC})_5\text{CrP}(\text{CH}_2\text{NPh})_3\text{PCr}(\text{CO})_5$, 28 A solution of 0.10 g (0.31 mMol) of 14 and 0.14 g (0.62 mMol) of $\text{CH}_3\text{CNCr}(\text{CO})_5$ in 10 mL of methylcyclohexane was heated at 80° for three hours. After cooling to room temperature, the solvent was removed under reduced pressure leaving a green solid. This solid residue was extracted with 3 x 15 mL of diethyl ether. The ether was removed under reduced pressure to leave a white solid. The ^{31}P NMR of this solid indicated the presence of 27 and 28 in a ratio of approximately 1:6, along with other impurities. Further extraction with 2 x 25 mL of 1:1, V:V of ether:hexane and removal of the solvent produced 0.10 g (42% yield) of 28 as a white solid (^1H NMR (CDCl_3) 3.81 (d, 2H, $^3\text{J}_{\text{PH}} = 5.0$ Hz, CH_2) 6.5-7.4 (m, 5H, Ph)). Isolation of 27 was precluded by the small amount of the material present.

RESULTS AND DISCUSSION

Synthesis

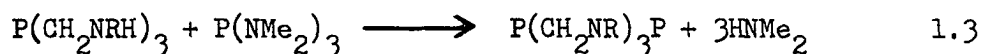
The phosphonium salt $P(CH_2OH)_4Cl$ reacts with primary and secondary alkyl amines according to equation 1.1 to form the tris-(alkyl or dialkylaminomethyl)phosphine (15). Extraction of the aqueous reaction mixture with benzene removes only the phosphine. The tris(dialkylaminomethyl)phosphines are distillable liquids, but the tris(alkylaminomethyl)phosphines decompose before distilling even at reduced pressures. In the case of aniline ($R_1 = H$, $R_2 = Ph$), a stable phosphonium salt is formed (equation 1.2) but this salt is easily



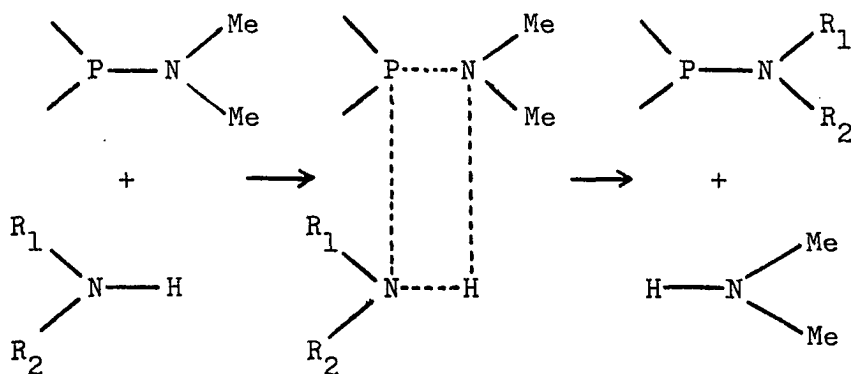
reduced with anhydrous ammonia (16) to the tris(anilinomethyl)phosphine 11.

The bicyclic compounds 2,6,7-trimethyl-2,6,7-triaza-1,4-diphosphabicyclo[2.2.2]octane, 12, 2,6,7-triethyl-2,6,7-triaza-1,4-diphosphabicyclo[2.2.2]octane, 13, and 2,6,7-triphenyl-2,6,7-triaza-1,4-diphosphabicyclo[2.2.2]octane, 14, are formed by transamination of the appropriate triamine (9, 10 or 11) with tris(dimethylamino)phosphine

(equation 1.3). The generality of this reaction was demonstrated by



Burgada (18) and was utilized by Laube *et al.* (7) in the preparation of 6. Yields were maximized when the reactions were performed in the absence of a solvent. Such reactions can be interpreted as occurring through a tetragonal transition state or intermediate (19).



Two factors which can affect the activation energy of the reactions of interest here are the nucleophilicity of the attacking amine and the electrophilicity of the phosphorus. The pi bonding of the nitrogen atoms of 11 with the phenyl rings reduces the nucleophilicity of these nitrogens compared to the nitrogens in 9 or 10. A qualitative indication of this effect is found in the longer reaction time to form 14 (72 hours) compared to 12 or 13 (20-24 hours). The second factor (electrophilicity of phosphorus) would also predict a longer reaction time (higher activation energy) for the formation of 14

compared to 12. The ability of nitrogen to donate electrons to phosphorus is lower for 11 than for 9 or $P(NMe_2)_3$ so that as the dimethylamino groups of $P(NMe_2)_3$ are replaced by the nitrogens of 11, the phosphorus becomes more electrophilic. The more electrophilic phosphorus attracts more electrons from the remaining dimethylamino groups making the latter less nucleophilic and less reactive. An important factor which certainly favors the formation of 12-14 is the volatility of dimethylamine which provides a driving force for the reaction.

All attempts to purify 12 and 13 by fractional distillation were unsuccessful. Apparently either the impurity boils within 0.5 degree of the cage or the cage decomposes at its boiling point. Chromatography on silica gel or Florisil columns also proved fruitless as 12 and 13 both decompose on the column. Purification of 14 by chromatography followed by recrystallization from ethyl acetate provides nice crystals of pure 14.

The sulfuration of 12 and 13 in benzene solution is exothermic and in both cases readily yields the disulfide 17 and 19, respectively. In the case of 13, the monosulfide 18 was also isolated. No evidence for the monosulfide having the sulfur bonded to the aminophosphine was found, indicating that the phosphine end of the molecule reacts more readily than the aminophosphine. The reaction of 12 and 13 with $KSeCN$ under mild conditions (13) readily gave the diselenides of both compounds, 20 and 21, respectively. The reactivity of 14 toward

sulfur and selenium is in direct contrast to 12 and 13. Reaction of 14 with excess sulfur in refluxing benzene or toluene gave only unreacted starting materials and some unidentified decomposition products of 14. Direct reaction of 14 with sulfur in a sealed tube decomposed the cage. Reaction of 14 with KSeCN under mild conditions (60°) and with red selenium under more vigorous conditions (refluxing toluene) yielded only unreacted 14. The unexpected lack of reactivity of the aminophosphine moiety of 14 compared to 12 and 13 may be rationalized by the pi bonding of the nitrogen lone pair with the phenyl ring, which renders the nitrogen less able to donate electrons to phosphorus. The phosphorus could then become a "harder" base and hence less reactive toward the soft acid (sulfur) (20). The unreactive phosphine phosphorus in 14 does not lend itself to any satisfying rationalization at this time, since the triamine 11 readily reacts with sulfur (16).

All three cages 12, 13, and 14 were reluctant to form oxides. Trialkylphosphines are normally oxidized by atmospheric oxygen (21) but pure oxygen bubbled through solutions of the cages even at $60-80^{\circ}$ failed to produce any oxides. Other oxidizing agents which also failed to oxidize the cages include KO_2 , H_2O_2 (aqueous), O_3 (-78°), and benzoyl peroxide. Smith and Sisler (22) found that $(Ph)_2PNR_2$ compounds were resistant to oxidation by the usual oxidizing agents but were readily oxidized by activated MnO_2 . Treatment of 12 with activated MnO_2 at 100° in toluene oxidized the phosphine end of the cage, but

not the aminophosphine, forming 15. Treatment of a hexane solution of 14 with gaseous N_2O_4 at -78° produced a small amount of the dioxide 16. Similar reactions with 12 and 13 failed to produce any isolable oxides. An interesting observation made while monitoring the reaction of 12 with H_2O_2 using ^{31}P NMR spectroscopy revealed that the impurity phosphines normally present with 12 were oxidized by the initial addition of H_2O_2 but after all of these impurities had reacted, further addition of H_2O_2 caused decomposition of the cage structure.

Phosphine selenides are easily converted to the corresponding phosphine oxide upon treatment with peroxides (23). The reaction of 20 with H_2O_2 (30%) was monitored with ^{31}P NMR spectroscopy. As the reaction progressed, the two doublets due to 20 decreased in intensity as two new doublets grew in intensity. The aminophosphine resonance shifted very little while the phosphine resonance was shifted downfield by 13 ppm indicating that the selenium on the phosphine end was being replaced by oxygen while the aminophosphine end remained a selenide. Mass spectral analysis of the solution revealed that 22 was indeed the product. Further addition of H_2O_2 did not displace the aminophosphine selenide and upon standing the cage structure decomposed.

The metal carbonyl complexes $\text{CH}_3\text{CNM}(\text{CO})_5$ ($\text{M} = \text{Cr}, \text{W}$) were prepared from the $[\text{M}(\text{CO})_5]\text{Et}_4\text{N}$ salts (14, 24) to furnish a ligand (CH_3CN) which is easily displaced by phosphorus. The phosphine and aminophosphine phosphorus atoms of 12, 13, and 14 readily displace the

acetonitrile to form the bis(pentacarbonyl)metal complexes 23, 24, 26, and 28, respectively. The mono-substituted complexes of 14 (25 and 27) were isolated with the phosphine end of the cage showing preferential coordination.

Mass Spectra

Although no parent ions were observed in the mass spectra of 9 and 10, this is not an unexpected result for secondary amines (25). All other compounds showed strong parent ions except 14 for which chemical ionization techniques were required to obtain the expected parent ions. The isotopes of selenium (^{74}Se , 0.87%; ^{76}Se , 9.02%; ^{77}Se , 7.58%; ^{78}Se , 23.52%; ^{80}Se , 49.82%; ^{82}Se , 9.19%) give an interesting and characteristic pattern to the parent ion region of the mass spectrum of selenium-containing compounds. For compounds 20, 21, and 22, the average of the intensities of all the peaks in the parent ion region for ten spectra were compared to the theoretical values as calculated by the program MASP (12). The experimental values agreed with the calculated values to within 10% for all three compounds. The parent ion region for 21, which contains two selenium atoms, is shown in Figure 1.1. The fragmentation pattern for the same compound is shown in Figure 1.2. As in all of the cage compounds, a favored fragmentation mechanism is loss of one bridging group ($m/e = 336$) followed by loss of a second bridging group ($m/e = 279$) as shown in Figure 1.3.

Figure 1.1. Parent ion region of the mass spectrum
of $\text{Se}=\text{P}(\text{CH}_2\text{NEt})_3\text{P}=\text{Se}$, 21

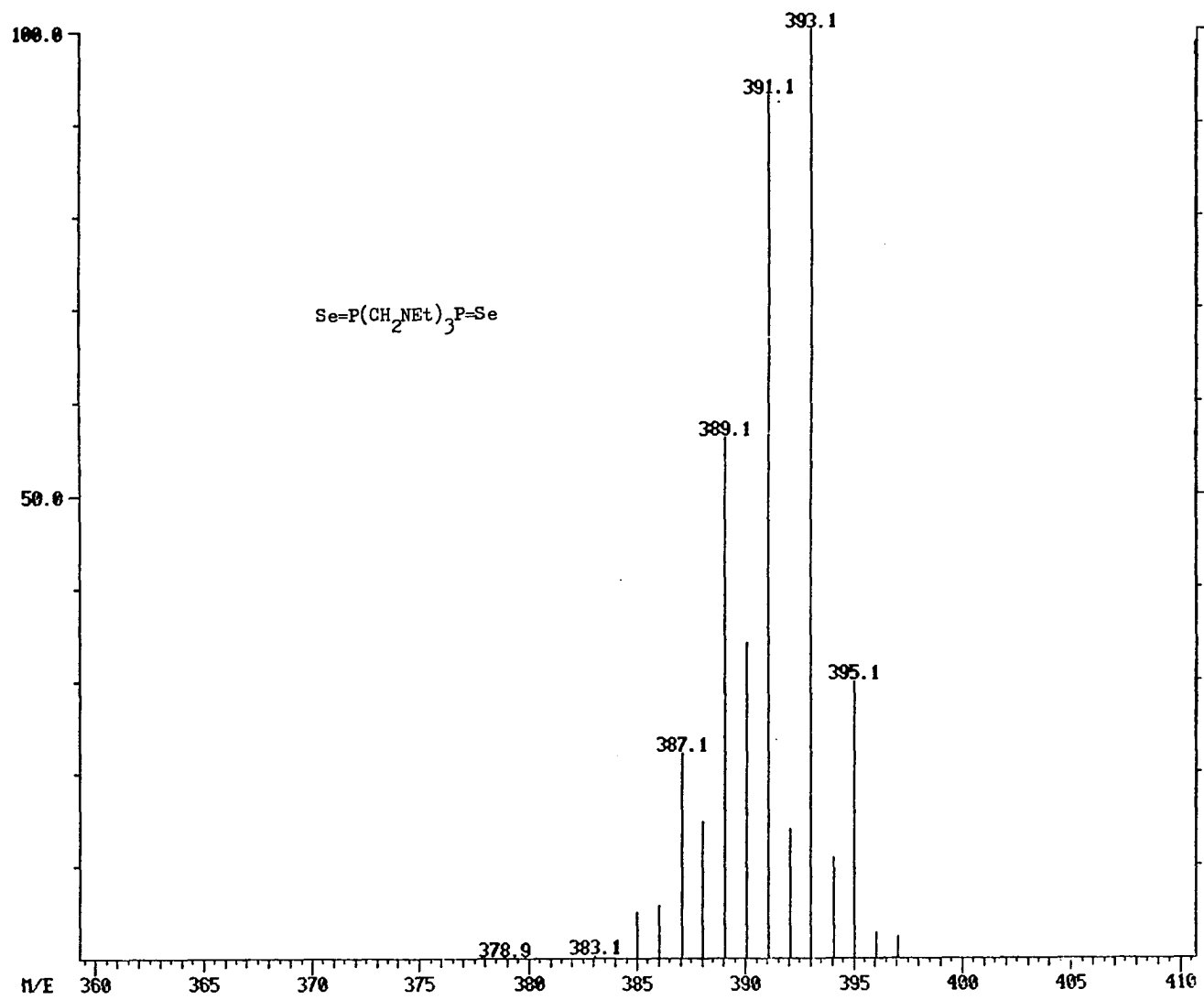
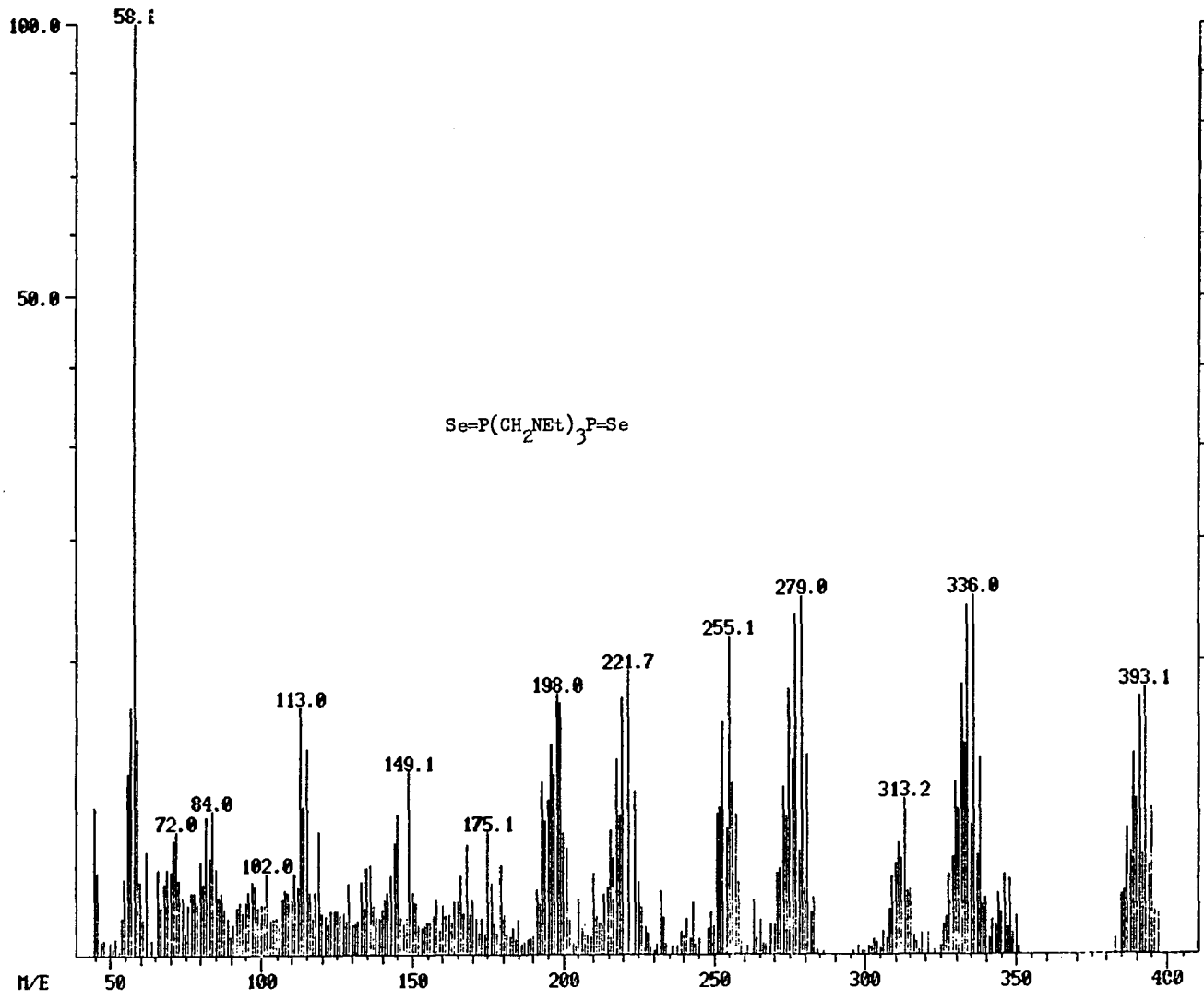


Figure 1.2. Mass spectral fragmentation pattern for $\text{Se}=\text{P}(\text{CH}_2\text{NEt})_3\text{P}=\text{Se}$, 21



11

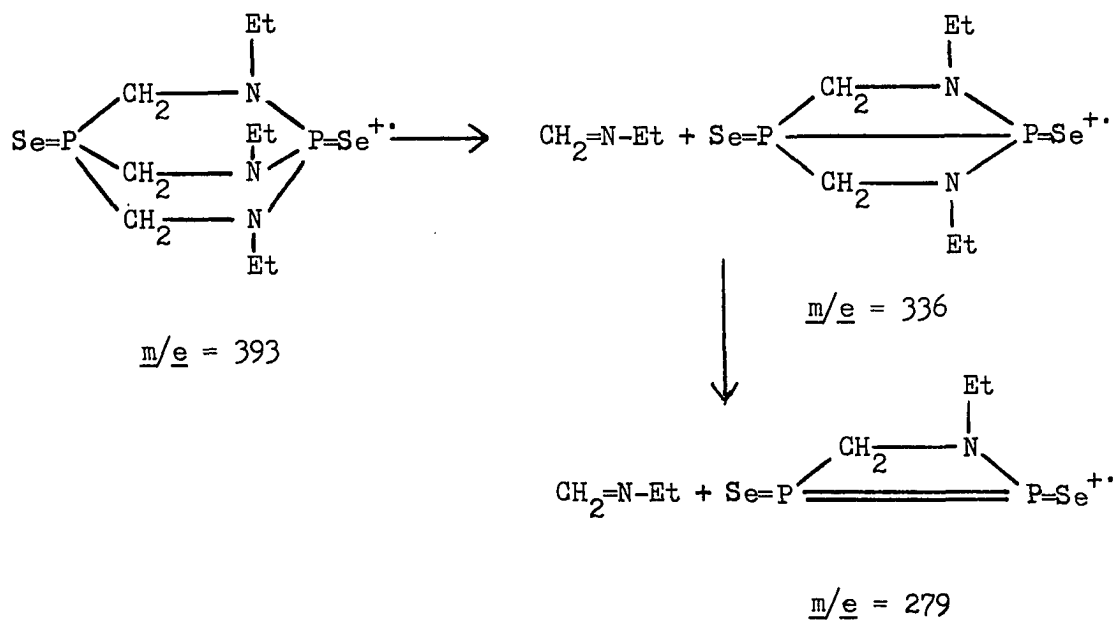


Figure 1.3. Fragmentation mechanism for mass spectrum of cage compounds. $\text{Se}=\text{P}(\text{CH}_2\text{NEt})_3\text{P}=\text{Se}$, 21 is used as an example

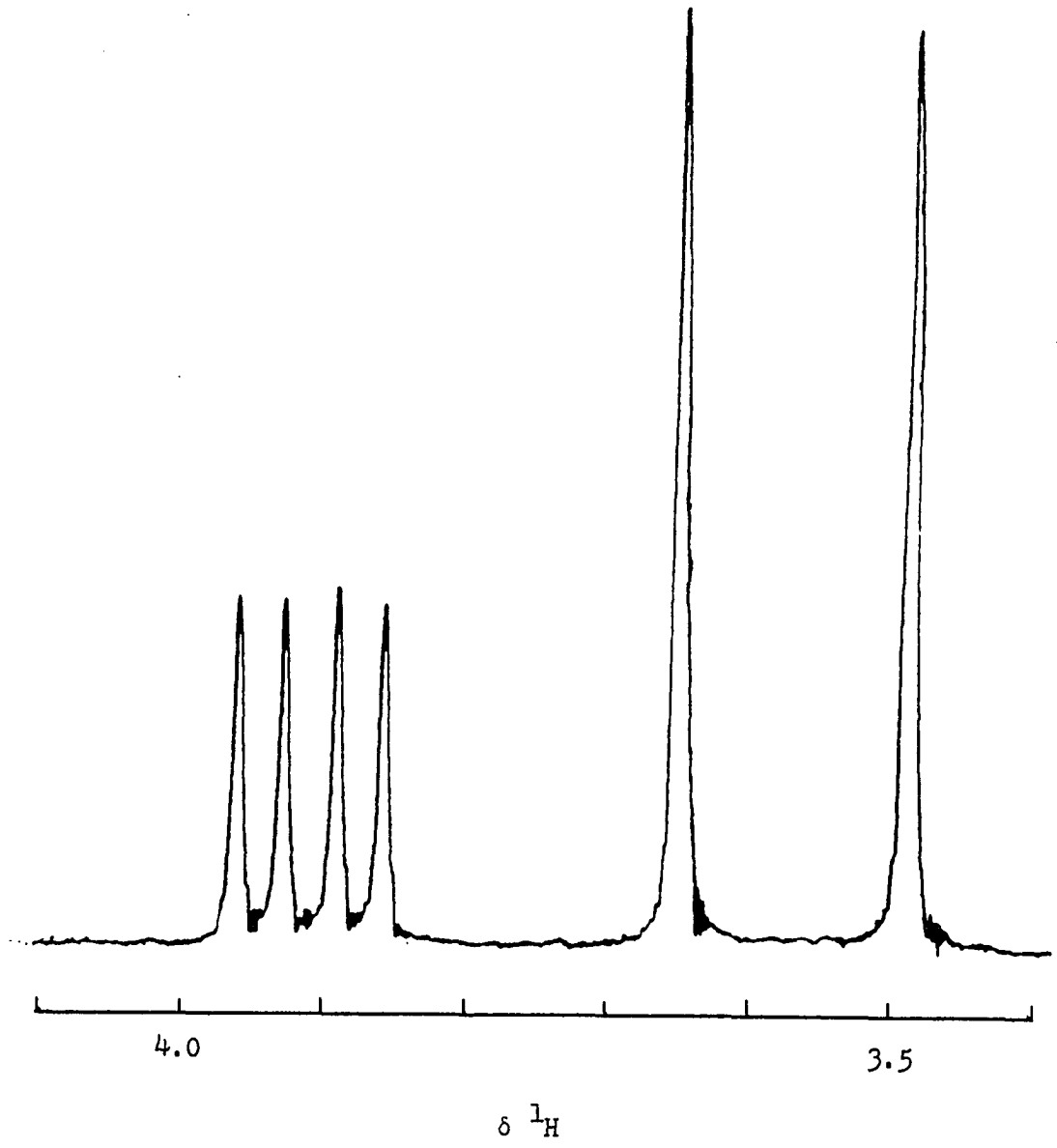
NMR Spectra

 ^1H NMR

The presence of two phosphorus atoms, each with a magnetic spin of $\frac{1}{2}$, causes interesting spin-spin splitting patterns in the ^1H NMR spectra of the cage compounds. Both phosphorus atoms have the potential of coupling to the protons on the carbon of the bridge as well as to the N-methyl protons of 12 or the methylene protons of the N-ethyl group of 13. The complexity of the phenyl resonances of 14 precludes assignment of any PH couplings for the phenyl protons of this compound, although phosphorus couplings were detectable for the phenyl carbons in the ^{13}C NMR spectrum of 14.

The ^1H NMR spectrum of 12 is shown in Figure 1.4. The bridging methylene protons appear as a doublet of doublets with the assignments of $^2J_{\text{PH}} = 6.8$ Hz and $^3J_{\text{PH}} = 3.2$ Hz being made by selective decoupling of the phosphorus nuclei. The N-methyl protons couple to the aminophosphine phosphorus, but not to the phosphine phosphorus. This is consistent with the lack of observable PH coupling for the N-methyl protons of 9. The more downfield position of the methylene resonances compared to those of the N-methyl peaks is expected from electronegativity considerations. The ^1H NMR chemical shift is dominated by the diamagnetic term of the Ramsey equation (26), so the presence of two electronegative atoms (N and P) adjacent to the methylene carbon should deshield the methylene protons more than the protons of the N-methyl carbon which is bonded to only one atom of high electronegativity.

Figure 1.4. ^1H NMR spectrum of $\text{P}(\text{CH}_2\text{NMe})_3$, 12



In Figure 1.5 is shown the ^1H NMR spectrum of 17. The change in oxidation state of the phosphorus atoms has given rise to a considerable change in the PH coupling constants. The expected doublet of doublets for the methylene protons appears as an apparent triplet due to the equivalence of $^2J_{\text{PH}}$ and $^3J_{\text{PH}}$. The N-methyl protons of 17 show coupling to the phosphine phosphorus which is absent in the spectrum of 12.

The ^1H NMR spectrum of the bridging methylene protons and the methylene protons of the ethyl group for 19 is shown in Figure 1.6. The bridging methylene protons appear as an apparent triplet due to equivalent coupling to both phosphorus atoms. The splitting pattern for the methylene protons of the ethyl group is complex due to second order effects. The results of selective decoupling experiments performed to simplify the spectrum are diagrammed in Figure 1.7. Figure 1.7.b. shows that broadband decoupling of the phosphorus atoms reduces the spectrum to first order with the bridging methylene protons unsplit and the ethyl resonances showing the expected A_3X_2 system splitting. Selectively decoupling one phosphorus at a time (Figures 1.7.c. and 1.7.d.) again produces first order spectra due to splitting of both groups of methylene protons by the undecoupled phosphorus. The ethyl methylene protons (D) of Figure 1.7.c. appear as a deceptively simple pentet because $^3J_{\text{PH}} = ^3J_{\text{HH}} = 7.1$ Hz. Decoupling of the methyl protons of the ethyl group produces spectrum 1.7.e. The ethyl methylene protons do not show the expected doublet of doublets from coupling to

Figure 1.5. ^1H NMR spectrum of $\text{S}=\text{P}(\text{CH}_2\text{NMe})_3\text{P}=\text{S}$, 17

The CH_2 protons couple to both phosphorus atoms equally, resulting in an apparent triplet

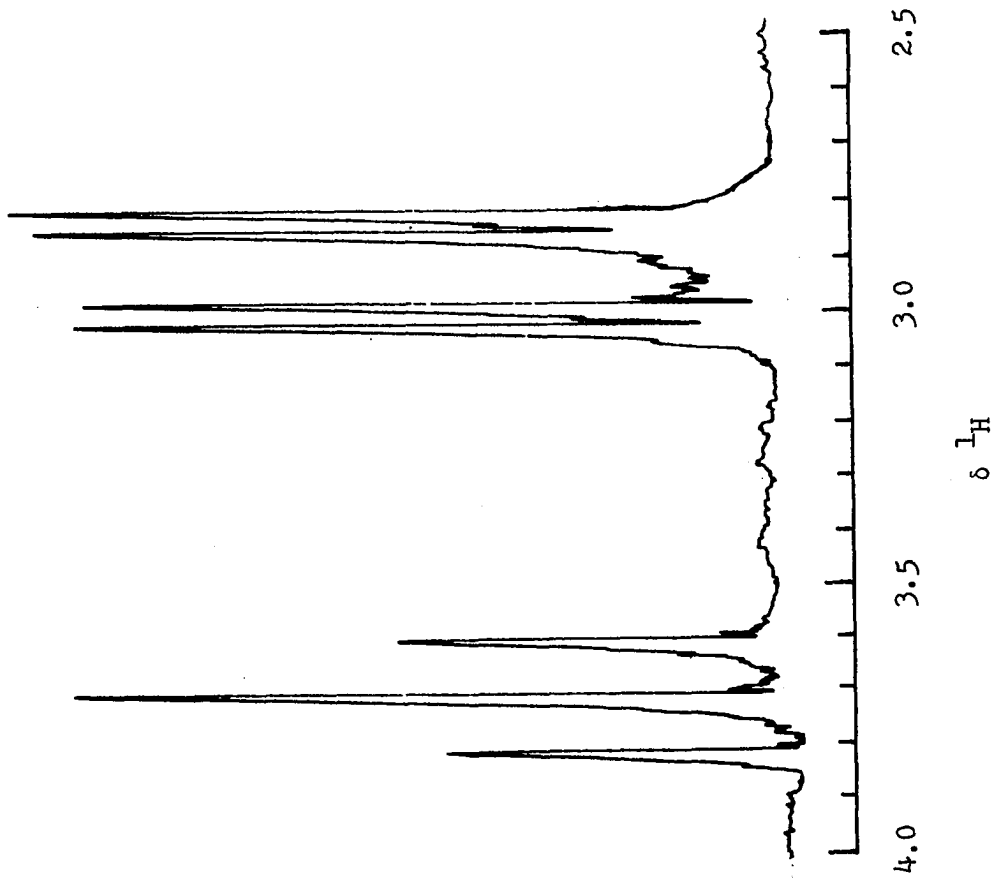


Figure 1.6. ^1H NMR spectrum of $\text{S}=\text{P}(\text{CH}_2\text{NEt})_3\text{P}=\text{S}$, 19
The triplet for the methyl protons of the ethyl group has been omitted.

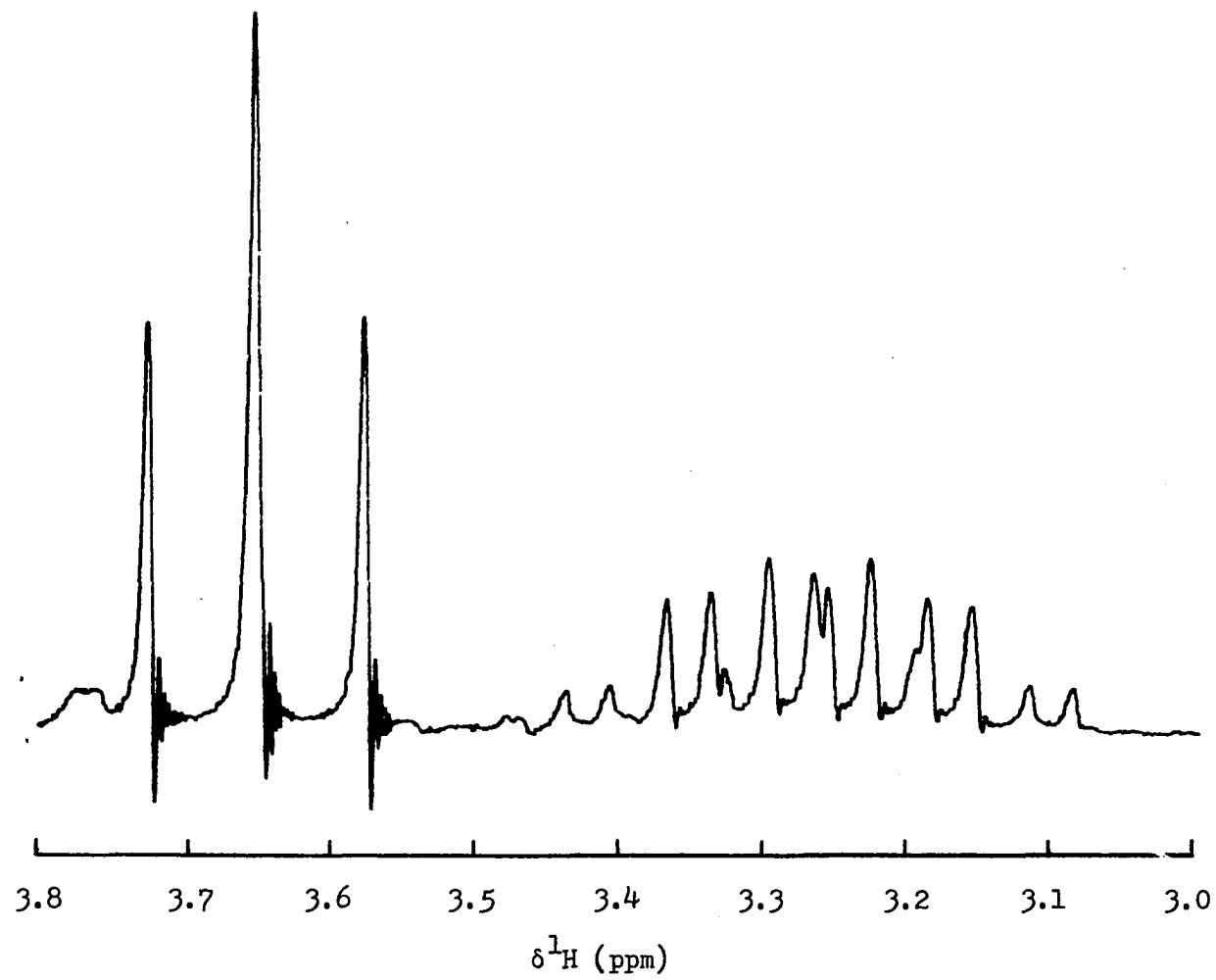
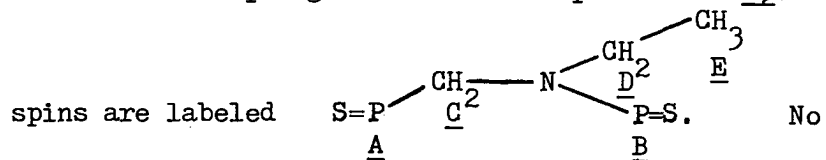


Figure 1.7. Selective decoupling of the ^1H NMR spectrum of 19. The



decoupling is present in (a). Both phosphorus atoms (A and B) are decoupled in (b). Only A is decoupled in (c) while B is decoupled in (d). The methyl protons E are decoupled in (e)

the phosphorus atoms, but rather what appears to be a doublet of triplets. The proximity of the resonances of the two sets of methylene protons made selective decoupling of these protons impossible on the spectrometers available. The second order effects are present only when coupling between the phosphorus atoms is allowed. Thus, the additional coupling must be transferred by the P-P system. In a strongly coupled spin system such as an ABC system, if A and C are both strongly coupled to B, the A and/or C part of the spectrum can show coupling effects known as "virtual" coupling to the other nucleus even if the A-C coupling constant is almost zero (25). Since the bridging methylene and ethyl methylene groups are both strongly coupled to the phosphorus atoms, the concept of virtual coupling may be invoked to rationalize the extra splitting noted in the ethyl methylene region of the spectrum.

^{13}C NMR

The ^{13}C chemical shifts of the bridging methylene carbons of 12 and 14 (44.8 and 40.4 ppm, respectively) are well upfield from the values reported (27) for the bridging methylene carbon of 6 (61.2 ppm) and 7 (62.9 ppm). In addition to the change in electronegativity between the phosphorus and carbon bridgeheads, the size of the bridgehead atom may affect the hybridization of the methylene carbon. The average NCC bond angle for the oxide 7 (107.5) is more than 4° smaller than the NCP angle (111.8°) of 14. A similar effect on the ^{13}C NMR

chemical shift of the bridging methylene carbon is seen when the carbon bridgehead of $(\text{P}(\text{OCH}_2)_3)_2\text{C}-\text{CH}_3$ ($\delta^{13}\text{CH}_2 = 71.4$ ppm (2), $\angle \text{OCC} = 110.0^\circ$ (28)), is replaced by phosphorus in 1 ($\delta^{13}\text{CH}_2 = 58.2$ ppm (29), $\angle \text{OCP} = 113.4^\circ$ (30)).

The spin-spin coupling between the aminophosphine phosphorus and the methyl carbon of 12 (35.4 Hz) is in sharp contrast to the lack of similar coupling in 6 but is more in line with the ${}^2J_{\text{PNCH}_3}$ couplings in the spectra of $\text{P}(\text{NMe}_2)_3$ (19.15 Hz (27)) and 3 (12.8 Hz (27)). The phenyl carbon resonances of 14 were assigned by analogy to HNMePh (31). Substantial PC couplings were observed for C_{11} (28.1 Hz) as well as C_{12} and C_{16} (18.3 Hz).

${}^{31}\text{P}$ NMR

The ${}^{31}\text{P}$ NMR chemical shift is a valuable tool for characterizing organophosphorus compounds. The shifts are quite sensitive to the nature of the substituents attached to phosphorus. Thus, by comparing the shifts of numerous compounds, ranges for the typical shift of classes of compounds such as phosphines or phosphites can be determined (32). The ${}^{31}\text{P}$ NMR chemical shifts for the compounds in Part I are contained in Tables 1.1 and 1.2.

When a phosphorus atom is constrained into a bicyclo[2.2.2]octane structure, the ${}^{31}\text{P}$ NMR chemical shift is generally found to be upfield of the analogous acyclic compound (see Part II of this dissertation). Two of the few examples which do not fit this trend are the phosphine phosphorus atoms of 12 and 13. The trend holds for the phosphine

Table 1.1. ^{31}P NMR data for precursors and derivatives of 12, 13, and 14 ^a

Compound	δ $^{31}\text{P}\text{N}_3$	δ $^{31}\text{P}(\text{CH}_2)_3$	J_{PP}
<u>9</u> $\text{P}(\text{CH}_2\text{NHMe})_3$		-60.8	
<u>10</u> $\text{P}(\text{CH}_2\text{NHEt})_3$		-60.8	
<u>11</u> $\text{P}(\text{CH}_2\text{NHPh})_3$		-31.9	
<u>12</u> $\text{P}(\text{CH}_2\text{NMe})_3\text{P}$	80.0	-55.0	-27.7
<u>13</u> $\text{P}(\text{CH}_2\text{NEt})_3\text{P}$	73.4	-54.0	-27.0
<u>14</u> $\text{P}(\text{CH}_2\text{NPh})_3\text{P}$	49.0	-46.0	-27.7
<u>15</u> $\text{O}=\text{P}(\text{CH}_2\text{NMe})_3\text{P}$	79.6	30.6	17.8
<u>16</u> $\text{O}=\text{P}(\text{CH}_2\text{NPh})_3\text{P}=\text{O}$	-7.4	35.6	72.1
<u>17</u> $\text{S}=\text{P}(\text{CH}_2\text{NMe})_3\text{P}=\text{S}$	62.3	35.1	116.5
<u>18</u> $\text{S}=\text{P}(\text{CH}_2\text{NEt})_3\text{P}$	70.4	6.2	8.9
<u>19</u> $\text{S}=\text{P}(\text{CH}_2\text{NEt})_3\text{P}=\text{S}$	58.2	35.9	107.6
<u>20</u> $\text{Se}=\text{P}(\text{CH}_2\text{NMe})_3\text{P}=\text{Se}$	64.7	19.1	111.0
<u>21</u> $\text{Se}=\text{P}(\text{CH}_2\text{NEt})_3\text{P}=\text{Se}$	53.5	12.5	107.6
<u>22</u> $\text{O}=\text{P}(\text{CH}_2\text{NMe})_3\text{P}=\text{Se}$	65.2	32.3	109.9

^aSpectra were obtained in CDCl_3 . Positive shifts are downfield from H_3PO_4 .

Table 1.2. ^{31}P NMR data for metal carbonyl complexes ^a

Compound	δ $^{31}\text{P}_{\text{N}_3}$	$\Delta\delta$	$^1J_{\text{WP}}$	δ $^{31}\text{P}(\text{CH}_2)_3$	$\Delta\delta$	$^1J_{\text{WP}}$	J_{PP}
<u>23</u> $(\text{OC})_5\text{WP}(\text{CH}_2\text{NMe})_3\text{PW}(\text{CO})_5$	110.7	30.7	_b	-2.2	52.8	226.4	64.4
<u>24</u> $(\text{OC})_5\text{WP}(\text{CH}_2\text{NEt})_3\text{PW}(\text{CO})_5$	106.8	33.4	344.0	-0.2	53.8	226.4	78.8
<u>25</u> $(\text{OC})_5\text{WP}(\text{CH}_2\text{NPh})_3\text{P}$	49.8	_c	_b	12.1	33.9	239.7	15.5
<u>26</u> $(\text{OC})_5\text{WP}(\text{CH}_2\text{NPh})_3\text{PW}(\text{CO})_5$	90.9	41.9	352.9	-19.1	65.1	225.3	46.6
<u>27</u> $(\text{OC})_5\text{CrP}(\text{CH}_2\text{NPh})_3\text{P}$	53.5	_c	_c	-36.9	82.9	_c	15.5
<u>28</u> $(\text{OC})_5\text{CrP}(\text{CH}_2\text{NPh})_3\text{PCr}(\text{CO})_5$	104.6	55.6	_c	-67.5	113.5	_c	44.4

^aSpectra were obtained in CDCl_3 solutions. Positive shifts are downfield from the 85% H_3PO_4 external standard.

^bNot observed.

^cNot applicable.

phosphorus of 14 as well as the aminophosphine phosphorus atoms of 12, 13, and 14. The aminophosphine phosphorus shifts of 12 and 13 are approximately 40 ppm to higher field than their analogous acyclic compounds $P(NMe_2)_3$ (123 ppm) and $P(NEt_2)_3$ (118 ppm) (32). The 49.0 ppm chemical shift of the aminophosphine of 14 is well upfield of "normal" aminophosphines (135-115 ppm) (32). Bonding of the phosphorus lone pair to an electron pair acceptor such as oxygen, sulfur, or selenium moves the chemical shift of phosphine ^{31}P in a downfield direction, while moving the aminophosphine ^{31}P shifts to higher field. In the cage systems 12, 13, and 14, the phosphine phosphorus atoms seem to be more sensitive to this oxidation process than the aminophosphines. For example, the $\Delta \delta$ for the phosphine of 12 upon sulfuration to 17 is 90.1 ppm while the $\Delta \delta$ of the aminophosphine phosphorus is only -17.7 ppm. The magnitude of $\Delta \delta$ for the phosphine phosphorus also depends upon the oxidation state of the aminophosphine phosphorus as demonstrated by the $\Delta \delta$ of 60 ppm in going from 13 to 18 in which the oxidation state of the aminophosphine phosphorus remains +3. However, when the oxidation state of both phosphorus atoms changes to +5, as in going from 13 to 19, $\Delta \delta$ is 89.9 ppm.

Group VIB metal carbonyls cause a downfield ^{31}P chemical shift upon coordination of both phosphines and aminophosphines. As in the chalcogenide case, the phosphine phosphorus of the cage compounds is more sensitive than the aminophosphine phosphorus, with $\Delta \delta PC_3$ being about 1.5 times greater than $\Delta \delta PN_3$ for 23, 24, and 26.

For most of the $W(CO)_5$ complexes, the major doublets in the ^{31}P NMR spectrum were flanked by two small satellite doublets due to coupling to the ^{183}W nucleus which has a spin of $\frac{1}{2}$ and a natural abundance of 14.40%. The value of $^1J_{WP}$ is the separation between the satellite doublets. The broad lines of the aminophosphine phosphorus resonances of 23 and 25 precluded the observation of the satellite peaks. Coupling constants between directly bonded atoms arise almost entirely from the Fermi contact interaction between nuclear spins and s orbital electron spins. The coupling constants between phosphorus and ^{183}W should yield information regarding the extent of s character contained in the P-W bond. The electronegativities of the substituents on phosphorus have been found to correlate with $^1J_{WP}$ for a variety of phosphorus ligands (1). The greater electronegativity of nitrogen compared to carbon results in considerably greater values for $^1J_{WP}$ for the aminophosphine phosphorus compared to the phosphine atoms of 24 and 26. The $^1J_{WP}$ values of the phosphines of 23, 24, and 26 show little variation among themselves or from values for typical phosphines (1). The aminophosphines of 24 and 26, however, have somewhat higher $^1J_{WP}$ values than $P(NMe_2)_3$ (297 Hz) or $P(NEt_2)_3$ (296 Hz) (33). The higher s character in the lone pairs of the aminophosphines of the cages 13 and 14 compared to those of the acyclic analogues, would result in a concomitantly smaller percentage of p character in the cage lone pairs. This phenomenon can be associated with reduced Lewis basicity for the cage compounds (34).

Determination of coupling constant signs

Indirect nuclear spin couplings represent intrinsic properties of molecules which are not in themselves dependent upon the magnetic resonance phenomenon. Indirect nuclear spin couplings have their origin in magnetic interactions between the nuclei and the electrons in the molecule. This magnetic interaction contributes to the total energy of the molecule. A positive nuclear spin coupling constant is conventionally defined as resulting from an interaction which minimizes the spin coupling energy when the two nuclear spins are antiparallel and a negative spin coupling constant corresponds to a minimum coupling energy when the nuclear spins are parallel (35). Thus, the nuclear spin coupling constants can provide significant information regarding the manner in which a magnetic perturbation in one part of the molecule is transmitted via electronic interactions to another part of the molecule. Theoretical determinations of nuclear spin couplings provide not only magnitudes, but also the absolute signs of the coupling constants. The experimental determination of signs and magnitudes of spin coupling constants can thus provide information of relevance to bonding patterns in a series of related molecules.

The absolute signs of indirect nuclear spin coupling constants may be obtained from high resolution NMR spectra of partially oriented molecules (36). This technique involves the application of a strong electric field to a sample of a polar molecule or alternatively, to a sample of the compound of interest dissolved in a liquid crystal matrix.

These experiments are quite difficult to carry out. The relative signs of spin coupling constants are accessible, however, by more conventional double resonance techniques. The double resonance technique of choice known as "spin tickling" involves the application of a weak radio signal which is applied to the sample at a frequency corresponding to that of a resonance frequency in the spectrum. The resulting perturbation causes mixing of the two states associated with this transition and thus causes secondary perturbations in transitions which are connected to these states. This process allows the connectedness of the transitions to be determined. If the absolute sign of one of the couplings is known, or can be inferred from other information, absolute signs of all the couplings can be assigned.

The spin tickling technique requires a system which contains at least three unique interacting nuclei. The two phosphorus atoms and the methyl protons of 17 are used as an example to demonstrate this approach. Both phosphorus and hydrogen have spin $\frac{1}{2}$ nuclei, each of which has two possible spin states (+ and -). A spin state of the system can be represented by a product of the spin states of the individual nuclei. Resonances observed in the NMR spectrum represent an absorption of energy by one of the nuclei upon going from the state of lower energy (+) to that of higher energy (-). For compound 17 there are nine protons and two phosphorus atoms, so that the product function of any single state of the system consists of eleven positive or negative spins. However, because of the magnetic equivalence of

the protons, the energy of a $+ \rightarrow -$ transition is the same for all of the protons and a transition of any one of the protons causes a resonance condition in the spectrum which for the protons of 17 is therefore multiply degenerate. Considering the degenerate protons as one spin, allows the spin states of the system to be represented by a product of three positive or negative spins. There are four product functions for the two phosphorus atoms ($++$, $+ -$, $- +$, $--$). Thus, each proton transition associated with any of these states causes a resonance in the proton spectrum resulting in a four-line spectrum in the proton region (Table 1.3, resonances 1-4).

Resonances in the ^{31}P spectrum are due to transitions involving a change of spin state for a phosphorus atom. The ^{31}P lines are actually decets due to the nine proton spins. Here these lines will be represented as a single line, however. Thus, lines 5 and 6 (Table 1.3) result from transitions of the aminophosphine sulfide phosphorus while lines 7 and 8 are caused by phosphine sulfide transitions.

The spin tickling experiment performed on this system consists of observing the proton spectrum while perturbing the phosphorus resonances one at a time with a weak irradiating signal. The results of this experiment are shown in Figure 1.8. Figure 1.8a shows the four resonances of the proton spectrum with no tickling. Irradiation of line 5 shows a strong perturbation on lines 1 and 3 of the proton spectrum while irradiation at 6 shows connectedness to lines 2 and 4. In Figure 1.8d line 7 is shown to connect with lines 1 and 2 while

Table 1.3. A representation of the origin and connectedness of the ^1H and ^{31}P NMR resonances of the system consisting of the methyl group and two phosphorus atoms of $\text{S}=\text{P}(\text{CH}_2\text{NMe})_3$, 17

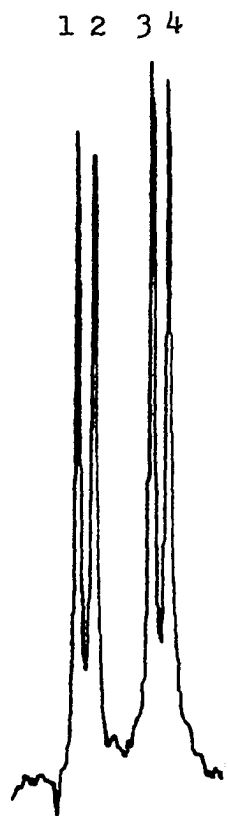
Resonance	Origin ^a	Connectedness
1	$(+)^{\text{b}}_{++} \rightarrow (-)_{++}$	5,7
2	$(+)_{-+} \rightarrow (-)_{-+}$	6,7
3	$(+)_{+-} \rightarrow (-)_{+-}$	5,8
4	$(+)_{--} \rightarrow (-)_{--}$	6,8
5	$(^1\text{H})^{\text{c}}_{++} \rightarrow (^1\text{H})_{-+}$	1,3
6	$(^1\text{H})_{+-} \rightarrow (^1\text{H})_{--}$	2,4
7	$(^1\text{H})_{++} \rightarrow (^1\text{H})_{+-}$	1,2
8	$(^1\text{H})_{-+} \rightarrow (^1\text{H})_{--}$	3,4

^aThe spin functions are ordered ^1H , $\text{SP}(\text{N})_3$, $\text{SP}(\text{C})_3$.

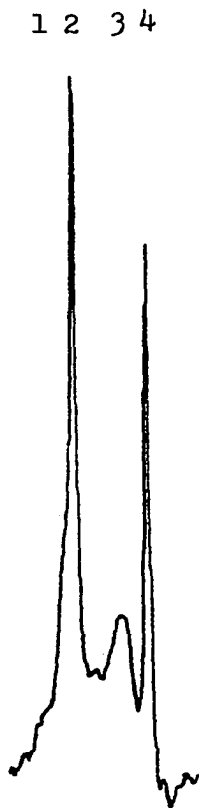
^bThe protons are considered as one spin (see text).

^cThe symbol (^1H) represents a product function of the nine proton spins.

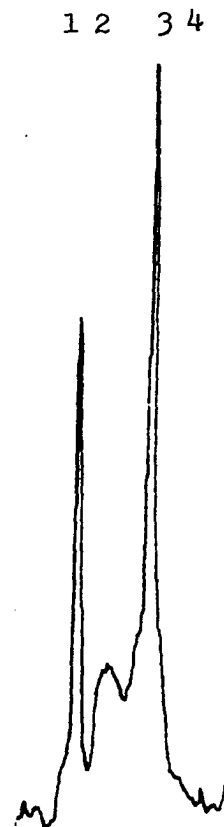
Figure 1.8. Effects of the spin tickling experiment on the ^1H NMR spectrum of the methyl protons of $\text{S}=\text{P}(\text{CH}_2\text{NMe})_3\text{P}=\text{S}$, 17.
(a) No second irradiating frequency (b) Spin tickling line 5 of Figure 1.7 (c) Spin tickling of line 6.



a



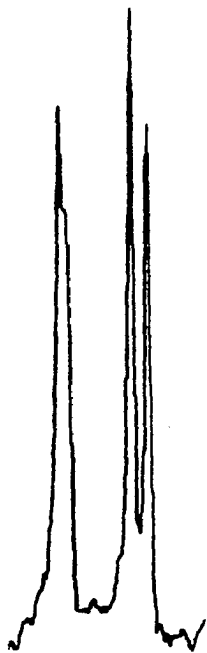
b



c

Figure 1.8. (Continued) (d) Spin tickling of line 7 (e) Spin tickling of line 8

1 2 3 4



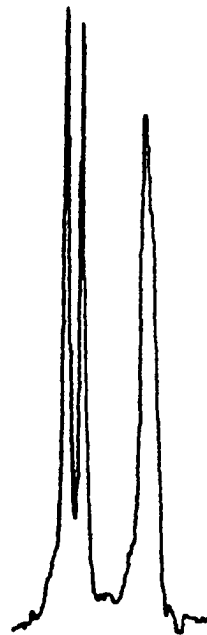
Irradiating

at

7

d

1 2 3 4



Irradiating

at

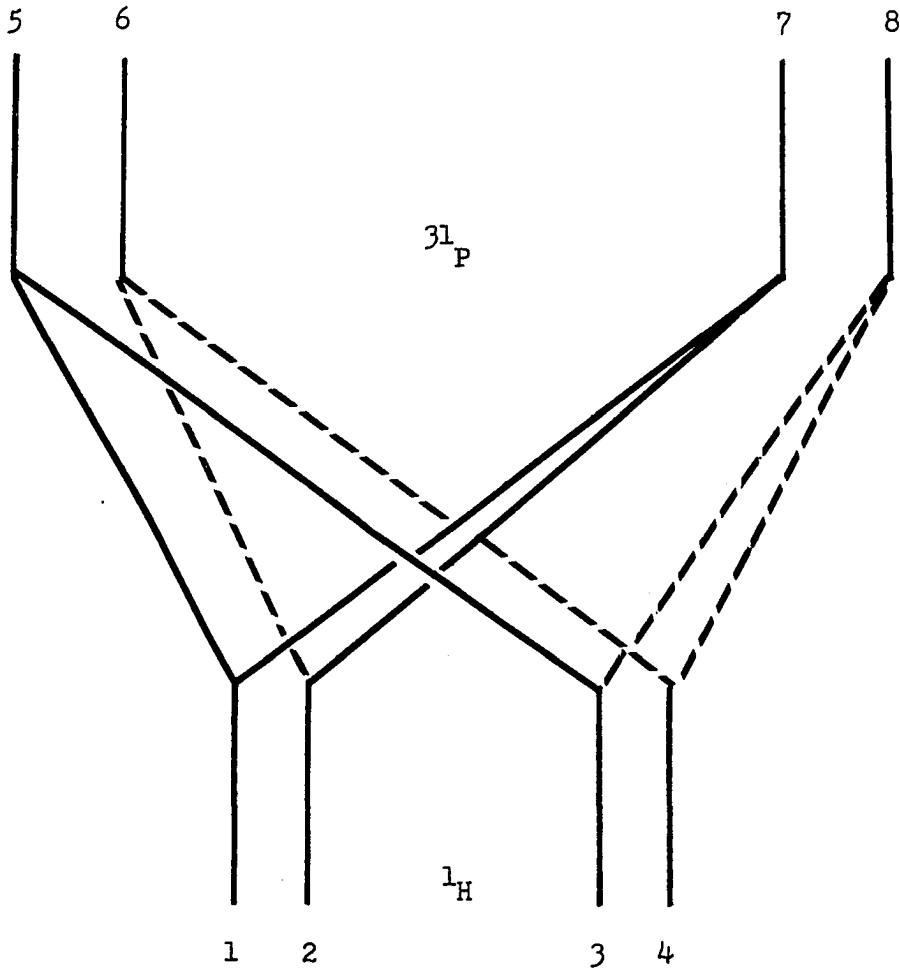
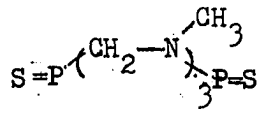
8

e

lines 3 and 4 are perturbed by irradiation of 8. The results of the tickling experiments are summarized in Figure 1.9. Friedman and Gutowsky (37) have developed a method for assigning the relative signs of the coupling constants from the connectedness of the transitions. It can be seen from Table 1.2 that the difference between lines 5 and 6 is a change in the spin state of the phosphine sulfide phosphorus. Observation of the effect on the proton spectrum of irradiation in the aminophosphine sulfide region (5 and 6) determines the relative ordering of the spin functions of the phosphine sulfide phosphorus as revealed by ${}^3J_{PP}$, to the ordering of the proton spin functions as revealed by ${}^4J_{PH}$. In an analogous manner the sign relationships between the coupling of the phosphorus nuclei and the coupling between the aminophosphine sulfide phosphorus and the protons is determined by irradiating the phosphine sulfide resonances (7 and 8). The connectedness of the lowest frequency 1H resonance (1) to the low-frequency member of the aminophosphine sulfide doublet (5) indicates that ${}^4J_{PH}$ and ${}^3J_{PP}$ have the same sign. Similarly, the low field arm of the phosphine sulfide doublet (7) is connected to the low field resonances of the proton spectrum. Thus, ${}^3J_{PH}$ and ${}^3J_{PP}$ also have the same sign and the magnitudes of these couplings can be read directly from the 1H spectrum and the ${}^{31}P$ spectrum, respectively.

Spin tickling also reveals the relative signs of ${}^3J_{PP}$ to the bridging methylene protons of 8. Here the analysis is slightly different due to overlap of lines 2 and 3 of the proton spectrum. However, from

Figure 1.9. The connectedness of the four proton resonances of the methyl protons in $S=P(CH_2NMe)_3P=S$ (lines 1-4) to the aminophosphine sulfide (lines 5 and 6) and the phosphine sulfide (lines 7 and 8)



the knowledge of the transition origins in Table 1.3, the connectedness of the high and low frequency lines of the proton spectrum allows the connectedness of lines 2 and 3 to be deduced (37). The coupling of the aminophosphine sulfide to the bridging methylenes, ${}^3J_{PH}$, has the same sign as ${}^3J_{PP}$ but the phosphine sulfide coupling to these protons, ${}^2J_{PH}$, has the opposite sign of ${}^3J_{PP}$.

In the analysis of the indirect spin coupling constants of $O=P(CH_2O)_3P=O$, Bertrand used an INDOR technique to determine the relative signs of ${}^3J_{PH}$ and ${}^1J_{CH}$ (4). The direct coupling, ${}^1J_{CH}$, has been found to always have a positive sign. Thus the absolute signs for the couplings within $O=P(CH_2O)_3P=O$ become attainable. In the case of other derivatives of 1 for which the INDOR technique did not permit determination of the relative signs of ${}^3J_{PH}$ to ${}^1J_{CH}$, the assumption was made that ${}^3J_{PH}$ is positive for all the compounds studied (5). Values of ${}^3J_{PH}$ for derivatives of 1 varied from +2.5 to +8.3. McFarlane found ${}^3J_{POCH}$ to be positive in a number of compounds (39). Although only a limited number of data are available, Mavel presumed ${}^3J_{POCH}$, ${}^3J_{PNCH}$, and ${}^3J_{PSCH}$ couplings to have the same signs (40). The magnitudes for ${}^3J_{PNCH}$ of 12, 13, 14, and their derivatives range from 1.5 to 8.0 Hz, which is similar to the ${}^3J_{POCH}$ range of derivatives of 1. The ${}^{13}C$ satellite peaks of the 1H spectrum of 17 necessary to relate the sign of ${}^1J_{PC}$ to that of ${}^3J_{PH}$ or ${}^4J_{PH}$ were obscured by spinning side bands which could not be removed by tuning the spectrometer probe. Therefore, the assumption will be made that ${}^3J_{PNCH}$ is positive

throughout the series of compounds studied. The signs and magnitudes of the spin coupling constants for 12, 17, and 19 as well as 1 and $S=P(CH_2O)_3P=S$ are found in Table 1.4. Comparison of the signs and magnitudes of couplings of analogous compounds of these two different cage types reveals great similarities between the two systems. The $^2J_{PH}$ values change sign when the oxidation state of the phosphorus atoms changes from +3 to +5. The change in sign and magnitude of $^3J_{PP}$ caused by this oxidation state change is also very similar for the two different cage compounds. Although no coupling constant signs were determined, the magnitudes of the $^3J_{PP}$ couplings for 3 and its derivatives determined by Kroshefsky (27) indicate an analogous sign change for $^3J_{PP}$ upon oxidation of the phosphorus atoms (Table 1.4). It would appear from the present evidence that the mechanism for transferring magnetic information from one phosphorus to the other in 1,4-diphoshabicyclo[2.2.2]octane structures is approximately independent of the identity of the bridging atoms. Because of this apparent lack of sensitivity to the bridging groups on $^3J_{PP}$ and the spatial proximity of the phosphorus atoms in the cage structure, the possibility of through-space coupling of the two phosphorus atoms across the cage must be considered.

Although few examples of through-space coupling outside of ^{19}F NMR have been reported for which the supporting evidence is convincing (39), the back lobes of the orbitals of the lone pairs or $P = X$ bonds of the cage compounds are suitably oriented for partial overlap (41).

Table 1.4. Spin-spin coupling constants for some cage compounds

Compound	$^2J_{PH}$	$^3J_{PH}(\text{endo})$	$^3J_{PH}(\text{exo})$	$^4J_{PH}$	$^3J_{PP}$
$P(\text{CH}_2\text{NMe})_3\text{P}$ <u>12</u>	+6.8	+3.2	+15.8	0	-27.7
$S=P(\text{CH}_2\text{NMe})_3\text{P=S}$ <u>17</u>	-7.5	+7.5	+12.2	+2.7	+116.5
$S=P(\text{CH}_2\text{NEt})_3\text{P=S}$ <u>19</u>	-7.1	+7.1	+7.1	+2.1	+107.6
$P(\text{CH}_2\text{O})_3\text{P}$ <u>1</u> ^a	+8.9	+2.5	-	-	-37.2
$S=P(\text{CH}_2\text{O})_3\text{P=S}$ ^a	-5.4	+8.6	-	-	+150
$P(\text{NMeNMe})_3\text{P}$ <u>2</u> ^b	-	-	15.0	-	32.0
$S=P(\text{NMeNMe})_3\text{P=O}$ ^b	-	-	11.0	-	105.3

^aReference 3.

^bReference 27.

Preliminary molecular orbital calculations (42) indicate the presence of a strong through-space interaction of the two phosphorus atoms of $\underline{1}$. Overlap of this type has been postulated to explain the large ${}^4J_{\text{PH}}$ coupling constant (7.2 Hz) in $\text{P}(\text{OCH}_2)_3\text{CH}$ (43) and ${}^3J_{\text{PP}}$ in $\underline{1}$ (44), but it must be kept in mind that the three bridging groups provide three pathways for through-bond coupling (4).

Quadrupolar effects

In addition to chemical shifts and coupling constants, a third type of information obtainable from high resolution NMR spectra pertains to nuclear relaxation times. Nuclear relaxation times are characteristic time constants representing the rate of change of the longitudinal or transverse components of the macroscopic nuclear magnetization and are determined by the interaction of spins within the system and between the spins and the lattice. In a system of dipolar nuclei (spin $\frac{1}{2}$) the main interaction is generally the magnetic dipole-dipole interaction between the nuclei.

Nuclei with spin greater than $\frac{1}{2}$, such as ${}^{14}\text{N}$ (spin = 1), possess a non-spherical nuclear charge distribution and therefore have a quadrupole moment. If a spin $\frac{1}{2}$ nucleus is spin-spin coupled to the quadrupolar nucleus via scalar interactions involving the bonding electrons, the fluctuating magnetic field of the quadrupole provides a relaxation mechanism which dominates the relaxation process of the dipolar nucleus. The effect on the NMR spectrum of the spin $\frac{1}{2}$ nucleus is determined by several factors including the scalar coupling constant,

the temperature, and the quadrupolar coupling constant (45). The temperature effect arises from the rapid nuclear quadrupole transitions induced by rapid molecular motion. Thus at high temperatures, the quadrupole relaxes quickly and the quadrupole relaxation time becomes longer and the line widths of the spin $\frac{1}{2}$ nucleus broaden. The quadrupolar coupling constant is a result of the interaction of the quadrupole moment with the electric field gradient. The electric field gradient is very sensitive to the changes in geometry at the quadrupolar nucleus. Increasing the symmetry around the quadrupole reduces the electric field gradient and the effect of the quadrupolar coupling constant on the spectrum of the spin $\frac{1}{2}$ nucleus is reduced.

The aminophosphine phosphorus atoms of the cage compounds 12-28 are coupled to the three quadrupolar ^{14}N atoms of the cage structure. Figure 1.10 shows the effect of temperature upon the ^{31}P NMR line shape of 12. At low temperatures the quadrupolar effect is relatively small due to slow molecular motion and the aminophosphine resonance is a slightly broadened doublet. At -70° the line widths at half height of the aminophosphine phosphorus resonances are 1.5 times as broad as the phosphine phosphorus. As the temperature is raised, the quadrupolar effect becomes stronger and the aminophosphine doublet gradually broadens into a broad singlet at higher temperatures. The quadrupolar effect on the room temperature ^{31}P spectrum of 17 (Figure 1.11) is much less than that for 12 (Figure 1.12). This phenomenon must be a result of either a smaller P-N scalar coupling for 17 or a more symmetrical environment

Figure 1.10. The effect of temperature on the ^{31}P NMR line shape of the aminophosphine phosphorus, PN_3 , of $\text{P}(\text{CH}_2\text{NMe})_3$, 12. Impurities are labeled x

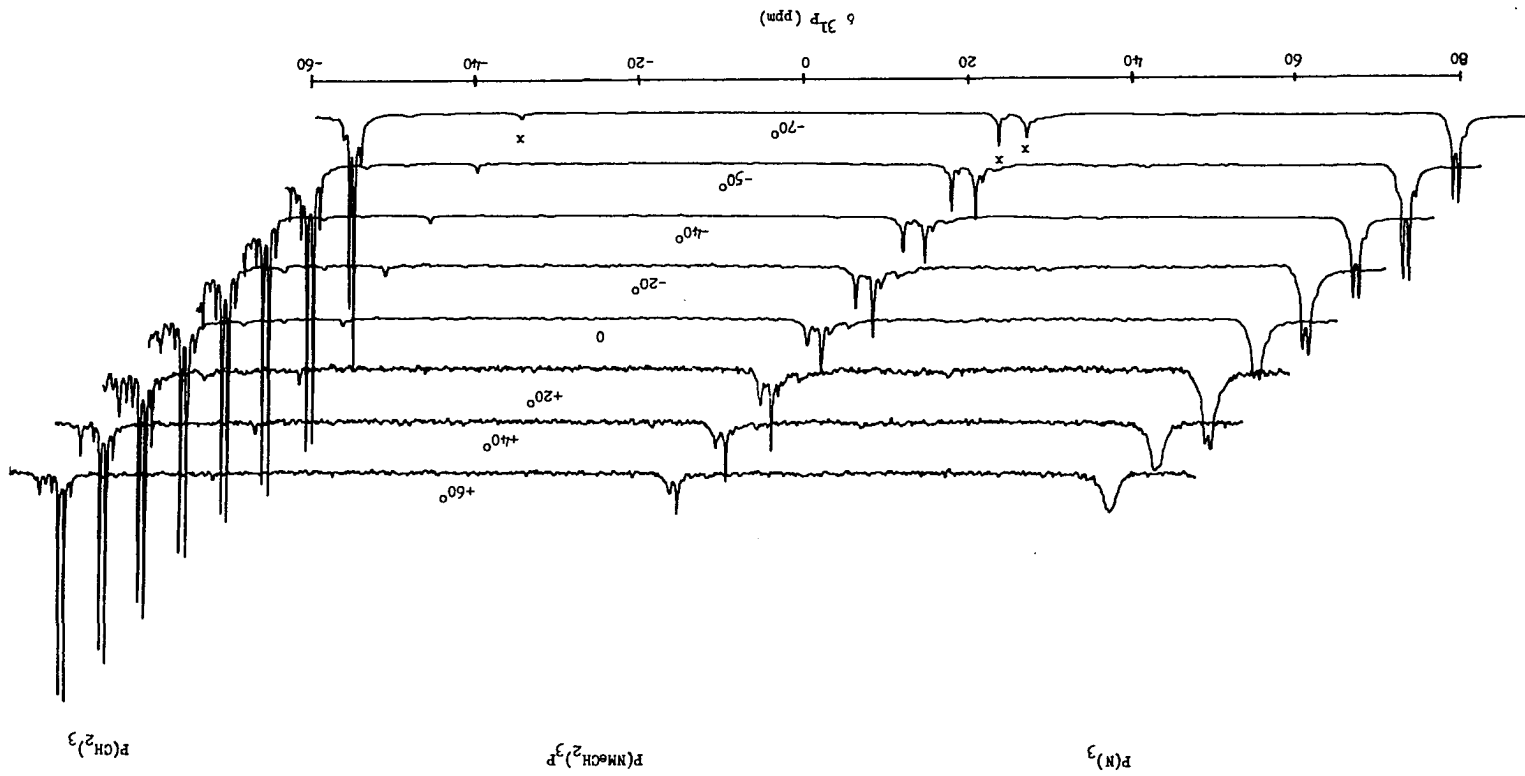


Figure 1.11. ^{31}P NMR spectrum of $\text{S}=\text{P}(\text{CH}_2\text{NMe})_3\text{P}=\text{S}$, 17

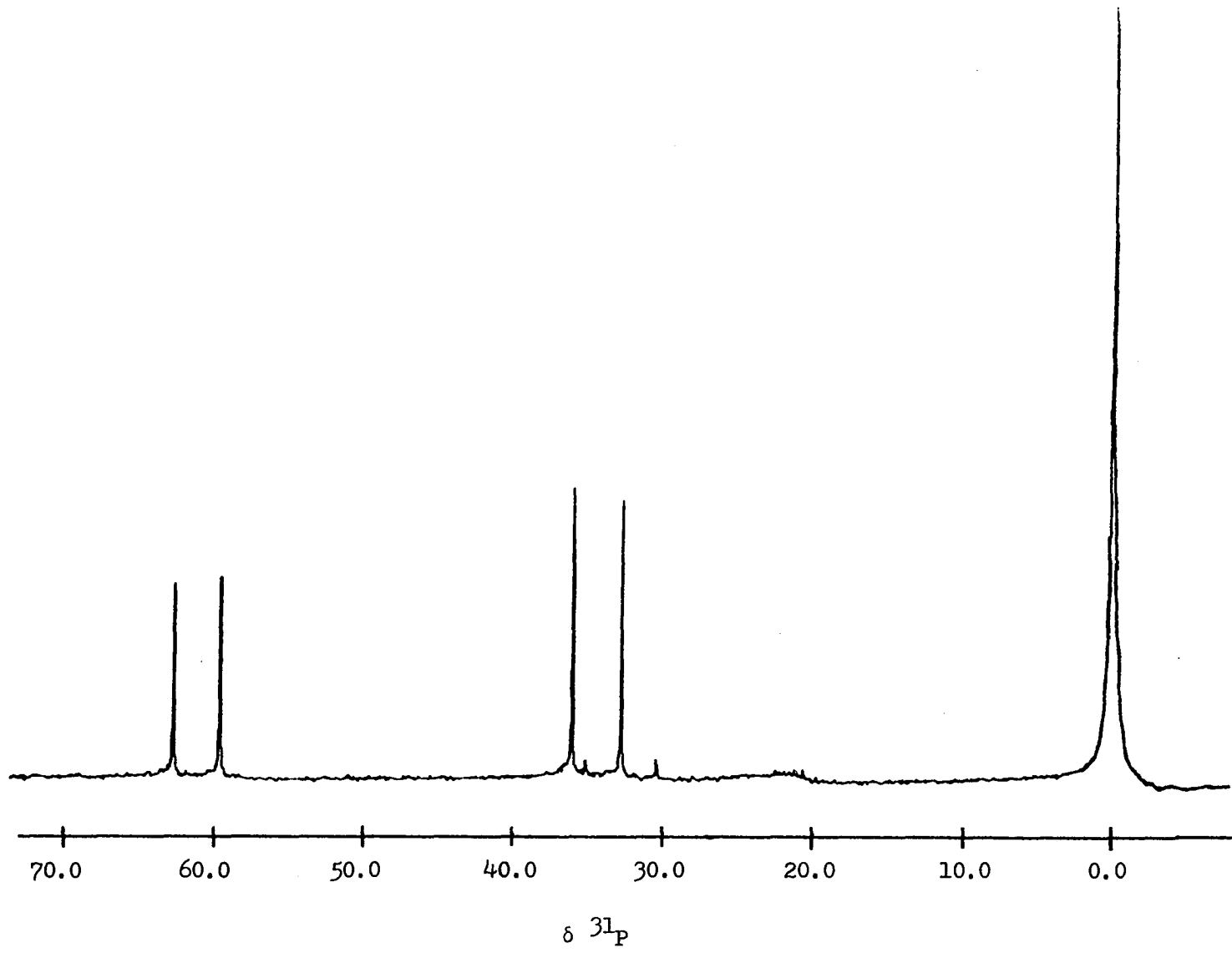
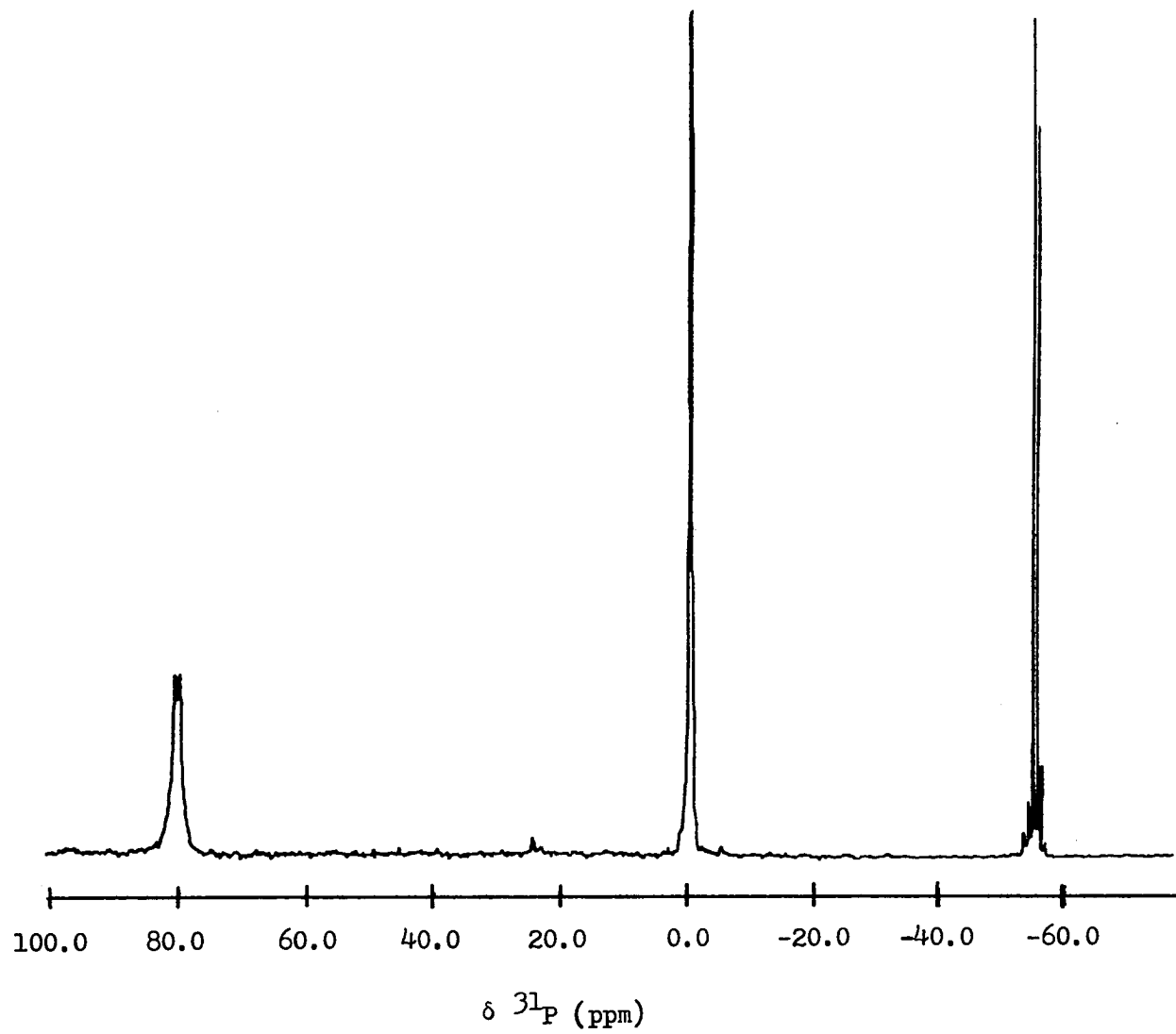


Figure 1.12. ^{31}P NMR spectrum of $\text{P}(\text{CH}_2\text{NMe})_3$, 12, at room temperature.
Note the quadrupolar broadening of the aminophosphine
doublet ($\delta = 80.0$ ppm)



around the nitrogens of 17 compared to 12 resulting in a smaller electric field gradient.

Infrared Spectra

The use of carbonyl group IR stretching frequencies and force constants in metal carbonyl complexes of phosphorus ligands to describe M-P bonding as well as ligand donor and acceptor properties has been an area of active study for many years (1,27). The cage phosphite $\text{P}(\text{OCH}_2)_3\text{CMe}$, 59, and aminophosphine, 6, cause higher $\nu(\text{CO})$ values than the acyclic analogues $\text{P}(\text{OMe})_3$ and $\text{P}(\text{NMe}_2)_3$. This stereoelectronic effect (the "hinge effect") in cage phosphates has been ascribed to the consequences of constraint on the pi character of the bonds of phosphorus to the esteratic oxygens, arising from rehybridization of these oxygens and the orientation of the lone pairs on these oxygens relative to the $\text{O} = \text{P}$ bond. This hybridization change increases the pi acidity and decreases the sigma basicity of the phosphorus atoms (46). The phosphite and phosphine phosphorus of 1 show unexpectedly similar effects on the CO frequencies of Group VI metal carbonyls so that only one set of stretching bands is observed rather than two (4).

The $\nu(\text{CO})$ values for 23, 24, and 26, as well as $(\text{OC})_5\text{WP}(\text{NMe}_2)_3$, are presented in Table 1.5. Like the bridged complexes of 1, the ligand-bridged compounds 23, 24, and 26 show only one set of $\nu(\text{CO})$ values. The results for 23, 24, and 26 are not as unexpected as those for 1, since the donor and acceptor properties of phosphines and aminophosphines are more similar than phosphines and phosphites. Two general trends

Table 1.5. CO stretching frequencies of metal complexes ^{a,b}

Compound	A ₁ ²	B ₁	A ₁ ¹	E	E(¹³ C)
$\begin{array}{c} \text{Me} \\ \\ (\text{OC})_5\text{WP}(\text{CH}_2\text{N})_3\text{PW}(\text{CO})_5 \end{array} \quad (23)$	2077	1986 (s)	1960 (sh)	1952 (vs)	1907 (w)
$\begin{array}{c} \text{Et} \\ \\ (\text{OC})_5\text{WP}(\text{CH}_2\text{N})_3\text{PW}(\text{CO})_5 \end{array} \quad (24)$	2068	1983 (s)	1956 (sh)	1950 (vs)	1915
$\begin{array}{c} \text{Ph} \\ \\ (\text{OC})_5\text{WP}(\text{CH}_2\text{N})_3\text{PW}(\text{CO})_5 \end{array} \quad (26)$	2074	1977 (s)	1959 (sh)	1946 (vs)	1910
(OC) ₅ WP(NMe ₂) ₃	2074.9	1980.5	1943.4 (sh)	1937.4 (vs)	1903.3 (vw)

^aFrequencies are in cm⁻¹.

^bw = weak, m = medium, s = strong, sh = shoulder.

appear in Table 1.5. The values for the complex of 12 are generally higher than those of the other two cage ligands and the values for the cage ligand complexes are in most cases higher than the $(OC)_5WP(NMe_2)_3$ values. The latter trend can be attributed to the hinge effect but the differences in the frequencies are small and so no further characterization of the ligand properties can be achieved from these values.

Crystal and Molecular Structure of $P(CH_2NPh)_3P$

A crystal of 14, grown by slow evaporation of an ethyl acetate solution, was cut to the approximate dimensions 1.0 mm X 1.0 mm X 1.0 mm and sealed in a glass capillary. Five preliminary ω -oscillation photographs taken at various χ and ϕ settings on a four-circle diffractometer, provided the coordinates of eighteen independent reflections which were input into an automatic indexing program (47). This indexing procedure and systematic extinctions predicted a monoclinic system of space group $P_{2/n}$. When difficulty arose in solving the structure, a closer look at the data revealed systematic extinctions ($h0l$ absent if $h + l = 2n + 1$, $0k0$ absent if $k = 2n + 1$) which correctly identified the space group as $P_{2_1/n}$.

Lattice parameters were obtained by a least-squares refinement of the precise $\pm 2\theta$ ($|2\theta| > 25^\circ$) measurements of 18 strong independent reflections at $27^\circ C$ using graphite-monochromated $Mo K\alpha$ radiation ($\lambda = 0.70954 \text{ \AA}$). The lattice parameters are: $a = 10.546(4)$, $b = 18.819(4)$, $c = 10.266(3) \text{ \AA}$; $\beta = 108.66(3)^\circ$ and there are four molecules per unit cell.

An automated four-circle diffractometer described previously by Rohrbaugh and Jacobson (48) was used to measure 6303 reflections (four octants) within a 2θ sphere. There was no significant crystal decomposition as judged by repeated measurements of three standard reflections. Correction for Lorentz-polarization effects and averaging of equivalent data yielded 3063 observed reflections ($F_o \geq 3\sigma$). Estimated deviations in the structure factors were calculated by the finite difference method (49). Due to the cubic shape of the crystal and the relatively limited variation of the transmission factor ($0.702 < T < 0.779$), no absorption corrections were made. During the latter stages of refinement, the data set was corrected for data overflow with five very intense reflections being discarded.

The two phosphorus atoms, three nitrogen atoms, and fifteen of the twenty-one carbon atoms were located using the Patterson superposition technique. The remaining carbon atoms were found by electron density map calculations (50). Hydrogens were put in at positions 1.05 \AA from the corresponding carbons and their isotropic temperature factors fixed at 4.5 \AA^2 . The parameters of all nonhydrogen atoms were refined via a block diagonal least-squares refinement, minimizing the function $(|F_o| - |F_c|)^2$ where $\omega = 1/\sigma_F^2$. A final full-matrix least-squares refinement converged to a conventional $R_F = 7.0\%$ and the weighted $R_w = 9.4\%$. The scattering factors used for nonhydrogen atoms were those of Hanson *et al.* (51) while the parameter for hydrogen was that of Stewart *et al.* (52). The final positional and thermal parameters

are listed in Tables 1.6 and 1.7, respectively. Bond lengths between nonhydrogen atoms are provided in Table 1.8 and bond angles in Table 1.9.

Perspective drawings of 14 appear in Figures 1.13, 1.14, and 1.15 (53). Figure 1.13 displays the whole molecule showing the disposition of the phenyl rings around the cage structure. Figure 1.14 shows the cage structure with the phenyl groups omitted for clarity. Figure 1.15 views the molecule down a vector connecting the two phosphorus atoms. The CH_2N groups forming the bridges between the phosphorus atoms are skewed rather than planar as in 8 and 7. The PNCP torsion angles in 14 average 34.1° . It is interesting to note that 4 and 5 have twisted bridging groups with torsion angles of 20.0° and 18.6° , respectively, while the trivalent 3 has planar bridges. The source of the bridge twisting in 14, 4, and 5 is not clear.

The plane of each phenyl ring might be expected to bisect the HCH angle of the bridging methylene in order to minimize the steric interaction between the rings, but this is not the case. The phenyl groups are canted to one side to form a paddle wheel arrangement around the cage. The reason for this distortion is probably repulsion between the methylene protons and a phenyl proton. Calculations performed on the system assuming that the phenyl group bisects the HCH angle of a planar bridge indicate the H-H distance between the proton of C_{11} and methylene protons of C_1 would be 1.88 \AA , well within the sum of the Van der Waals radii of 2.4 \AA (54). Van der Waals repulsion between the methyl groups

Table 1.6. Final fractional coordinates of 14.

Atom	x	y	z
P(1)	0.8394(1)	0.6822(1)	0.9490(1)
P(2)	0.6668(1)	0.6049(1)	0.6821(1)
N(1)	0.7632(3)	0.6043(2)	0.9662(3)
N(2)	0.7074(3)	0.7269(2)	0.8397(3)
N(3)	0.9156(3)	0.6537(2)	0.8346(3)
C(1)	0.7176(4)	0.5558(2)	0.8472(4)
C(2)	0.6019(4)	0.6856(2)	0.7403(4)
C(3)	0.8342(4)	0.6389(2)	0.6918(4)
C(11)	0.7170(3)	0.5937(2)	0.0796(4)
C(12)	0.6984(4)	0.5241(2)	0.1192(4)
C(13)	0.6520(5)	0.5135(2)	0.2298(4)
C(14)	0.6269(5)	0.5697(2)	0.3025(4)
C(15)	0.6475(4)	0.6379(2)	0.2649(4)
C(16)	0.6911(4)	0.6500(2)	0.1525(4)
C(21)	0.6830(3)	0.7974(2)	0.8666(3)
C(22)	0.5548(4)	0.8229(2)	0.8464(4)
C(23)	0.5348(5)	0.8942(2)	0.8766(5)
C(24)	0.6420(5)	0.9390(2)	0.9279(5)
C(25)	0.7693(5)	0.9145(2)	0.9474(5)
C(26)	0.7913(4)	0.8447(2)	0.9152(4)

Table 1.6. (Continued)

Atom	x	y	z
C(31)	0.0524(3)	0.6579(2)	0.8676(4)
C(32)	0.1364(4)	0.6533(2)	0.0065(4)
C(33)	0.2754(4)	0.6601(2)	0.0400(4)
C(34)	0.3368(4)	0.6695(2)	0.9369(5)
C(35)	0.2523(4)	0.6720(2)	0.7998(5)
C(36)	0.1150(4)	0.6666(2)	0.7641(4)

Table 1.7. Final thermal parameters^a for 14

Atom	β_{11}	β_{22}	β_{33}	β_{12}	β_{13}	β_{23}
P(1)	0.0074(1)	0.0025(1)	0.0070(1)	-0.0003(1)	0.0018(1)	-0.0006(1)
P(2)	0.0096(1)	0.0032(1)	0.0082(1)	-0.0011(1)	0.0022(1)	-0.0016(1)
N(1)	0.0117(3)	0.0025(1)	0.0083(3)	-0.0008(1)	0.0040(3)	-0.0008(1)
N(2)	0.0078(3)	0.0026(1)	0.0094(3)	-0.0003(1)	0.0003(3)	-0.0010(1)
N(3)	0.0080(3)	0.0037(1)	0.0077(3)	-0.0005(2)	0.0029(3)	-0.0012(2)
C(1)	0.0142(6)	0.0027(1)	0.0099(4)	-0.0012(2)	0.0041(4)	-0.0013(2)
C(2)	0.0081(4)	0.0033(1)	0.0133(5)	-0.0006(2)	0.0007(3)	-0.0015(2)
C(3)	0.0098(4)	0.0038(1)	0.0079(4)	-0.0006(2)	0.0031(3)	-0.0012(2)
C(11)	0.0082(4)	0.0027(1)	0.0076(4)	0.0000(2)	0.0019(3)	0.0000(2)
C(12)	0.0145(5)	0.0028(1)	0.0109(5)	-0.0004(2)	0.0055(4)	0.0000(2)
C(13)	0.0174(6)	0.0034(2)	0.0118(5)	-0.0010(2)	0.0064(4)	0.0004(2)
C(14)	0.0159(6)	0.0043(2)	0.0104(5)	-0.0008(2)	0.0065(4)	0.0003(2)
C(15)	0.0126(5)	0.0037(1)	0.0105(5)	0.0007(2)	0.0047(4)	-0.0005(2)

^a β_{ij} are defined by: $T = \exp [-(h^2\beta_{11} + k^2\beta_{22} + l^2\beta_{33} + 2hk\beta_{12} + 2hl\beta_{13} + 2lk\beta_{23})]$.

Table 1.7. (Continued)

Atom	β_{11}	β_{22}	β_{33}	β_{12}	β_{13}	β_{23}
C(16)	0.0095(4)	0.0029(1)	0.0087(4)	0.0002(2)	0.0031(3)	-0.0002(2)
C(21)	0.0093(4)	0.0025(1)	0.0066(3)	-0.0002(2)	0.0018(3)	-0.0002(2)
C(22)	0.0096(4)	0.0031(1)	0.0099(5)	0.0004(2)	0.0016(4)	-0.0002(2)
C(23)	0.0141(6)	0.0033(1)	0.0129(5)	0.0020(2)	0.0033(5)	0.0001(2)
C(24)	0.1830(7)	0.0026(1)	0.0149(6)	0.0010(3)	0.0030(5)	-0.0001(2)
C(25)	0.0160(6)	0.0025(1)	0.0130(5)	-0.0018(2)	0.0030(5)	-0.0003(2)
C(26)	0.0106(5)	0.0029(1)	0.0094(4)	-0.0009(2)	0.0022(3)	0.0004(2)
C(31)	0.0073(4)	0.0026(1)	0.0100(4)	-0.0001(1)	0.0032(3)	-0.0004(2)
C(32)	0.0093(4)	0.0034(1)	0.0090(4)	0.0006(2)	0.0023(3)	-0.0002(2)
C(33)	0.0092(4)	0.0043(2)	0.0116(5)	0.0007(2)	0.0022(4)	-0.0006(2)
C(34)	0.0083(5)	0.0049(2)	0.0166(6)	-0.0001(2)	0.0044(4)	-0.0002(2)
C(35)	0.0167(4)	0.0034(1)	0.0130(6)	0.0002(2)	0.0053(4)	0.0003(2)
C(36)	-0.0103(4)	0.0030(1)	0.0103(5)	0.0003(2)	0.0055(4)	0.0003(2)

Table 1.8. Bond lengths between all nonhydrogen atoms of 14

Atoms	Bond Length (Å)
P(1)-N(1)	1.704(4)
P(1)-N(2)	1.708(4)
P(1)-N(3)	1.704(3)
P(2)-C(1)	1.852(4)
P(2)-C(2)	1.852(4)
P(2)-C(3)	1.845(4)
N(1)-C(1)	1.476(5)
N(2)-C(2)	1.469(5)
N(3)-C(3)	1.472(4)
N(1)-C(11)	1.412(4)
N(2)-C(21)	1.393(5)
N(3)-C(31)	1.382(5)
C(11)-C(12)	1.392(5)
C(12)-C(13)	1.387(7)
C(13)-C(14)	1.369(6)
C(14)-C(15)	1.366(5)
C(15)-C(16)	1.397(6)
C(16)-C(11)	1.375(6)
C(21)-C(22)	1.385(5)
C(22)-C(23)	1.397(5)
C(23)-C(24)	1.379(6)

Table 1.8. (Continued)

Atoms	Bond Length (Å)
C(24)-C(25)	1.377(7)
C(25)-C(26)	1.385(5)
C(26)-C(21)	1.414(5)
C(31)-C(32)	1.417(6)
C(32)-C(33)	1.392(6)
C(33)-C(34)	1.416(6)
C(34)-C(35)	1.409(6)
C(35)-C(36)	1.377(6)
C(36)-C(31)	1.414(6)

Table 1.9. Bond angles between nonhydrogen atoms of 14.

Atoms involved	Bond angle (°)
N(1)-P(1)-N(2)	100.3(2)
N(2)-P(1)-N(3)	99.6(2)
N(3)-P(1)-N(1)	98.2(2)
P(1)-N(1)-C(1)	118.8(3)
P(1)-N(2)-C(2)	118.6(3)
P(1)-N(3)-C(3)	119.6(3)
N(1)-C(1)-P(2)	111.9(2)
N(2)-C(2)-P(2)	112.1(3)
N(3)-C(3)-P(2)	111.3(3)
C(1)-P(2)-C(2)	98.4(2)
C(2)-P(2)-C(3)	98.5(2)
C(3)-P(2)-C(1)	97.3(2)
P(1)-N(1)-C(11)	120.6(2)
P(1)-N(2)-C(21)	120.4(2)
P(1)-N(3)-C(31)	120.1(2)
C(1)-N(1)-C(11)	119.2(3)
C(2)-N(2)-C(21)	119.0(3)
C(3)-N(3)-C(31)	119.0(2)
N(1)-C(11)-C(12)	119.5(2)
N(1)-C(11)-C(16)	120.9(2)

Table 1.9. (Continued)

Atoms involved	Bond angle (°)
C(11)-C(12)-C(13)	119.3(4)
C(12)-C(13)-C(14)	121.3(4)
C(13)-C(14)-C(15)	119.3(4)
C(14)-C(15)-C(16)	120.7(4)
C(15)-C(16)-C(11)	119.8(4)
C(16)-C(11)-C(12)	119.6(4)
N(2)-C(21)-C(22)	122.6(3)
N(2)-C(21)-C(26)	119.1(3)
C(21)-C(22)-C(23)	120.5(4)
C(22)-C(23)-C(24)	120.6(4)
C(23)-C(24)-C(25)	119.5(4)
C(24)-C(25)-C(26)	120.9(4)
C(25)-C(26)-C(21)	120.1(4)
C(26)-C(21)-C(22)	118.4(3)
N(3)-C(31)-C(32)	120.6(4)
N(3)-C(31)-C(36)	121.7(4)
C(31)-C(32)-C(33)	120.9(4)
C(32)-C(33)-C(34)	121.5(3)
C(33)-C(34)-C(35)	116.4(4)
C(34)-C(35)-C(36)	122.9(4)

Table 1.9. (Continued)

Atoms involved	Bond angle (°)
C(35)-C(36)-C(31)	120.6(3)
C(36)-C(31)-C(32)	117.6(4)

Figure 1.13. Perspective of 14 showing all atoms and
indicating the numbering scheme.

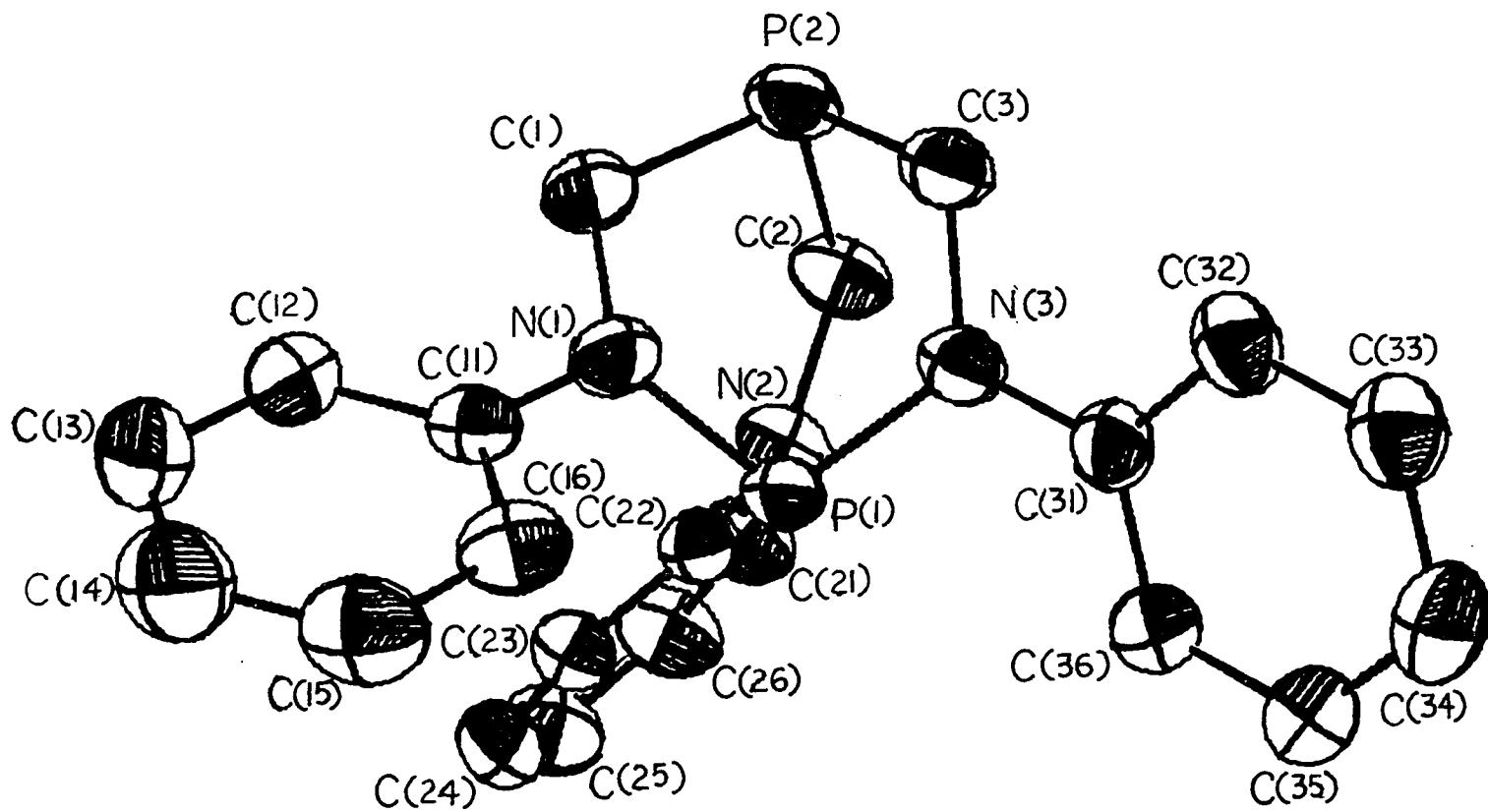


Figure 1.14. Perspective drawing of 14 excluding
the phenyl carbons for clarity

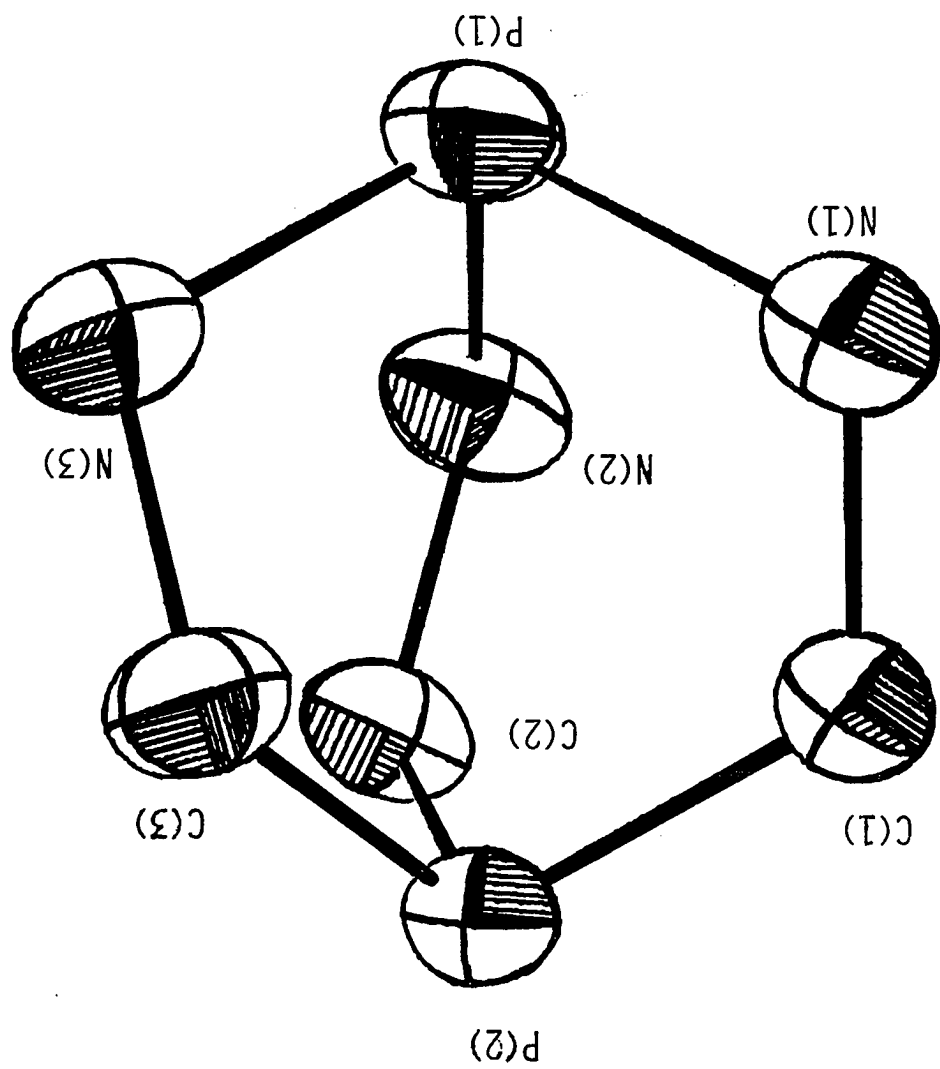
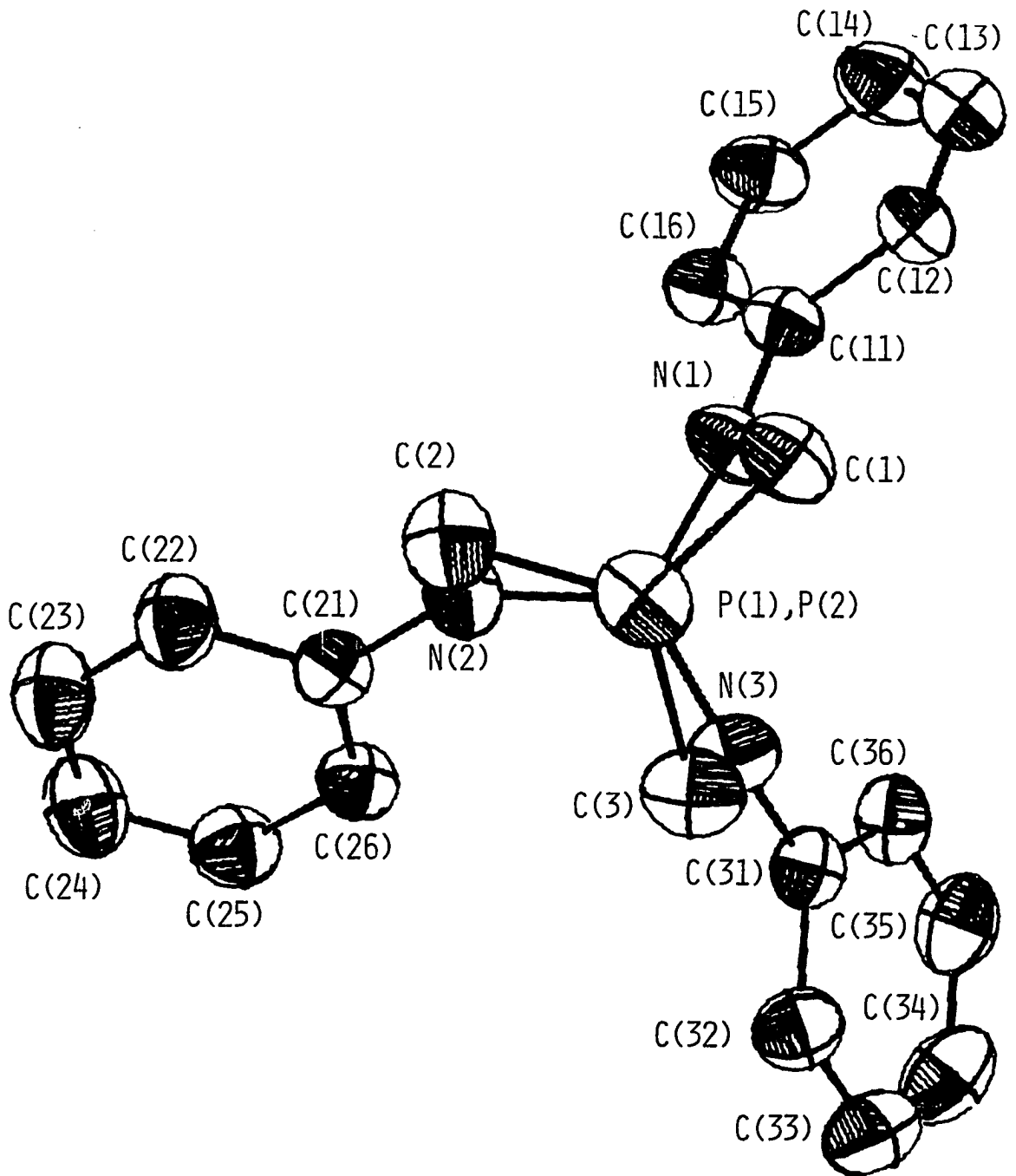


Figure 1.15. View of 14 down the P-P vector.
Note the twist of the bridging
groups



of 3, 4, and 5 are believed responsible for the deviation from planarity of the nitrogen atoms in these compounds (11). The rotation of the phenyl groups in 14 appears to be an energetically favored way to minimize repulsive intramolecular interactions.

The P-P distance of the 1,4-diphosphabicyclo[2.2.2]octane compounds for which structural data are available and 30 are compared to the 3.122 Å value for 14 in Table 1.10. All of the values in Table 1.10 are less than the sum of the Van der Waals radii of 3.8 Å (54) for two phosphorus atoms, but at the same time they are longer than the normal P-P single bond of 2.3 Å (54). The phosphorus atoms in these structures are certainly spatially oriented for possible through-space interaction, but the extent of this interaction is difficult to assess. The P-P distance in 14 is the longest of the cage structures in Table 1.10. The angles around tricoordinate phosphorus are smaller than in tetra-coordinate compounds, and phosphine angles are smaller than those in aminophosphines. The combination of a tricoordinate phosphine and aminophosphine in 14 therefore tends to push the bridgehead atoms of the cage away from each other.

The P-N bond lengths of numerous compounds have been recorded (11). These values range from 1.84 Å for the exocyclic P-N bonds of $(\text{Me}_2\text{N})_8\text{P}_4\text{N}_4$ to 1.49 Å for PN. The P-N bond length for phosphazenes, which are considered to have considerable double bond character, range from 1.51 to 1.66 Å. The 1.71 Å P-N bond in 14 is similar to the 1.70 Å reported for $\text{P}(\text{NMe}_2)_3$ and is longer than the 1.68 Å of 3 and 30. Thus,

Table 1.10. P-P separations of compounds for which structural data are available.

Compound	P-P Distance (\AA)
<u>29</u>	2.994
<u>2</u>	3.024
<u>3</u>	2.99
<u>4</u>	2.82
<u>5</u>	2.844
<u>14</u>	3.122
<u>30</u>	3.500

on the basis of this criterion the amount of P-N π - π bonding does not appear to be great in 14.

The average sum of the bond angles around the nitrogens of 14 is 358.4° which is well within the range (355 - 360°) suggested by Clardy *et al.* for classifying nitrogens with this geometry as trigonal planar (11). The CPC bond angle of 98.1° for 14 is only slightly larger than the 97.1° for the uncoordinated phosphine of 2 and the 97.6° in 29, all of which can be considered as normal phosphine angles (55). Compound 30 and 14 both have NPN bond angles of 99.4° , slightly smaller than the 100° average for 3. The tetracoordinate derivatives 4, 5, 7, and 8 have NPN angles between 102° and 105° showing the expected opening of the phosphorus angles upon coordination. This opening of the NPN angle causes a decrease in the endocyclic bond angle at nitrogen. The PNN bond angle of 3 (117°) is approximately 3° larger than in the derivatives 4 (113.6) and 5 (114). The 119.0° PNC angle of 14 is considerably larger than the tetracoordinate compounds 8 (114°) and 7 (116°). Oxidation of phosphorus in a cage phosphite ($\text{P}(\text{OCH}_2)_3\text{C}-\text{CH}_2\text{Br}$) to a phosphate ($\text{O} = \text{P}(\text{OCH}_2)_3\text{C}-\text{CH}_3$) causes a similar decrease in POC from 117.5° (28) to 115.1° (56).

It is concluded that the phosphorus atoms in the cage compounds 14, 15, and 16 have some properties which are different from acyclic phosphines and aminophosphines. In general, the ^{31}P chemical shifts of the trivalent cages are upfield from the analogous acyclic compounds. The resistance to oxidation of all three cages 14, 15, and 16, and

sulfuration and selenation of 16 may be due to the intramolecular electronic effects of the cage structure.

The signs and magnitudes of PP coupling constants for 1,4-diphosphabicyclo[2.2.2]octane compounds are very similar regardless of the nature of the bridging groups. The attractive rationalization of this phenomenon by direct through-space coupling of the phosphorus nuclei is presently impossible to verify.

The X-ray crystal structure determination of 14 reveals a P-P separation which is intermediate between a P-P single bond and the sum of the Van der Waals radii for two phosphorus atoms. The nitrogen atoms have the planar geometry favored by aminophosphines. The NPN and CPC angles are similar to those in acyclic compounds which is consistent with the "hinge effect" proposed for $OP(OR)_3$ systems (46) in which the angles of the bridging groups flex in preference to the angles around phosphorus.

PART II. ^{31}P NMR OF POLYCYCLIC PHOSPHORUS COMPOUNDS

INTRODUCTION

Theory of ^{31}P NMR Chemical Shifts

The NMR experiment involves placing a nucleus (which is a magnetic dipole) in a static magnetic field B_0 . The nucleus interacts with B_0 and acquires energy as expressed in the following equation.

$$E = -\mu B_0 \quad 2.1$$

Since the nucleus has angular momentum, it will align itself with respect to B_0 , but it will also precess at an angle θ about B_0 . The precession frequency, called the Larmor frequency, is defined in equation 2.2.

$$\omega_0 = \nu B_0 \quad 2.2$$

The proportionality constant, ν , is the magnetogyric ratio. If the frequency of an electric field normal to B_0 is the same as ω_0 , the nucleus will absorb energy and a signal will be detected and recorded by the spectrometer.

The electrons around the nucleus influence the field actually felt at the nucleus so that the Larmor frequency for nucleus x becomes:

$$\omega_x = \nu_x (1 - \sigma_x) B_0 \quad 2.3$$

where σ_x is the shielding constant for x. The general theory of magnetic shielding as applied to nuclear magnetic resonance was first developed by Ramsey (57). Saika and Slichter (58) suggested that

the screening expression, σ , could be subdivided into three contributions:

$$\sigma = \sigma^d + \sigma^p + \sigma^n \quad 2.4$$

where σ^d is a diamagnetic term arising from electron circulation induced by the magnetic field on the atom of interest, σ^p is a paramagnetic term which has its origin in the intrinsic angular momentum of nonspherical orbitals centered on the same atom, and σ^n is a term which includes both diamagnetic and paramagnetic screening contributions from all other atoms in the molecule.

Saika and Slichter found that the diamagnetic term for atoms reasonably larger than hydrogen makes a very minor contribution to the chemical shift. Rough calculations for the phosphorus atom estimate the contribution from the paramagnetic term to be ten to one-hundred times greater than that from the diamagnetic term. The shielding effects of electrons on neighboring atoms fall off as a function of $1/r^3$ and were discounted in the calculations of Saika and Slichter. Since the core electrons of neighboring atoms are not easily polarized and the valence electrons are only partially associated with the atom of interest, the effect of both groups of electrons are minimized. The paramagnetic term for neighboring atoms can become important for phosphorus when it is bonded to atoms with many core electrons such as metals (59) but this contribution is small for organophosphorus compounds. Therefore, it is generally accepted that the only term of importance is the paramagnetic contribution from electrons in the

valence-state orbitals associated with the atom in question. In an LCAO-MO treatment by Pople (60), the paramagnetic term is approximated by equation 2.5:

$$\sigma_p = (-e^2 \hbar^2 / 2m^2 c^2) 1/\Delta E \langle 1/r^3 \rangle \sum_B Q_{AB} \quad 2.5$$

where ΔE is an average excitation energy, $\langle 1/r^3 \rangle$ is the average value of the non-s-orbital radius, and the Q_{AB} 's are the elements of the "charge density bond order" matrix of the LCAO molecular orbitals.

Letcher and Van Wazer have formulated the only quantum mechanical treatment of the ^{31}P NMR chemical shift (32). In their analysis, the NMR chemical shift, δ_o , can be expressed as follows:

$$\delta - \delta_o = -(2e^2 \hbar^2 / 3\Delta m^2 c^2) [\langle r^{-3} \rangle_p \xi_1 + \langle r^{-3} \rangle_d \xi_2] \quad 2.6$$

or

$$\delta - \delta_o = B \xi_1 + Bf \xi_2 \quad 2.7$$

$$\text{where } B = (-2e^2 \hbar^2 / 3\Delta m^2 c^2) \langle r^{-3} \rangle_p \quad 2.8$$

$$\text{and } f = \langle r^{-3} \rangle_d / \langle r^{-3} \rangle_p \quad 2.9$$

The constants e , h , m , and c have their normal meanings. The mean excitation potential, Δ , and the average value of the non-s-orbital radius, r^{-3} , may vary from molecule to molecule, but Letcher and Van Wazer chose to assume that the value for B remains constant within a group of compounds in which the coordination number of the phosphorus remains constant. The basis for this assumption is not clear. The

values of f may be estimated from atomic spectral data and are constant for a given coordination number.

The ξ_1 and ξ_2 terms are expressions which attempt to determine the elements of the charge-bond-order matrix by relating a physical observable to a function of the orbital occupation numbers.

Unfortunately, there is no physical observable which properly relates these entities. Letcher and Van Wazer have resorted to the Coulson-modified (61) Pauling definition of the ionic character of a bond between two atoms, h_z , and a function of the bond angles around phosphorus, μ :

$$\xi_1 = (6 - 6h_z + 3/2h_z^2) - \mu (6 - 9h_z + 3h_z^2) \quad 2.10$$

$$\text{where } h_z = 1.0 + 0.16 (\chi_z - \chi_p) + 0.035 (\chi_z - \chi_p)^2 \quad 2.11$$

$$\text{and } \mu = 1/(1 - \cos\theta) \quad 2.12$$

In 2.12, θ is the Z-P-Z angle determined from diffraction experiments.

χ_z and χ_p are the Pauling electronegativities of Z and phosphorus, respectively. ξ_2 describes the contribution from the d orbitals and is reasonably approximated by the linear function:

$$\xi_2 = A \gamma_6^2 \quad 2.13$$

where A is a constant equal to 16.8 and γ_6^2 is the occupation number for the π orbitals.

Although NMR chemical shifts can be related to electronegativity of substituent atoms, the Pauling numbers apply to bonds between two

atoms of a diatomic molecule and, therefore, cannot accurately describe phenomena of polyatomic molecules. Letcher and Van Wazer did attempt to use group electronegativities (32), but values for only a limited number of substituents are available (62).

The inadequacy of the electronegativity part of the Letcher and Van Wazer approach sometimes causes exaggeration of the bond angle effect. For example, when ethoxy groups of $P(OCH_2CH_3)_3$ are replaced by other alkoxy groups (63), it was claimed that a 10 ppm shift in the ^{31}P NMR spectrum was caused by a 0.25° change in the O-P-O bond angle θ . Haemers *et al.* (64) question the physical significance of an angular difference of 0.2° between two compounds for the discussion of NMR parameters. The NMR experiment reflects average geometries and is an average value of all of the vibrational states. Even in the lowest state, the vibrational zero point energy (or the Heisenberg uncertainty principle) introduces a probability function for the angular value, and thus leads to an uncertainty in θ . Figure 2.1 shows a semi-classical approach for visualizing this uncertainty. The parabola describes

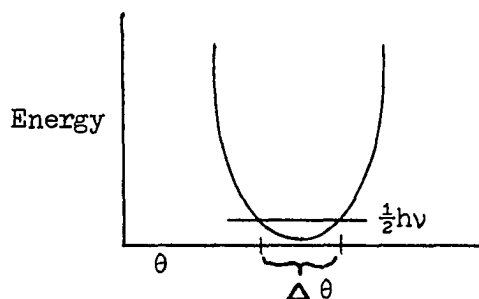


Figure 2.1. Uncertainty of θ

the harmonic motion of the O-P-O vibration which fits the equation $E = k/2 (\theta - \theta_0)^2$. The two abscissas of the interaction points of a horizontal line having the ordinate $\frac{1}{2} h\nu$ with the parabola, yield the upper and lower limits of the θ uncertainty. In the case of the O-P-O angle, θ varies between $\theta_0 + 3.9^\circ$ and $\theta_0 - 3.9^\circ$. In view of this uncertainty in θ (θ being $\theta_0 \pm \theta$), the physical significance of a so-called $\Delta \theta$ of 0.2° is not clear. Only a $\Delta \theta_0$ has a physical significance, but to obtain a true $\Delta \theta_0$ it is not only necessary that the relation between σ and θ be strictly linear (which seems to be the case in the Van Wazer theory) but also the vibrational motion must be harmonic. This is certainly not the case for the low frequency O-P-O bending mode ($\sim 290\text{cm}^{-1}$) (65). Another example of an improper prediction by the Letcher and Van Wazer theory is the predicted value of the C-P-C bond angles in tri (t-butyl) phosphine. While the theory predicted a bond angle of 105.7° (66), the crystal structure determination (67) revealed angles of 109.9° .

Grim and co-workers (68) have developed an empirical method of calculating ^{31}P chemical shifts of phosphines and phosphonium salts using the concept of additive group contributions (GC) to the chemical shift. The relationship is expressed by equation 2.14.

$$\delta = A - B \sum \text{GC} \quad 2.14$$

A and B are constants for each type of phosphine (primary, secondary, or tertiary) or phosphonium salt. The GC for alkyl groups can be

calculated using formula 2.15:

$$GC = 21 - 14 \beta_c + 3 \gamma_c \quad 2.15$$

where β_c and γ_c are the number of beta and gamma carbons in the group. These group contributions are probably a combination of the electronegativity of the group along with its steric requirements and its ability to interact with the phosphorus through hyperconjugation (68).

It has been proposed (69) that the same phenomena which control ^{13}C chemical shifts also control the ^{31}P chemical shifts for trivalent phosphorus. Cheney and Grant (69) have published a series of papers using a valence-bond formulation to derive the ^{13}C chemical shifts. This theory explains changes in the chemical shift in terms of type and proximity (α , β , or γ substitution) of groups to the carbon atom of interest. The two most important factors in explaining these substituent effects are the orbital radii (the $\langle 1/r^3 \rangle$ integrals of equation 2.5) and the effective nuclear charge of the orbitals, ϵ_a . The orbital radius is related to the orbital effective nuclear charge by:

$$\langle 1/r^3 \rangle_a = \epsilon_a^3 / 24 \quad 2.16$$

The orbital effective nuclear charge is defined as:

$$\epsilon_a = \epsilon_0 B' - S \sum_{b \neq a} q_b \quad 2.17$$

where ϵ_0 is the atomic effective nuclear charge obtained from Slater's rules, B' is a parameter accounting for changes in the effective

nuclear charge due to bond formation, S is the Slater screening factor, and q_b is the ionic charge in orbital b . Note that q_b is a function of the electronegativity of the atoms involved in bond formation, and therefore suffers one of the same problems found in the Letcher and Van Wazer theory.

Substitution of a more electronegative group for a less electronegative group next to the atom of interest causes a downfield movement in the chemical shift. This "alpha" effect is due to removal of electron density from the atom of interest, thus increasing the effective nuclear charges of the remaining orbitals. The resultant contraction of the orbitals is reflected in the shielding (σ_p of equation 2.5) by the enlarged $\langle 1/r^3 \rangle_a$ term.

Substitution at the β position also causes a downfield movement in the chemical shift. The nature of this "beta" effect is not as clear as the alpha effect. Grant's theory predicts that the inductive ability (electronegativity) of the β substituent is not transmitted through the alpha position, and thus has little effect on the shielding. Similarly, delocalization via hyperconjugation, as suggested by Grim et al. (68) cannot account for the magnitude of the observed β effect. Grant proposes a steric interaction between the β group and the atom of interest which causes a slight contraction of the orbitals on that atom. Such an effect may be reflected in the B' parameter used to calculate the effective nuclear charges (equation 2.17). Only a small variation in this parameter is needed to account for observed β shifts.

An upfield movement is noted in the chemical shift of carbon atoms upon substitution in the gamma position. This shift can be explained for alkanes (69) by a slight charge polarization in the H-C bond when a proton on the carbon of interest is in the vicinity of a proton on the gamma group as in Figure 2.2.

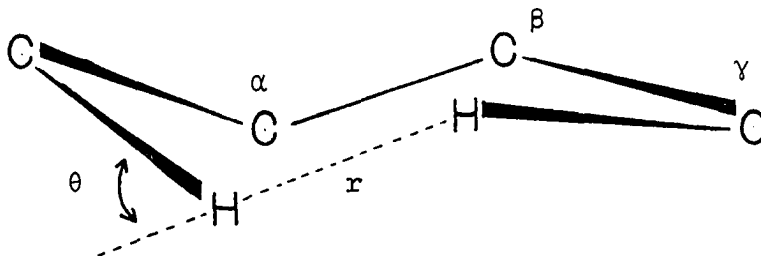


Figure 2.2 Steric γ effect

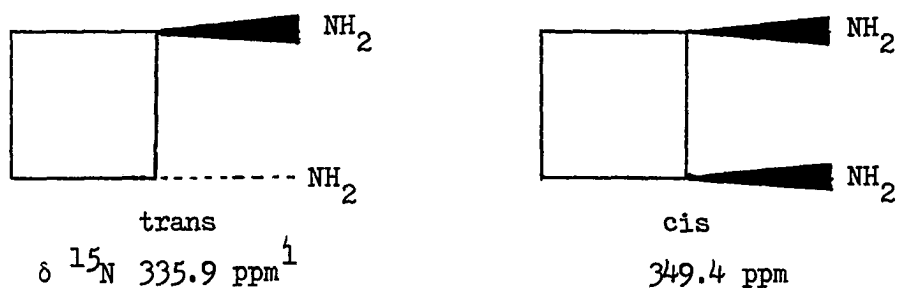
This transfer of electron charge is due to the nonbonded repulsion existing between electrons centered on the proximal hydrogens. The size of the change in the chemical shift is a function of r and θ in Figure 2.2 and can be calculated using equation 2.18.

$$\delta^{13}\text{C} = +1680 \cos \theta \exp(-2671 r) \quad 2.18$$

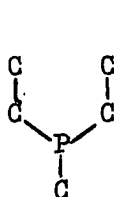
The calculated value of +1.8 ppm shift for a rotating n-butane system agrees reasonably well with the experimental +2.9 ppm (69).

Quin *et al.*, found the steric γ effect in phosphorus compounds of the type $\text{X}_2\text{P n-Bu}$ ($\text{X} = \text{alkyl, Cl, or OMe}$) in both the ^{31}P and ^{13}C spectra to range between +0.5 and +1.5 ppm (70). A combination of steric and electronic effects of the substituents were used by Lichter and

Roberts (71) to explain the difference in chemical shift between cis- and trans-1,2-diamino-cyclobutane.

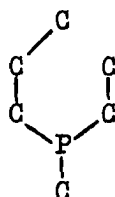


A steric γ effect was also postulated by Quin and Breen (72) for the 20 ppm variation of $\delta^{31}\text{P}$ in the series 64-66. As will be seen in



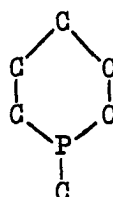
64

-34 ppm



65

-39 ppm (calcd)



66

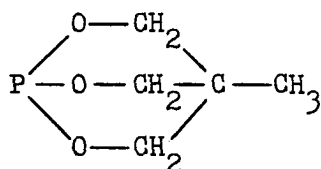
-53.7 ppm

the following discussion, this interaction may be a combination of steric and electronic effects.

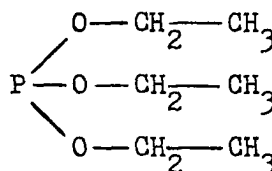
¹Chemical shifts relative to 10 M Nitric Acid.

Orbital Interactions of Cage Compounds

When a phosphorus atom is constrained into a cage-like structure such as compound 59, the $\delta^{31}\text{P}$ value is shifted upfield from the acyclic analogues e.g., 58 (73).

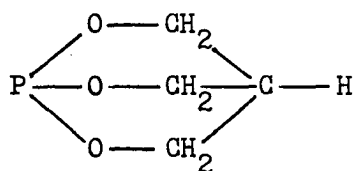
59

$$\delta^{31}\text{P} = 91.5$$

58

$$\delta^{31}\text{P} = 137.0$$

A through-space interaction of the nonbonding lobes of orbitals of similar energy on the bridgehead carbon and phosphorus atoms of 60 has been proposed to explain the large four-bond spin-spin coupling constant (${}^4J_{\text{POCCH}} = 7.2 \text{ Hz}$) in 60 (43). It was also noted, however, that 60 has three routes for transfer of coupling information in the

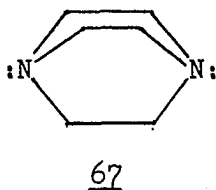
60

cage structure (43). Both the through-space and the through-bond mechanisms postulated for this phenomenon would lead to delocalization

of the electron density in the phosphorus lone pair orbital.

Delocalization of the phosphorus lone pair could account for the upfield ^{31}P shift noted for 60 since the resulting lone pair orbital radius increase would cause a decrease in the $(1/r^3)$ value used to calculate the NMR shielding parameter σ_p . The decrease in σ_p in turn would produce an upfield shift in the NMR resonance signal (69).

The interaction of the nitrogen lone pairs of 1,4-diazabicyclo [2.2.2]octane 67 has been extensively studied (74, 75, 76, 77) and these investigations may serve as a model for phosphorus cage



compounds. The lone pairs of 67 can interact by either a through-space or a through-bond mechanism.

The through-space interaction is a direct overlap of the two lone pair orbitals (Figure 2.3).

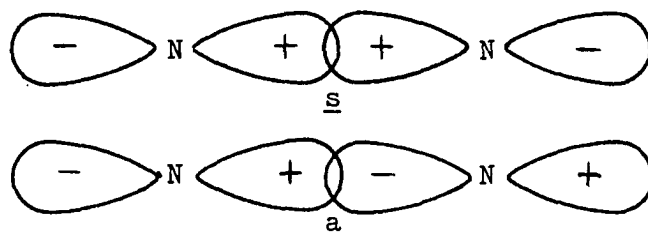


Figure 2.3 Interaction of N lone pairs of 67

This interaction results in a symmetric, s, and an antisymmetric, a, combination of orbitals. Since the a combination contains a node, it would be assumed to have a higher energy than the s combination. It has been found (74), however, that when the overlap integral is small (as it is in 67), the sign of the interaction is sensitive to very small geometrical changes and to the type of semi-empirical SCF model (e.g. SPINDO, MINDO/2, CNDO/2) used for the M.O. calculation. Using the MINDO/2 model, the through-space interaction of the nitrogen lone pairs causes a 0.28eV difference between s and a with a having the lower energy.

The through-bond mechanism requires that both lone pairs interact with another orbital which acts as a "relay" orbital. The symmetry of 67 is D_{3h} (78) so the s combination of the nitrogen lone pairs is included in the A_1 irreducible representation while the a combination fits the A_2 irreducible representation. Also included in the A_1 set are three symmetry-adapted linear combinations of molecular orbitals (SLMO's) derived from the C-C, C-N and C-H bonds of the cage. The A_2 set contains SLMO's from combinations of C-N and C-H orbitals. When all orbitals of appropriate symmetry are allowed to mix, it is found that s interacts strongly with the C-C sigma bond while a interacts almost as strongly with the C-N orbitals. Both s and a interact to a smaller extent with the C-H bonds. The effect on the energies of the orbitals due to the through-space and through-bond interactions for 67 is shown in Figure 2.4.

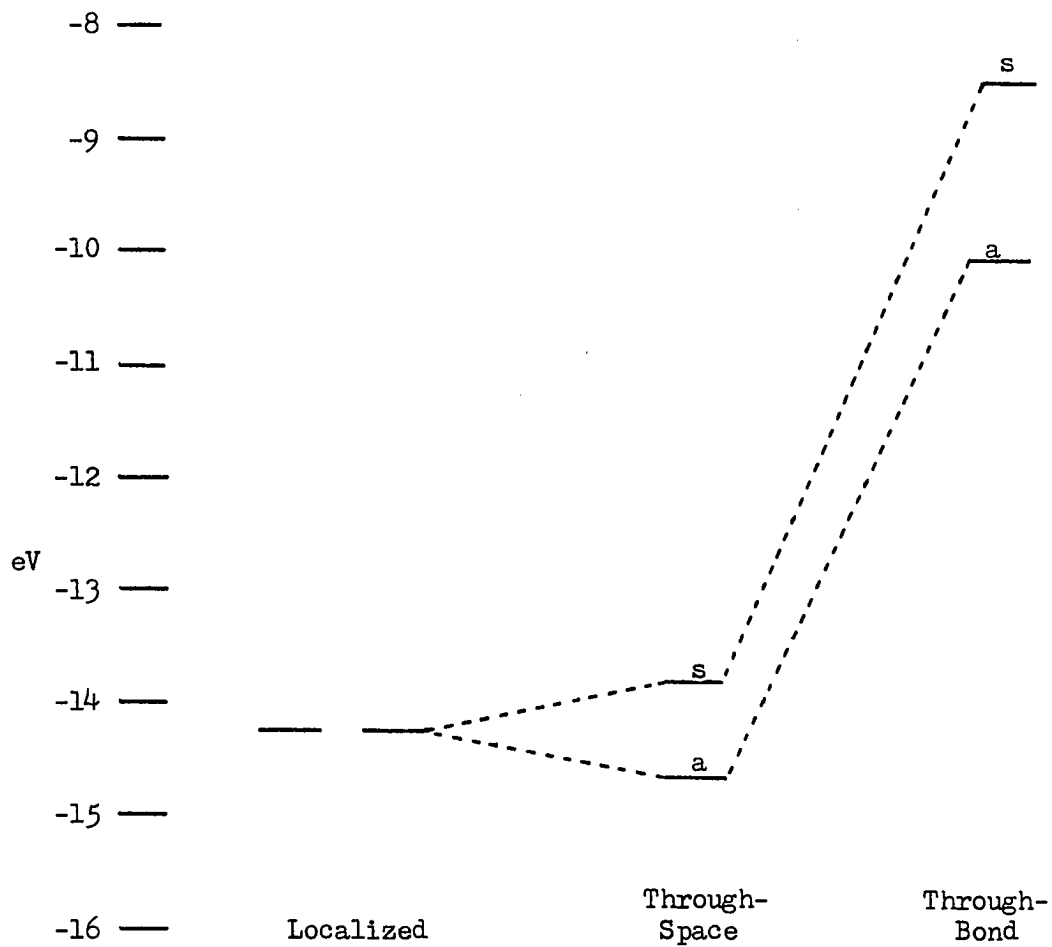
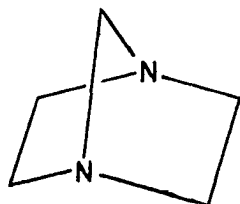
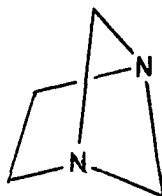
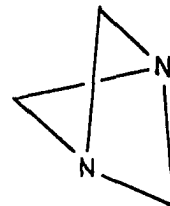


Figure 2.4. Energy diagram for the interaction of nitrogen lone pairs in 67

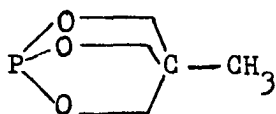
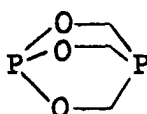
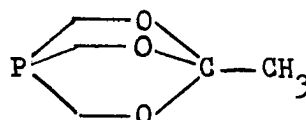
The destabilization of 5.52eV and 4.00eV for s and a, respectively, for the through-bond interaction compared to the 0.14eV destabilization of s and 0.14eV stabilization of a from the through-space interaction demonstrates the dominance of the through-bond mechanism for the bicyclo[2.2.2]octane structure.

According to Hoffmann *et al.* (77) two-atom bridges optimize the through-bond mechanism but as one-atom bridges replace the two-atom bridges as in 67-70, the through-bond mechanism becomes less efficient while the through-space mechanism becomes more efficient. Calculations (77) predict the through-space interaction of the lone pairs of 70 to be

686970

similar in magnitude to the through-bond interaction of 67 while both the through-space and through-bond interactions in 68 and 69 are substantially less due to inefficient coupling mechanisms.

A preliminary report of calculations done on the phosphorus cages 59, 1, and 45, indicates that both the through-space and the

59145

through-bond mechanisms are of importance (42). It also seems that the phosphorus-carbon bridgehead interactions are stronger than the phosphorus-phosphorus interaction.

Roberts has postulated a through-space interaction as the cause of an upfield shift in the ^{13}C NMR of carbons in some norbornyl derivatives (79). Roberts found that when a substituent (X) was placed at the 2 position of the norbornane structure, (Figure 2.5) the α effect discussed by Cheney and Grant (69) was seen at atom 2 and a β effect was noted at the 1 and 3 positions. The steric γ effect caused by X was seen in the chemical shift of carbon 6 when X was in the



Figure 2.5. γ interactions of norbornyl systems

endo position (Figure 2.5a), but when X was in the exo position (Figure 2.5b), carbon 7 showed this steric effect. In addition, with X in the exo position there was an effect at carbon 6 which was not related to the steric size of the substituent but rather to its electronegativity. This led Roberts to postulate an interaction of the back lobes of the σ bonding orbitals of carbons 2 and 6.

A similar electronic γ effect may be responsible for the transmission of the inductive effect of X observed in the ^{19}F NMR of

4-substituted γ -fluorobicyclo[2.2.2.]octanes as the X group is varied
(Table 2.1) (80).

Table 2.1. Remote substituent effect on $\delta^{19}\text{F}$ of 1-fluoro bicyclo[2.2.2.]octanes



<u>4-Substituent</u>	<u>Substituent Chemical Shift</u>
H	0.00
CO ₂ Et	+4.47
F	+9.23

Eliel et al. have postulated a hyperconjugative interaction to rationalize the upfield shift of the resonance for γ carbon atoms which are anti-periplanar to N, O, or F substituents (81). A lone pair of the substituent interacts with the C _{α} - C _{β} sigma bond which in turn interacts with a bonding orbital on the γ carbon (Figure 2.6).

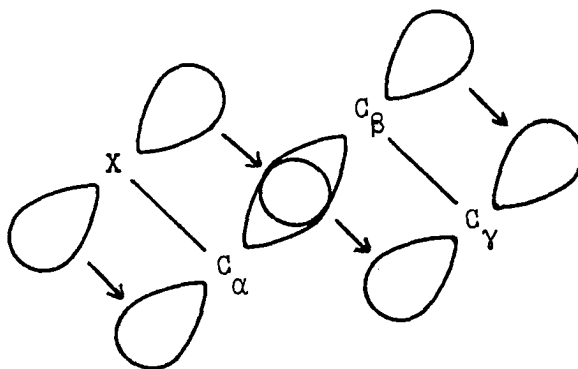
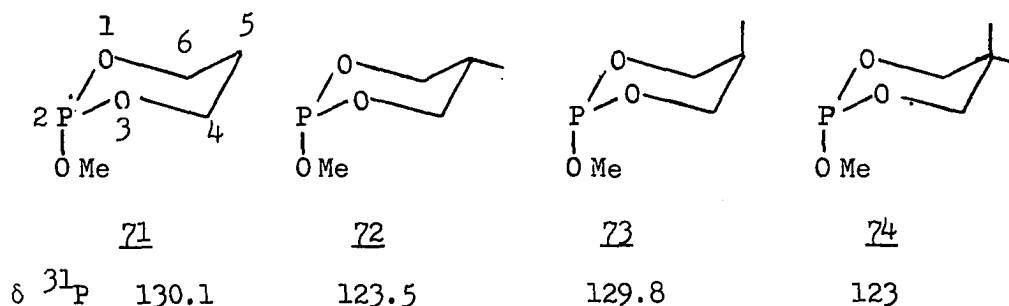


Figure 2.6 Hyperconjugative interaction of lone pair electrons with the γ carbon

The magnitude of the interaction is reduced when the stereochemical orientation is gauche or when the X substituent is a third-row element such as S or Cl. The larger orbital radii of third-row substituents compared to the second-row elements may lead to less favorable overlap with the carbon orbitals.

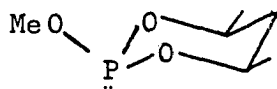
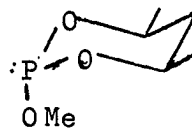
Haemers et al. have found that the effect on the ^{31}P chemical shift of adding a methyl group at the 5-position of compound 71 is stereospecific (64). The shift difference between 71 and 72 is



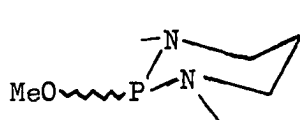
6.6 ppm while that between 71 and 73 is negligible. In these same compounds and in 74, the $^4J_{\text{PC}}$ coupling is also stereospecific (the coupling to the equatorial carbons being between 1 and 2 Hz while the axial carbon-to-phosphorus coupling is unobserved).

White et al. (82) rationalized the difference in $\delta \ ^{31}\text{P}$ between 71 and 74 to a narrowing of the O-P-O angle in response to the decrease in the C-C-C angle on alkyl substitution of hydrogens on

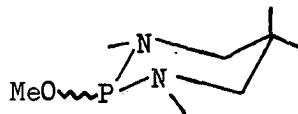
C(5). Another possible explanation for the stereospecific changes of chemical shift and coupling constant involves either a through-bond or through-space interaction of the phosphorus lone pair and back lobes of the exocyclic bonds of C(5). In the chair conformation adopted by the six-membered rings, the equatorial orientation of the phosphorus lone pair and the C(5) bonding orbital would provide the proper symmetry for maximum orbital interaction with each other as well as the σ framework of the ring. The preferred axial orientation of OMe at phosphorus provides an equatorial lone pair in 71 - 74. Compounds 72 and 74 have equatorial methyl groups and exhibit the upfield shift expected on energetic grounds; thus, the methyl C-C σ bond is closer in energy to that of the C-O σ , C-C σ , and phosphorus lone pair, than is the C(5)-H σ bond and so the mixing of the C-C bond with the other bonds in the system would be greater than that for C(5)-H σ . The larger $^4J_{PC}$ coupling of the methyl carbon can also be explained by the increased orbital interaction. When the stereochemistry at phosphorus is changed by converting the axial lone pair in compound 75 to equatorial in 76, the increased interaction of the equatorial lone pair is manifested in a 4.3 ppm upfield shift (64).

75 $\delta = 131.5$ 76 $\delta = 127.2$

A similar effect of 5,5-dimethyl substitution on $\delta^{31}\text{P}$ was seen in N,N -dimethyl-2-phospha-1,3-diazocyclohexanes 77 and 78 (83). It was postulated that 77 might have one N-methyl axial and the other

77 $\delta^{31}\text{P}$

131.6

78

122.6

equatorial while the 5,5-dimethyl substituents strongly favor diequatorial N-methyls for 78. The $^3J_{\text{PH}}$ coupling constants and ^{31}P NMR chemical shifts did not support this hypothesis so the interaction of the phosphorus lone pair with the C(5) bonding orbitals previously discussed for 2-phospha-1,3-dioxacyclohexanes appears to be the best explanation for the change in $\delta^{31}\text{P}$ upon 5,5-dimethyl substitution.

Electronegativity Considerations

It is evident from the previous discussion that both the Letcher - Van Wazer theory and the Grant theory of NMR chemical shifts suffer from the inability to describe mathematically the polarity of the bonds between atoms. While an electronegativity-type function is needed for the substituents bonded to the atom of interest, this function should reflect the inductive nature of the substituent group as a whole. A step in this direction was taken by Huheey (84) when he extended the work of Hinze and Jaffe' (85) and Mulliken (86) on the concept of orbital electronegativity. Mulliken suggested that the attraction

of an atom for electrons should be the average of the ionization energy and the electron affinity of the atom. Mulliken electronegativities can be estimated with equation 2.19:

$$\chi_M = 0.168 (IE + EA - 1.23) \quad 2.19$$

where the valence state ionization energy (IE) and the electron affinity (EA) are in electron volts. This formulation allows consideration of hybridization effects by using valence state ionization energies and electron affinities which are adjusted for the promotional energy from the ground state.

Jaffé proposed that the electronegativity is a function not only of hybridization but also of charge (85). A plot of the ionization energies against electron affinities for an element gives a curve approximated by the quadratic 2.20:

$$E = \alpha q + \beta q^2 \quad 2.20$$

where E is the total energy of the atom and q is the ionic charge. The slope of the curve dE/dq has been suggested (87) as a measure of the electronegativity. For the neutral atom this corresponds exactly to the Mulliken definition of electronegativity as a function of charge:

$$\chi = \frac{dE}{dq} = \alpha + 2\beta q \quad 2.21$$

which may be expressed in terms of partial charge (δ) instead of ionic charge (q) and the constants may be changed for convenience ($a = \alpha$ and $b = \beta$) so that:

$$\chi = \frac{dE}{dq} = a + b\delta \quad 2.22$$

The inherent or neutral-atom electronegativity of an atom is given by a . This is the electronegativity of a particular valence state as estimated by the Mulliken method. The parameter b may be termed the charge coefficient and measures the rate of change of electronegativity with charge. Large, soft atoms have low values of b while small, hard atoms tend to have higher values.

Sanderson (88) has suggested that when a bond forms between two atoms, electron density will shift from one atom to the other until the electronegativities have become equalized. Initially, the more electronegative element will have a greater attraction for electrons, but as the electron density shifts toward that atom in bond formation, it will become negative and tend to attract electrons less. Conversely, the atom which is losing electrons becomes somewhat positive and attracts electrons better than it did when neutral. This process will continue until the electronegativities have been equalized and charge transfer will cease:

$$\chi_A = a_A + b_A \delta_A = \chi_B = a_B + b_B \delta_B \quad 2.23$$

For a group such as $-W \begin{matrix} \swarrow X \\ \searrow Y \end{matrix}$, Huheey (84) found that equations 2.24-2.27 could be used to obtain equation 2.28.

$$a_W + b_W \delta_W = a_X + b_X \delta_X = a_Y + b_Y \delta_Y \quad 2.24$$

$$\delta_W + \delta_X + \delta_Y = 0 \text{ (radical)} \quad 2.25$$

$$\delta_W + \delta_X + \delta_Y = 1 \text{ (cation)} \quad 2.26$$

$$\delta_W + \delta_X + \delta_Y = -1 \text{ (anion)} \quad 2.27$$

$$\chi_{WXY} = \frac{a_W b_X b_Y + a_X b_W b_Y + a_Y b_W b_X + b_X b_Y b_W \delta_{WXY}}{b_X b_Y + b_W b_X + b_W b_Y} \quad 2.28$$

Similar equations can be derived for other geometries. Group electronegativities calculated for the group attached to phosphorus might be expected to provide a more sensitive measurement of the substituent inductive effect than the more rigid Pauling numbers.

The purpose of the present work is twofold. First, the NMR chemical shift values of the bridgehead atoms of bicyclic phosphorus molecules will be compared to the chemical shifts of the same atoms in analogous acyclic systems in an attempt to determine if molecular orbital interactions favored by physical constraint imposed by the bicyclic structure can account for upfield chemical shifts of the interacting atoms. Secondly, the ^{31}P NMR chemical shifts of a series of compounds having the structure $\text{P}(\text{CH}_2\text{NR}_1\text{R}_2)_3$ determined herein will be compared. If the ^{31}P NMR chemical shifts of these compounds


were predicted by the Letcher and Van Wazer theory, it would be assumed that pi bonding would be negligible and the electronegativity of the atoms bonded to phosphorus would not change. Thus, the only factor which should affect the chemical shift would be the bond angles around phosphorus. The methods of Huheey (84) will be used to calculate the group electronegativity of the $(-\text{CH}_2\text{NR}_1\text{R}_2)$ groups bonded to phosphorus so that the effect of group electronegativity on the ^{31}P chemical shift can be compared to the structural effects suggested by Letcher and Van Wazer.

EXPERIMENTAL

Techniques

Materials

All solvents were reagent grade or better. Benzene was dried by refluxing with and distilling from NaK alloy. Methanol was dried by refluxing with and distilling from CaH_2 .

The $\text{HN}(\text{n-Bu})_2$, $\text{H}_2\text{N}(\text{n-Bu})$, HNEtPh , $\text{CH}_3\text{C}(\text{OEt})_3$, and $\text{CH}_3\text{C}(\text{CH}_2\text{OH})_3$ were obtained from Aldrich Chemical Co. and were used as received. The HNMe_2 (40% in H_2O) was attained from J. T. Baker Co. Eastman chemicals was the source of HNMePh and $\text{P}(\text{OMe})_3$. Trimethyl phosphite was refluxed over sodium and vacuum distilled immediately before use. The HNEt_2 , HNPh_2 , H_2NPh , and HN  were acquired from Fisher Chemical Co. Mallinckrodt Chemical Co. was the source of piperidine and PCR Chemicals Inc. supplied $\text{CH}_3\text{Si}(\text{OMe})_3$.

The $\text{P}(\text{CH}_2\text{OH})_4\text{Cl}$ was obtained as an 85% solution from ROC/RIC. It can be converted to a hygroscopic crystalline solid by the following procedure. Most of the water is removed by azeotropic distillation with 1-propanol. The remaining oil is further dehydrated with 2,2-dimethoxypropane (Aldrich). The solid $\text{P}(\text{CH}_2\text{OH})_4\text{Cl}$ is then recrystallized from 2-propanol.

NMR spectroscopy

Proton NMR spectra were obtained on either a Varian HA-100 or an A-60 spectrometer using CDCl_3 or $(\text{CD}_3)_2\text{CO}$ as solvent. Me_4Si was used

as an internal standard and it served as the internal lock for the HA-100 instrument.

^{31}P NMR spectra were obtained on solutions in 10 mm tubes with a Bruker HX-90 spectrometer operating at 36.434 MHz in the Fourier transform (FT) mode while locked on the ^2H resonance of the deuterated solvent. The external standard was 85% H_3PO_4 contained in a 1 mm capillary tube held coaxially in the sample tube by a Teflon vortex plug. The spectrometer was interfaced with a Nicolet Instruments 1080 minicomputer system. Negative shifts are upfield from H_3PO_4 .

^{13}C NMR spectra were obtained on the Bruker HX-90 spectrometer operating at 22.63 MHz in the FT mode locked on the solvent ^2H resonances. The solvent carbons were used as references.

^{29}Si NMR spectra were also obtained on the Bruker HX-90 spectrometer operating at 17.88 MHz in the FT mode and locked on the solvent ^2H resonances. $\text{Si}(\text{OEt})_4$ was used as internal standard and $\text{Cr}(\text{acac})_3$ was added as a paramagnetic impurity to decrease the T_1 times and allow faster data collection. Pulse-modulated proton wide-band decoupling was used to obtain proton decoupled spectra while suppressing the Nuclear Overhauser Effect (89).

Mass spectrometry

Mass spectra were obtained on an AEI MS-902 high-resolution mass spectrometer. Exact masses were obtained by peak matching.

Preparation of compounds

$P(CH_2O)_3$, 31 This compound was prepared by the method of Vande Griend (2) which is a modification of the procedure given by Rathke et al. (90).

$P(CH_2NMe_2)_3$, 31 This compound was prepared according to the method of Coates and Wilson (15). Purification by vacuum distillation gave pure product in 86% yield ($b_{0.2} = 59-61^\circ$; lit. $b_{0.4} = 65-67^\circ$ (15)); 1H NMR ($(CD_3)_2CO$) 2.31 (s, 6H, Me), 2.59 (d, 2H, $J = 3$ Hz, PCH_2N); mass spectrum, m/e for P^+ 205.17079 measured, 205.17079 calculated).

$P(CH_2NEt_2)_3$, 32 This phosphine was prepared using a method analogous to the preparation of 31. Vacuum distillation produced pure 32 in 8% yield ($b_{0.05} = 108-109^\circ$; lit. $b_{0.2} = 131^\circ$ (15)); 1H NMR ($CDCl_3$), 1.05 (t, 3H, $J = 7.0$ Hz, CH_3), 2.62 (q, 2H, $J = 7.0$ Hz, NCH_2C), 2.70 (d, 2H, $J = 3.0$ Hz, PCH_2N)).

$P(CH_2N\text{-}n\text{-Bu}_2)_3$, 33 This compound was prepared by the method of Coates and Wilson (15). Purification by vacuum distillation was unsuccessful due to thermal decomposition of the product. All volatile impurities were removed by dynamic vacuum (6 hrs.) leaving 33 as a colorless liquid (68% yield, 1H NMR ($CDCl_3$) 0.70-1.75 (m, 14H, $CCH_2CH_2CH_3$), 2.53 (br t, 4H, $^3J_{HH} = 7.0$ Hz, NCH_2C), 2.74 (br d, 2H, $^2J_{PH} = 2.5$ Hz, PCH_2N)).

$P(CH_2N(H)n-Bu)_3$, 34 This compound was prepared and purified in the same manner as compound 33. (78% yield, 1H NMR ($CDCl_3$) 0.68-1.63 (m, 7H, $CCH_2CH_2CH_3$), 2.19-3.68 (m, 5H, $PCH_2N(H)CH_2$); mass spectrum m/e for P^+ - H_2NBu 216.17545 measured, 216.17554 calculated).

$P(CH_2N\text{---}O)_3$, 35 This compound was prepared in the same manner as compound 33. As with compound 33, thermal decomposition prevented vacuum distillation. (1H NMR ($CDCl_3$) 2.4-2.8 (m, 6H, $PCH_2-N(CH_2)_2$), 3.55-3.80 (m, 4H, $O(CH_2)_2$); mass spectrum m/e for P^+ 331.20125 measured, 331.20249 calculated).

$P(CH_2NMePh)_3$, 36 This compound was prepared by the method of Daigle et al. (91). (mp = 79-81°; lit. = 80-81.5° (91)).

$P(CH_2NEtPh)_3$, 37 This phosphine was prepared using a procedure analogous to compound 36 (91). The product 37 was filtered from the reaction mixture in 62% yield as colorless crystals (mp = 44.5-46.0°; 1H NMR ($CDCl_3$) 1.08 (t, 3H, $J = 7.0$ Hz, CH_3), 3.51 (q, 2H, $J = 7.0$ Hz, NCH_2C), 3.80 (d, 2H, $J = 4.2$ Hz, PCH_2N), 6.45-7.20 (m, 5H, Ph); mass spectrum m/e for P^+ 433.26467 measured, 433.26469 calculated).

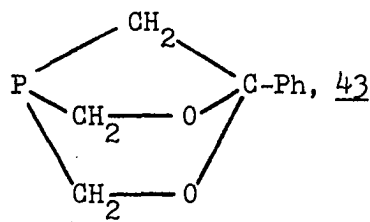
$P(CH_2NPh_2)_3$, 38 The preparation of this phosphine has been described elsewhere (91). (mp = 172-173°; lit. = 173-175° (b)) 1H NMR ($CDCl_3$) 3.82 (d, 2H, $J = 5.0$ Hz, $P-CH_2N$), 6.7-7.4 (m, 10H, Ph)).

$O=P(CH_2NMe_2)_3$, 39 Phosphine 31 was rapidly and quantitatively oxidized to the phosphine oxide 39 upon exposure to atmospheric oxygen. Recrystallization from benzene gave colorless crystals of pure 39 (mp = 153-155°; 1H NMR ($CDCl_3$) 2.38 (s, 6H, CH_3), 2.77 (d, 2H, J = 7.0 Hz, PCH_2N); ^{31}P NMR ($CDCl_3$) +47.6; mass spectrum, m/e for P^+ 221.16571 measured, 221.16496 calculated).

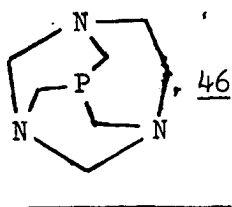
$O=P(CH_2N(n-Bu)_2)_3$, 40 The phosphine oxide derivative 40 was prepared by passing a stream of oxygen through a hexane solution of 33 at 60°. The hexane was removed under reduced pressure leaving a quantitative yield of 40 as an oil. (1H NMR ($CDCl_3$) 0.80-1.60 (m, 14H, NCC_3H_7), 2.45-2.65 (m, 4H, NCH_2C_3), 2.93 (d, 2H, J = 6.5 Hz, PCH_2N); ^{31}P NMR ($CDCl_3$) +48.8; mass spectrum, m/e for P^+ 473.447414 measured, 473.448405 calculated).

$P(CH_2OH)_3$, 41 Many procedures have been published for the preparation of this compound (90-98). A modification of the procedure published in reference (90) is described here. To a solution of 2.98 g (55.1 mMol) of freshly prepared $NaOCH_3$ in 200 mL of dry methanol was added 10.0 g (52.5 mMol) of crystalline $P(CH_2OH)_4Cl$. After stirring for thirty minutes, the $NaCl$ was filtered and the methanol removed under vacuum. The remaining oil was subjected to dynamic vacuum for eight hours after which time it was a viscous liquid. The 1H and ^{31}P NMR spectral parameters agree with literature values (99).

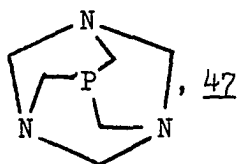
$\text{P}(\text{CH}_2\text{O})_3\text{Si-CH}_3$, 42 The preparation of this cage was carried out as previously described (90) with the following modifications. During the first two hours of the reaction of $\text{P}(\text{CH}_2\text{OH})_3$ with $\text{CH}_3\text{Si}(\text{OCH}_3)_3$, a water-cooled condenser retained the methanol formed in the reaction flask. An air-cooled condenser then replaced the water-cooled condenser and the methanol was removed with a nitrogen flush. Pure 42 was obtained in 43% yield by sublimation at 60° (0.1 mm). The melting point and ^1H NMR spectrum agree with published values (90).



This compound was prepared according to a published procedure (100) (^1H NMR (CDCl_3) 2.0 (d, 2H, $J = 8.4$ Hz, PCH_2C), 4.1-4.3 (m, 4H, PCH_2O), 7.1-7.7 (m, 5H, Ph); mass spectrum, m/e for P^+ 194.05223 measured, 194.049671 calculated).



The preparation of this compound has been reported (101).



This cage was prepared by the method of Daigle and Pepperman (102).

$\text{CH}_3\text{-C}(\text{OCH}_2)_3\text{C-CH}_3$, 56 This compound was prepared according to reference (103) except that triethyl orthoacetate was substituted for trimethyl orthoacetate. The yield was 86% while the literature yield (103) was given as 32%.

RESULTS AND DISCUSSION

The compounds to be discussed here are listed by number in Table 1. Most compounds in Part II were prepared by known methods so their syntheses will not be discussed further. The mass spectrum of 33 did not display a parent ion peak due to the ease of losing a small stable amine (25). The phosphine oxide 40 is more stable in the mass spectrometer and its characterization substantiates the synthesis of the precursor phosphine 33. The interpretation of the ^1H NMR spectrum of 43, however, does warrant further comment. The earlier workers (100) reported a doublet for the OCH_2 protons. These protons can be viewed as axial and equatorial substituents on a six-membered ring in the boat form and are therefore magnetically nonequivalent. The NMR spectrum for these protons is, therefore, a complex multiplet due to second order splitting in contrast to the reported simple doublet (100).

Cage Compounds

The discussion of δ ^{31}P of phosphorus cage compounds is divided into two parts; the bicyclic systems will be discussed first, followed by the tricyclic compounds. The change in chemical shift resulting from imposing the constraint of the cage structures will be described in terms of through-space and through-bond interactions of molecular orbitals. NMR chemical shifts which were not determined in this work were taken from references 2, 27, and 32.

Bicyclic systems

In Table 2.2 the bicyclic cage compounds are divided into six series with each series incorporating one type of phosphorus. Chemical shifts are seen to increase across a series with the acyclic species having the most downfield shift in each case. There are two trends to note in these series. First, when a two atom bridge of the bicyclic system is replaced by a one atom bridge (Series I, II, and IV) the ^{31}P chemical shift of the bicyclo[2.2.1]heptane compound has an intermediate value between the acyclic and the bicyclo[2.2.2]octane analogues. Secondly, $\delta^{31}\text{P}$ of the bicyclo[2.2.2]octane structures is dependent upon the nature of the second bridgehead atom.

The calculations of Hoffmann (77) for cage compounds consisting of two nitrogen atoms separated by three bridges indicate that the lone pairs will have a strong through-bond interaction when two-atom bridges



are present. When the bridges possess only one atom, a strong through-space interaction of the lone pairs is predicted. A combination of one and two-atom bridges decreases the effectiveness of both interaction mechanisms so that the interaction of the lone pairs in bicyclo[2.2.1]heptane and the hypothetical bicyclo[2.1.1]hexane structures is predicted to be considerably smaller than the bicyclo[2.2.2]octane compounds. If one assumes that the interaction mechanisms behave similarly for other bridgehead atoms such as phosphorus and carbon, the chemical shifts of the phosphorus cages with bicyclo[2.2.1]heptane

Table 2.2. Phosphorus cage compounds

Series I - Phosphites

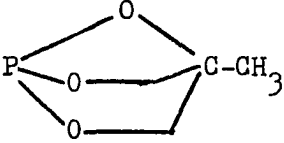
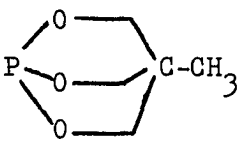
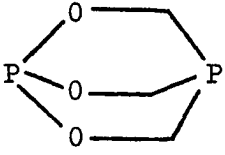
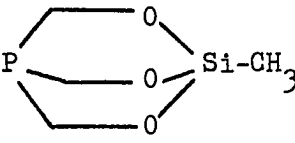
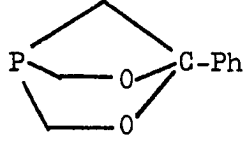
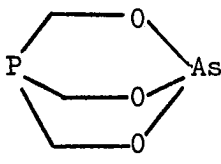
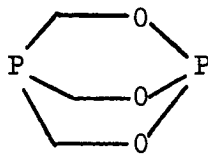
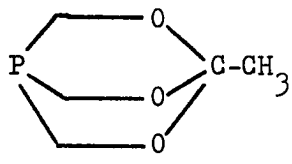
$P(OCH_2CH_3)_3$		
<u>58</u>	<u>61</u>	<u>59</u>
$\delta \text{ } ^{31}\text{P} \text{ } 138.0$	113.7	91.5
		
	<u>1</u>	
	89.8 (PO_3)	

Table 2.2. (Continued)

Series II - Phosphines

$P(CH_2OH)_3$		
<u>41</u>	<u>42</u>	<u>43</u>
$\delta \text{ } ^{31}\text{P}$ -24.0	-39.4	-46.9
		
<u>44</u>	<u>1</u>	<u>45</u>
$\delta \text{ } ^{31}\text{P}$ -66.7	-67.0 (PC_3)	-80.5

Series III - Aromatic Phosphines

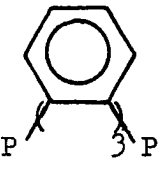
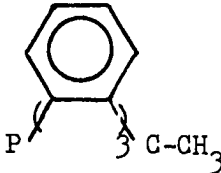
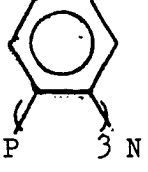
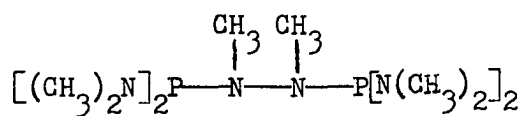
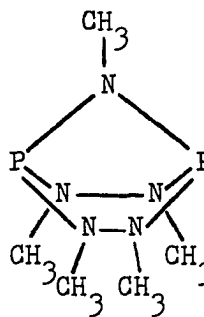
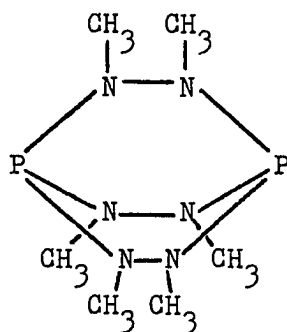
PPh_3			
	<u>49</u>	<u>50</u>	<u>51</u>
$\delta \text{ } ^{31}\text{P}$ -8	-43	-64.8	-80

Table 2.2. (Continued)

Series IV - Hydrazino Phosphines

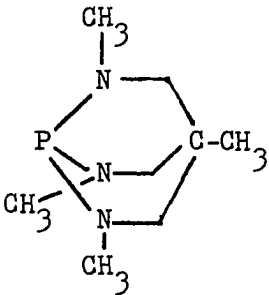
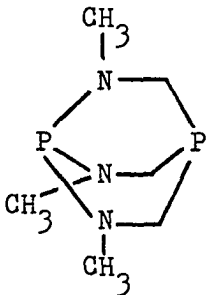
53 δ ^{31}P 123.154

117.8

3

107.4

Table 2.2. (Continued)

Series V - Aminophosphines			
$P[N(CH_3)_2]_3$			
<u>52</u>	<u>6</u>	<u>12</u>	
$\delta \text{ } ^{31}\text{P}$ 120.9	84.0	79.2 (PN ₃)	

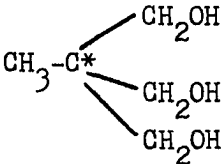
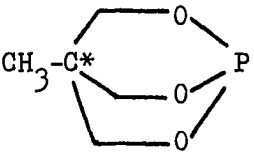
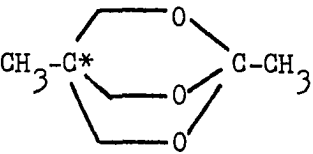
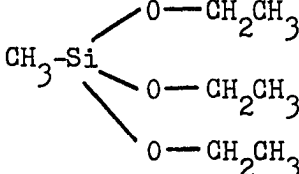
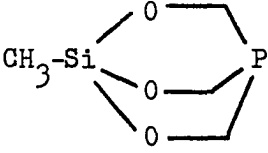
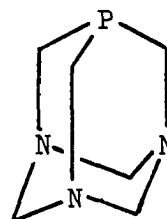
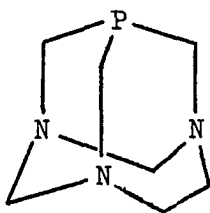
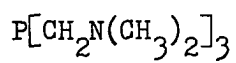
Series VI - Non-Phosphorus Bridgehead			
			
<u>55</u>	<u>59</u>	<u>56</u>	
$\delta \text{ } ^{13}\text{C}^*$ 41.9	32.3	29.6	
			
<u>57</u>	<u>42</u>		
$\delta \text{ } ^{29}\text{Si}$ 39.3	42.4		

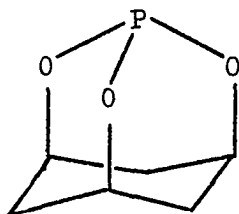
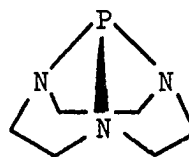
Table 2.2. (Continued)

Series VII - Tricyclic Systems

314647 $\delta \text{ } ^{31}\text{P}$ -56.8

-88.5

-98.6

6263 $\delta \text{ } ^{31}\text{P}$ 137.0

142 or 155

structures can be rationalized. The upfield shift in $\delta^{31}\text{P}$ of 61, 43, and 54 in comparison to the acyclic analogues 58, 41, and 53 indicates that an interaction of the phosphorus lone pair with the cage MO system is taking place, but the interaction in the bicyclo[2.2.2]octane structures 59, 45, and 3 is more efficient and a more upfield $\delta^{31}\text{P}$ is noted for the latter compounds.

The diverse nature of the second bridgehead atom of the bicyclic phosphorus compounds studied makes difficult the task of determining which characteristic of the bridgehead atom is mainly responsible for affecting the $\delta^{31}\text{P}$ value. The through-bond mechanism predicts a strong interaction of the sigma bond between the two bridging atoms and orbitals of proper symmetry on the bridgehead atoms. For Group VA atoms such as P and As, the interacting orbital will be the lone pair orbital while on Group IVA atoms, such as C and Si, it will be a bonding orbital. In addition, Group VA atoms tend to deviate from tetrahedral geometry while the Group IVA atoms deviate little from this geometry. It is therefore likely that comparisons between groups would be tenuous at best so comparisons will be restricted to each group individually. It is known from simple molecular orbital theory (104) that when two orbitals have the proper symmetry for interaction, the extent of interaction increases as the difference between their energies decreases (see Figure 2.7).

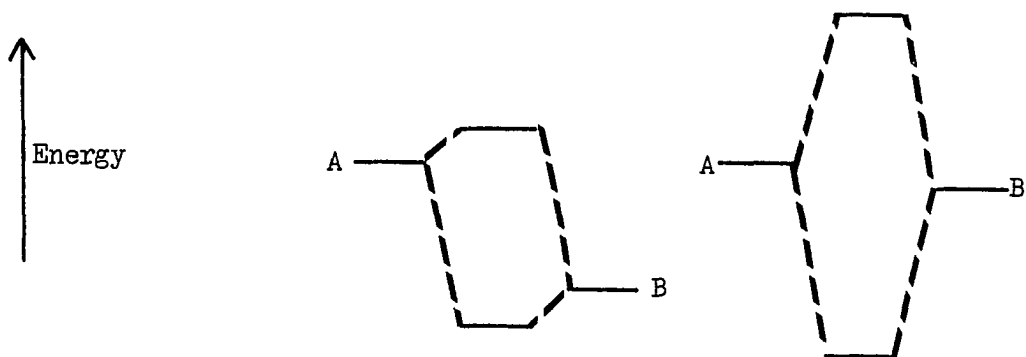
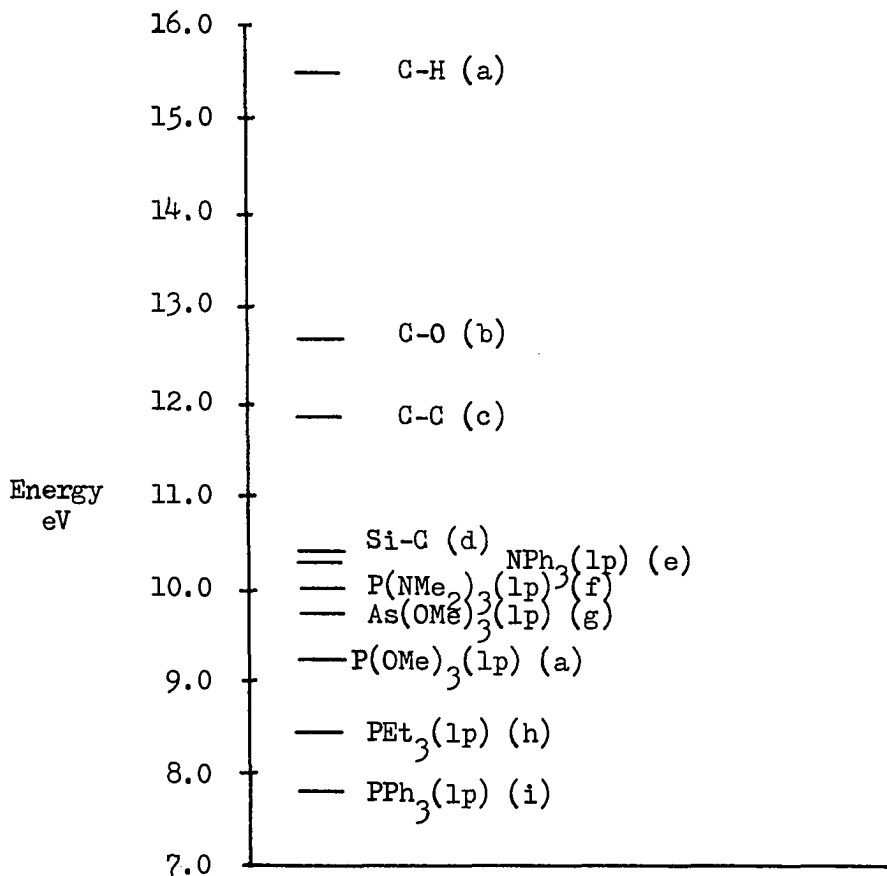


Figure 2.7. MO interaction as a function of energy of combining orbitals

The orbitals on the bridgehead atoms of Series II will interact with the C-O σ bond. In the photoelectron spectrum of $\text{P}(\text{OCH}_3)_3$ (105) the ionization band for the C-O σ bond overlaps with the P-O σ bond bands, all of which come above 12eV. Figure 2.8 contains an energy level diagram comparing the ionization energies of the lone pairs of $\text{P}(\text{OCH}_3)_3$ and $\text{As}(\text{OCH}_3)_3$ along with the ionizations from the C-C, C-O, and Si-C σ bonds. The C-C ionization energy of 11.8eV is much closer to the C-O energy (12.6eV) than is the Si-C bond ionization energy of 10.4eV. This is consistent with a more extensive interaction of the orbitals in 45 compared to that in 42, and thus a more upfield shift in the NMR of 45 may be expected. The smaller bond angles around As in $\text{As}(\text{OCH}_3)_3$ compared to those around P in $\text{P}(\text{OCH}_3)_3$ cause the As lone pair to have a higher ionization energy than P (106). One would expect the $\delta^{31}\text{P}$ of 44 to be upfield of 1 but the $\delta^{31}\text{P}$ values are very nearly the same. The P lone pair is less diffuse and has more p character than the As

Figure 2.8. Vertical ionization potentials from photoelectron spectra of selected compounds



	Compound	Reference
a	P(OMe) ₃	105
b	MeOH	107
c	Neopentane, Benzene	108 109
d	SiMe ₄	110
e	NPh ₃	111
f	P(NMe ₂) ₃	112
g	As(OMe) ₃	106
h	PEt ₃	105
i	PPh ₃	111

lone pair, and these factors may permit better overlap of the P lone pair with the σ bonds, thus leading to a stronger interaction. The nitrogen lone pair is closer in energy to the sigma bond of the benzene bridge than is the phosphorus lone pair. Thus, the bridgehead-bridgehead interaction in 51 is stronger than that in 49 leading to the appearance at higher field of the ^{31}P shift of 51.

The effect of orbital interaction on the NMR chemical shift of the second bridgehead atom (Series VI) appears to be applicable in the case of carbon but not silicon. The available theories of shielding apparently do not explain the chemical shift trends of the ^{29}Si nucleus (113), and so speculation on the origin of the downfield movement of δ ^{29}Si upon cage formation in 57 and 42 is not warranted. The carbon bridgeheads of 59 and 56 in Series VI show the upfield shift relative to the acyclic analogue 55, reminiscent of the phosphorus cages. Although the δ ^{31}P values for both phosphorus atoms of 1 are upfield from the acyclic analogues 58 and 41, the phosphine phosphorus of 12 is slightly downfield from the acyclic analogue 31. No rationale for the latter reversal is presently apparent.

In summary, the ^{31}P NMR chemical shifts of most of the bicyclic phosphorus cage compounds can now be rationalized on the basis of molecular orbital interactions which are facilitated by geometry. Cage formation causes an upfield shift for all types of phosphorus atoms except the aminomethyl phosphine 12. Overlap reduction, which occurs from a bicyclooctane to a more strained bicycloheptane structure,

accounts for the greater upfield shift of the bicyclooctane compounds in all cases. Finally, when the bicyclooctane compounds are separated into classes containing either a Group IVA or VA atom as the second bridgehead, trends within each class can be rationalized on the basis of relative orbital energies except for 44 and 1 for which hybridizational considerations were necessary to account for the data.

Tricyclic systems

The tricyclic phosphorus compounds of Series VII contain three bridgehead atoms of a second type in a different geometrical relationship to the first than was found for the single second bridgehead atom in the bicyclic systems just discussed. The nitrogen atoms of 47 are separated from the phosphorus atom by one-atom bridges which according to Hoffmann et al. (77) is conducive to through-space orbital interactions. The photoelectron spectrum of hexamethylenetetramine (114) which has a structure analogous to 47 (115,116) indicates a strong interaction among the nitrogen lone pair orbitals. A through-space interaction of the phosphorus lone pair with the three nitrogen lone pairs may thus be responsible for the 41.6 ppm upfield shift in $\delta^{31}\text{P}$ in going from 31 to 47. The substitution of a two-atom bridge for a one-atom bridge between nitrogens of 47 yields 46. This mixed-bridge system would reduce the efficiency of the through-space mechanism, thus accounting for the smaller upfield shift in the $\delta^{31}\text{P}$.

The adamantane-type structure of 47 is present in 62, but the $\delta^{31}\text{P}$ of 62 is very similar to the acyclic analogue 58. This apparent anomaly

is easily explained by comparing the energies of the orbitals involved (Figure 2.8). Whereas the energies of the phosphorus and nitrogen lone pairs would be quite similar, the C-H σ bond is of much higher energy and, therefore, has a small interaction.

The unusual structure of 63 contains pyramidal nitrogens adjacent to the phosphorus atom (117). The atomic arrangements, which gave rise to the orbital interactions postulated in the bicyclic systems and the adamantane-type tricyclic compounds, are not present in 63. Thus, no explanation is put forth for the downfield shift of δ ^{31}P for 63 compared to the acyclic analogue 52.

Compared to the number of tetracoordinate derivatives which could be synthesized from tricoordinate cage compounds, the number of chemical shifts recorded for such derivatives is relatively small and no trends are presently discernible. From the limited data available the trends seen for the tricoordinate phosphorus do not hold true for the tetra-coordinate analogues.

Electronegativity Considerations

Because of the complicated steric and electronic factors which can affect the NMR chemical shift (69), it is difficult to find a series of compounds in which only one parameter is varied. In an attempt to prepare such a series, a group of compounds with the general formula $\text{P}(\text{CH}_2\text{NR}_1\text{R}_2)_3$ was synthesized (Table 2.3). The first two atoms on each group bonded to phosphorus are the same, i.e. C-N. The fact that the

Table 2.3. Group electronegativities and $\delta^{31}\text{P}$ for aminomethylphosphines $\text{P}(\text{CH}_2\text{NR}_1\text{R}_2)_3$

	<u>R₁</u>	<u>R₂</u>	<u>Group EN</u>	<u>$\delta^{31}\text{P}$</u>
<u>31</u>	Me	Me	7.67	-56.832
<u>32</u>	Et	Et	7.61	-64.446
<u>33</u>	n-Bu	n-Bu	7.54	-66.487
<u>9</u>	H	Me	7.75	-60.822
<u>10</u>	H	Et	7.67	-63.807
<u>34</u>	H	n-Bu	7.60	-65.238
<u>35</u>	Morpholine		7.79	-61.096
<u>11</u>	H	Ph	8.60	-31.888
<u>36</u>	Me	Ph	7.94	-42.365
<u>37</u>	Et	Ph	7.88	-41.511
<u>38</u>	Ph	Ph	8.07	-34.599

groups which are varied are two atoms removed from phosphorus should minimize steric interactions of the R groups.

To see if the 35 ppm range in δ ^{31}P of the compounds in Table 2.3 could be correlated with the electronegativity of the groups on phosphorus, the group electronegativity of the $\text{CH}_2\text{-NR}_1\text{R}_2$ groups were calculated using the method of Huheey (84) (Table 2.3). Sample calculations are included in the Appendix 2. The compounds in Table 2.3 can be divided into two groups: Group I, in which both R groups are either hydrogen or alkyl groups (Figure 2.9), and Group II, in which at least one R group is a phenyl ring (Figure 2.10).

It is evident from Figure 2.9 that there is a linear correlation between the group electronegativity of the groups bonded to phosphorus and the ^{31}P chemical shift for six of the seven compounds. A linear regression analysis shows that if all the points of Figure 1 are included, the correlation coefficient is 0.42, but if the point for 31 is not used, the correlation coefficient is 0.96. It is not known why 31 does not fit the pattern. The chemistry of 31 also showed differences from similar compounds such as 32 in at least one respect. While 32 was indefinitely stable in air, 31 was rapidly oxidized by air to 39.

Figure 2.10 contains a plot of the relation between electronegativity and chemical shift for Group II compounds. Although more data would be necessary before a proper analysis of these systems can be performed, the four data points available gave a correlation coefficient of 0.75 which cannot be taken as support for a linear correlation.

Figure 2.9. A plot of the relationship between electronegativity and ^{31}P NMR chemical shift for Group I compounds

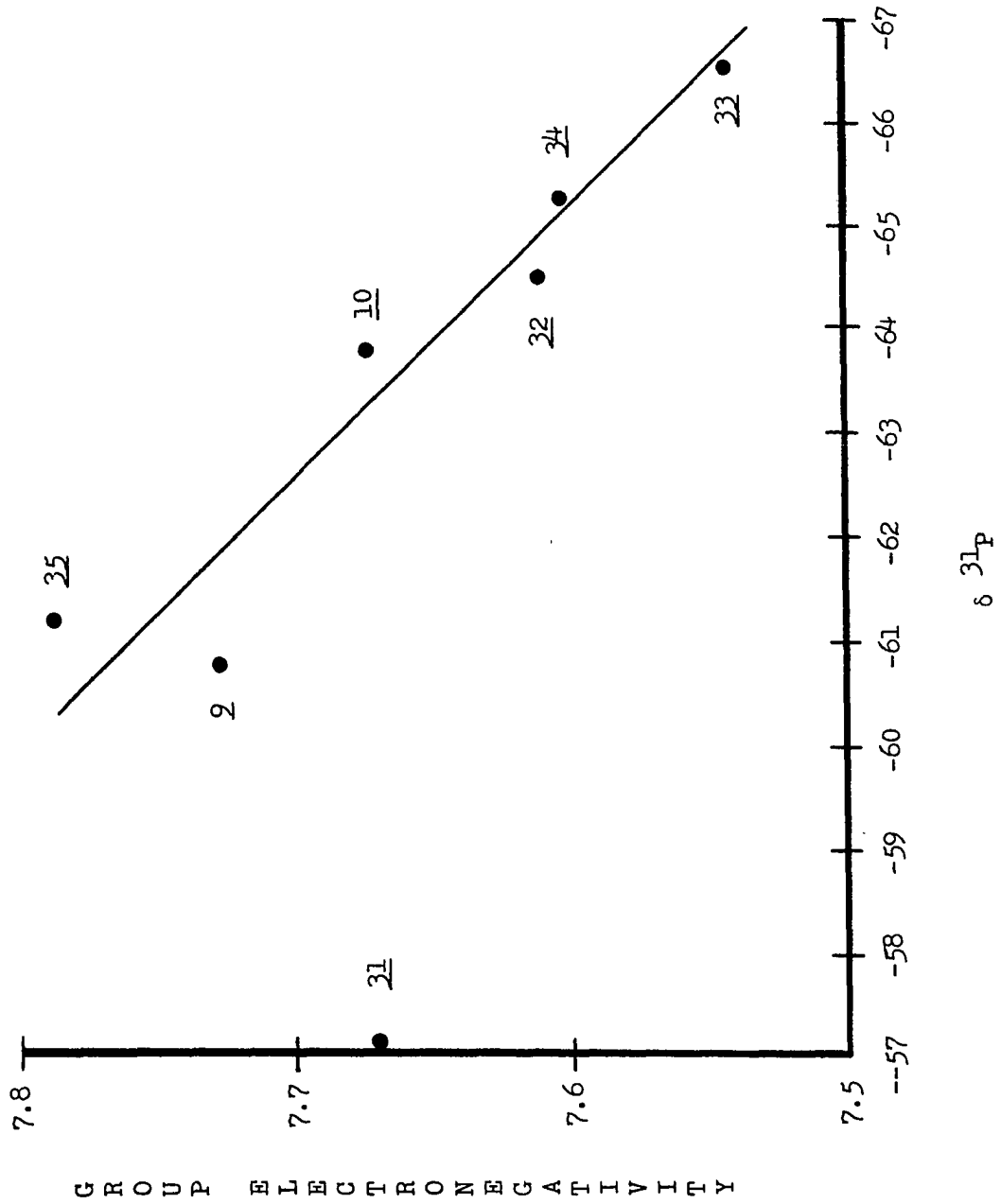
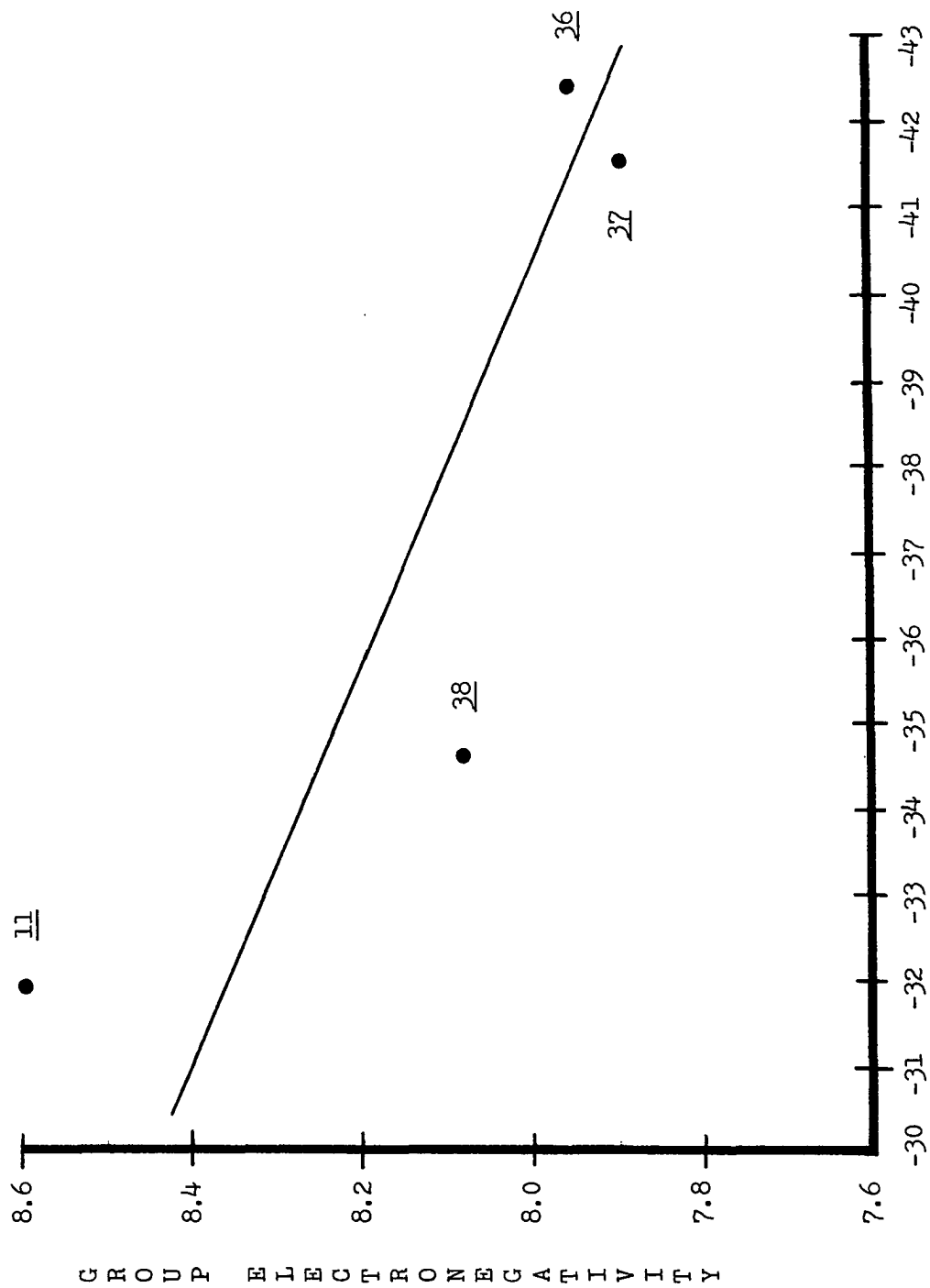


Figure 2.10. A plot of the relationship between electronegativity and ^{31}P NMR chemical shift for Group II compounds



$\delta^{31}\text{P}$

It is likely that the electronegativity is not the only factor affecting the NMR chemical shifts in Groups I and II, but it appears to be a dominant factor at least in Group I. Attempts to explain the trends of Group I and II using the MO theory of Letcher and Van Wazer in (32) or the hyperconjugation argument of Grim, et al. (68) were unsuccessful. Grim's theory predicts that 31, 32, 33, and 35 would all have the same chemical shift, which is not the case. The only variable which the Letcher and Van Wazer theory would expect to affect the δ ^{31}P for these phosphines is the bond angle around phosphorus. If the steric bulk of the R groups is causing an expansion of the angles around phosphorus, MO theory predicts a downfield shift in δ ^{31}P , but the opposite is observed. It appears that the group electronegativity argument must be given stronger consideration in the future development of theories for ^{31}P NMR chemical shifts.

PART III. $P(CH_2O)_3$ -BRIDGED SQUARE
COORDINATION COMPLEXES

INTRODUCTION

The nonchelating bifunctional ligand $\text{P}(\text{CH}_2\text{O})_3\text{P} \underline{1}$ can act as a bridge between two metal centers as in $(\text{OC})_4\text{FeP}(\text{CH}_2\text{O})_3\text{PFe}(\text{CO})_4$ and $(\text{OC})_5\text{WP}(\text{CH}_2\text{O})_3\text{PW}(\text{CO})_5$ (4). It appears that disubstituted complexes of $\underline{1}$ may be stabilized by dipole-dipole interactions of the ligand. Thus a head-to-tail orientation is found in the trans- $\text{P}(\text{CH}_2\text{O})_3\text{PFe}(\text{CO})_3\text{P}(\text{CH}_2\text{O})_3\text{P}$ (118). Reaction of $\underline{1}$ with $\text{Ni}(\text{CO})_4$ produces an insoluble polymer (3).

Metal complexes with cis or facial geometry of two or three $\underline{1}$ ligands provide the potential to prepare single or multiple ring coordination compounds. As the number of metal centers connected by $\underline{1}$ ligands increases, the solubility of the product is likely to decrease. The resultant polymeric material could have interesting potential in heterogeneous catalysis since it would have a large number of metal centers but would be insoluble in organic solvents. This would eliminate the difficult step of catalyst separation which prohibits the use of most homogeneous catalysts in industrial processes.

The purpose of the present work is to develop the synthetic techniques necessary to prepare a ring complex having metal centers at the corners of a square and $\underline{1}$ ligands oriented along the sides of the square:

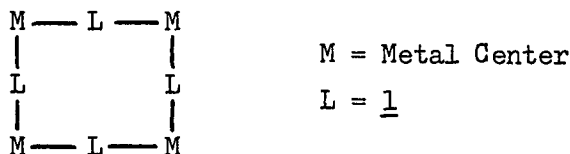


Figure 3.1. $\text{P}(\text{CH}_2\text{O})_3\text{P}$ -bridged square tetramer

Since the metals must possess a cis geometry throughout the synthesis, it was deemed preferable to begin with starting materials having this configuration. Conditions also had to be controlled to prevent random polymerization.

EXPERIMENTAL

A list of compounds cited in Part III is given in Table 1.

Techniques

All reactions involving metal complexes were performed under an inert atmosphere of dry nitrogen.

Materials

All solvents were reagent grade or better. Methylcyclohexane was dried by distilling from sodium. Chromium and tungsten hexacarbonyls were purchased from Pressure Chemical Co. Molybdenum hexacarbonyl was a generous gift from Climax Molybdenum Co. Norbornadiene (C_7H_8) and N,N,N',N' -Tetramethyl-1,3-propanediamine (tmpa) were purchased from Aldrich Chemical Co. and used as received.

NMR spectra

Proton NMR spectra were obtained on either a Varian HA-100 or an A-60 spectrometer using deuterated solvents. Me_4Si was used as an internal standard, and it served as the internal lock for the HA-100 instrument.

^{31}P NMR spectra were obtained on $CDCl_3$ solutions in 10 mm tubes with a Bruker HX-90 spectrometer operating at 36.434 MHz in the FT mode while locked on the 2H resonance of the deuterated solvent. The external standard was 85% H_3PO_4 sealed in a 1 mm capillary tube held coaxially in the sample tube by a Teflon vortex plug. The spectrometer is interfaced with a Nicolet Instruments 1080 minicomputer system.

Infrared spectra

Carbonyl stretching frequencies were measured on a Beckman IR4250 double beam spectrometer using NaCl optics. Absorption bands for the solutions were referenced to the 1601.8 cm^{-1} band of polystyrene.

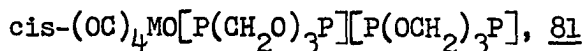
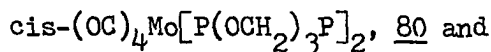
Preparation of compounds

$\text{cis}-(\text{OC})_4\text{CrC}_7\text{H}_8$ and $\text{cis}-(\text{OC})_4\text{MoC}_7\text{H}_8$ These two organometallic reagents were prepared from the metal hexacarbonyls and norbornadiene using the methods described by King (119).

$\text{cis}-(\text{OC})_4\text{WC}_7\text{H}_8$ This compound was prepared by the method of King and Fronzaglia (120).

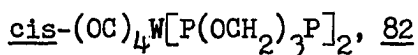
$\text{cis}(\text{OC})_4\text{Mo}(\text{tmpa})$ This material was prepared using the procedure of Dobson and Faber (121).

$\text{cis}-(\text{OC})_4\text{Cr}[\text{P}(\text{OCH}_2)_3\text{P}]_2$, 79 This compound was first prepared in 4% yield by Allison (3). The yield was improved to 49% using the following procedure. A solution of 0.53 g (2.1 mMol) of $\text{cis}-(\text{OC})_4\text{CrC}_7\text{H}_8$ in 25 mL of methylcyclohexane was added over a period of two hours to a solution of 0.69 g (4.6 mMol) of 1 in 25 mL of methylcyclohexane. While stirring for forty-eight hours, the yellow color of $\text{cis}-(\text{OC})_4\text{CrC}_7\text{H}_8$ gradually faded and a white solid precipitated. The solid was chromatographed on a Florisil column (acetone eluent) to yield 0.48 g (49%) of 79. The ^1H and ^{31}P NMR parameters agree with the values of Allison (3).



The preparation of these

compounds is recorded in a monthly report. Their synthesis is reported here for completeness. To a solution of 0.90 g (6.0 mMol) of 1 in 75 mL of methylcyclohexane was added 1.0 g (3.0 mMol) of cis-(OC)₄Mo(tmpa) in 50 mL methylcyclohexane over a period of one hour. A precipitate formed immediately when the addition commenced. After stirring for an additional two hours, the tan precipitate was filtered from the colorless solution. The crude product was purified by column chromatography on a Florisil column. A 3:1 mixture of hexane:ethyl acetate eluted excess 1 first, followed by 0.07 g (6.6%) of 81. Further elution with chloroform removed 0.33 g (31%) of 80 from the column. The ¹H and ³¹P NMR data for 81 agreed with the values reported by Allison (3). NMR also used to characterize 80 (¹H NMR (CDCl₃) 4.77 (apparent dt (spectrum is not first order - see text) ²J_{PH} = 9.0 Hz, ³J_{PH} = 5.0 Hz)). Reaction of 1 with cis-(OC)₄MoC₇H₈ produced only 80 in 20% yield.



A solution of 0.25 g (0.65 mMol) of

cis-(OC)₄WC₇H₈ in 15 mL of methylcyclohexane was added dropwise to a solution of 0.22 g (1.4 mMol) of 1 in 15 mL of methylcyclohexane at room temperature. After stirring for three hours, the precipitate which had formed was filtered. The crude solid was dissolved in 5 mL of chloroform and the solution was added to 100 mL of vigorously stirred pentane, precipitating 0.14 g (36%) of 82. (¹H NMR (CDCl₃) 4.88 (apparent dt (spectrum is second order - see text), ²J_{PH} = 8.5 Hz, ³J_{PH} = 5.5 Hz)).

$(OC)_{16}Cr_4[P(OCH_2)_3P]_4$, 83 A solution of 0.14 g (0.30 mMol) of 79 and 0.08 g (0.30 mMol) of $(OC)_4CrC_7H_8$ in 35 mL of methylene chloride was refluxed for twenty-four hours. The brown precipitate was filtered from the colorless solution. The solvent was removed under reduced pressure leaving a slightly yellow solid. The solid was dissolved in 3 mL of chloroform and the solution was added to 75 mL of vigorously stirred pentane. The white precipitate (0.16 g) represented a yield of 84% of 83. (1H NMR ($CDCl_3$) 4.80 (m)).

$(OC)_{16}Mo_4[P(OCH_2)_3P]_4$, 84 This compound was prepared from cis- $(OC)_4Mo(tmpa)$ and 80 in 86% yield using the same procedure as described for 83. (1H NMR ($CDCl_3$) 4.85 (m)).

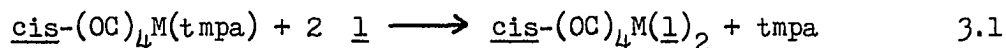
$(OC)_{16}W_4[P(OCH_2)_3P]_4$, 85 The same procedures used to prepare 83 produced 85 in 86% yield from cis- $(OC)_4WC_7H_8$ and 82. (1H NMR ($CDCl_3$) 4.80 (m)).

$(OC)_{16}Cr_2Mo_2[P(OCH_2)_3P]_4$, 86 This compound was prepared from cis- $(OC)_4Mo(tmpa)$ and 79 in 40% yield using the procedure described for 83. (1H NMR ($CDCl_3$) 4.77 (m)).

$(OC)_{16}Mo_2W_2[P(OCH_2)_3P]_4$, 87 Reaction of 82 with cis- $(OC)_4Mo(tmpa)$ in the same manner as described for the preparation of 86 produced 87 in 70% yield. (1H NMR ($CDCl_3$) 4.82 (m)).

RESULTS AND DISCUSSION

Group VI metal carbonyls have octahedral geometry which provides the 90° angles needed to form the square, tetrameric or "quadrameric"¹ compounds described in the Figure 3.1. The bridging 1 ligands must bind to the metal in a cis geometry in the quadramers so the cis-(OC)₄MC₇H₈ and cis-(OC)₄M(tmpa) complexes were chosen as starting materials (Reaction 3.1). The C₇H₈ and tmpa ligands ensure the cis



geometry and are readily displaced by the phosphines and phosphites under mild conditions (20°C) to avoid possible rearrangement to a trans isomer which could conceivably occur at higher temperatures. Methylcyclohexane is an ideal solvent for these reactions since the cis-(OC)₄M(1)₂ complexes are insoluble and precipitate from solution before they can undergo further reaction and form random polymers. The reaction of (OC)₄Mo(tmpa) with 1 produces two isomers (80 and 81) with 80 representing the major product. Reaction of cis-(OC)₄MoC₇H₈ with 1 yields only isomer 80 and in lower yields than the previous reaction. The cis-(OC)₄CrC₇H₈ and cis-(OC)₄WC₇H₈ complexes react with 1 to form

¹quadra: Latin, square, plinth, fillet; akin to Latin, quattuor, four.

-mer: from Greek meros, part; chem: member of a (specified) class. (123)

only the isomer which has both phosphite ends of the ligands coordinated to the metal (79 and 82). The cis configuration for the disubstituted complexes is confirmed by the presence of three of the four expected carbonyl IR modes (A_1^1 , A_1^2 , B_1 , and B_2). The two B bands are unresolved and are reported as one band in Table 3.1.

The ^{31}P NMR chemical shifts in Table 3.2 are extremely useful for characterizing these compounds. The phosphine and phosphite resonances are shifted downfield upon coordination to a Group VI metal. This coordination chemical shift ($\delta_{\text{complex}} - \delta_{\text{free ligand}}$) as defined by Grim et al. (124) is due, at least in part, to mixing of the phosphorus d orbitals with low-lying energy levels of the metal. Thus the effect on the ^{31}P chemical shift is greatest for small metals such as chromium for which the orbital overlap with phosphorus is most efficient (59). Whatever the origin(s) of the ^{31}P chemical shift, the empirical evidence of Grim et al. (124) allows the shifts of the compounds in Table 3.3 to be assigned to coordinated and uncoordinated phosphorus atoms and also to the metal involved in the coordination.

The ^1H NMR spectrum of 1 contains the expected doublet of doublets for the methylene protons due to coupling to both phosphorus atoms (see Part I of this dissertation). The ^1H NMR spectra of 79 and 81 were analyzed by Allison (3). The spectrum of 81 is first order but that of 79 contains second order effects. The same second order effects are present in the ^1H NMR spectrum of 80 (Figure 3.2) and 82. The two phosphite phosphorus atoms of 80 are chemically equivalent but

Figure 3.2. Proton NMR spectrum of 80.
The central peaks of the
apparent triplets are due
to virtual coupling

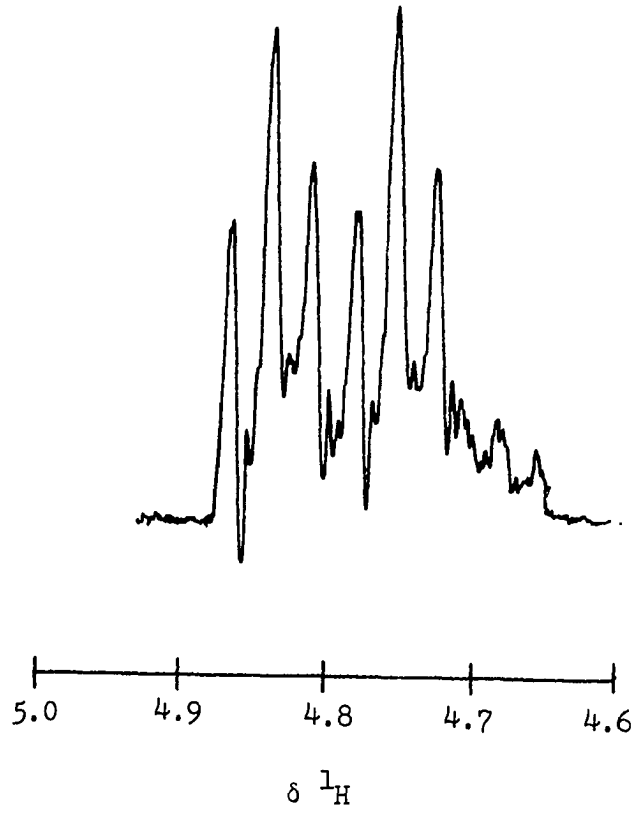


Table 3.1. Infrared frequency assignments for the carbonyl region

Compound	Frequencies (cm^{-1}) and assignments ^{a,b}		
	A_1^2	A_1^1	B_1B_2
<u>79</u>	2029 (w)	1943 (sh)	1926 (vs)
<u>80</u>	2041	1954	1938 (vs)
<u>81</u>	2039	1955 (sh)	1936 (vs)
<u>82</u>	2042 (w)	1955	1929 (vs)
<u>83</u>	2036	1960 (s)	1937 (vs)
<u>84</u>	2050, 2036	1970	1943 (vs)
<u>85</u>	2041	1963	1933 (vs)
<u>86</u>	2036	1959 (sh)	1938 (vs)
<u>87</u>	2040 (w)	1963	1936 (vs)

^a vs = very strong, sh = shoulder, s = strong, m = medium, w = weak. Values are precise to $\pm 2 \text{ cm}^{-1}$.

^b All spectra were taken in CH_2Cl_2 solutions.

Table 3.2. ^{31}P NMR chemical shifts for the compounds of Part III ^a

Compound	δPO_3	δPC_3	δMPO_3	δMPC_3
<u>1</u>	90.0	-67.0		
<u>79</u>		-68.1	157.4	
<u>80</u>		-68.4	133.5	
<u>81</u>	88.8	-69.1	134.1	-12.7
<u>82</u>		-68.6	109.9	
<u>83</u>			160.5	11.9
<u>84</u>			133.6	-14.6
<u>85</u>			112.6	-33.5
<u>86</u>			159.8	-11.9
<u>87</u>			111.2	-12.6

^a CDCl_3 solvent.

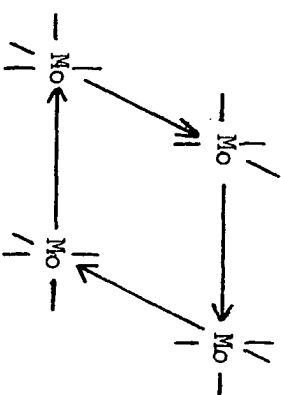
magnetically nonequivalent so that appreciable ${}^2J_{PP}$ coupling through the metal occurs. The protons are "virtually" coupled to this third phosphorus which causes an envelope of lines to appear between the proton doublet whose separation is ${}^3J_{PH}$ in the absence of second order effects (125). This doublet separation in the case of a virtually coupled spectrum is ${}^3J_{PH} + {}^5J_{PH}$. Because five-bond couplings are very small, ${}^5J_{PH}$ can be assumed to be zero (126), thus allowing ${}^3J_{PH}$ to be measured directly from the spectrum.

The reaction to form the quadramers from the disubstituted complexes $\text{cis}-(\text{OC})_4\text{M}(\underline{1})_2$ and either $\text{cis}-(\text{OC})_4\text{M}(\underline{7})\text{H}_8$ or $\text{cis}-(\text{OC})_4\text{M}(\text{tmpa})$ goes smoothly in high yields at 40°C in CH_2Cl_2 (Reaction 3.2).

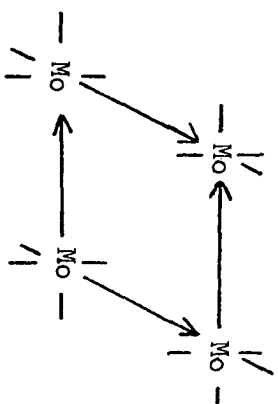
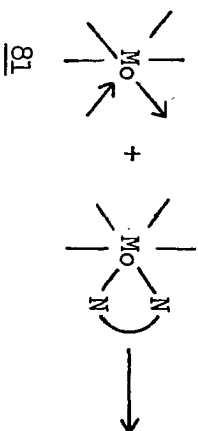


Tmpa is especially well suited for this reaction because it decomposes to a brown sticky solid under these conditions, and is thus removed from the reaction thereby providing a driving force for Reaction 3.2.

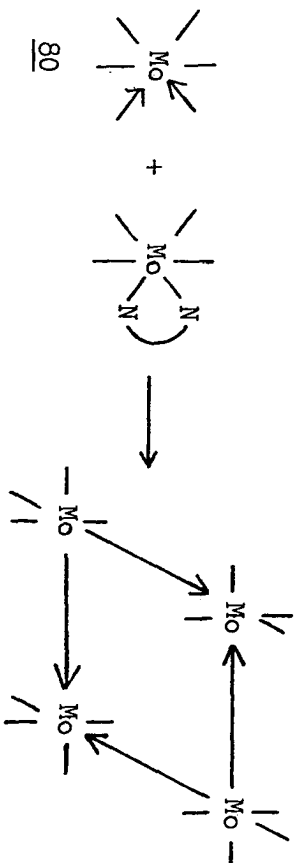
The two chemically different phosphorus atoms in $\underline{1}$, which are responsible for the two isomers $\underline{80}$ and $\underline{81}$, can also cause ligand isomerism in the quadramers. If isomer $\underline{81}$ is used to form the quadramer (Reaction 3.3; $\longrightarrow = \text{P}(\text{CH}_2\text{O})_3\text{P}$, arrowhead corresponds to phosphite P, $- = \text{CO}$), there are two possible isomers, \underline{a} and \underline{b} . But if the isomer $\underline{80}$ is used to form the quadramer, (Reaction 3.4) compound $\underline{84}$ is the only possible isomer which can be formed. The spectroscopic methods used to characterize these compounds (IR and ${}^1\text{H}$



3.3



b



3.4

84

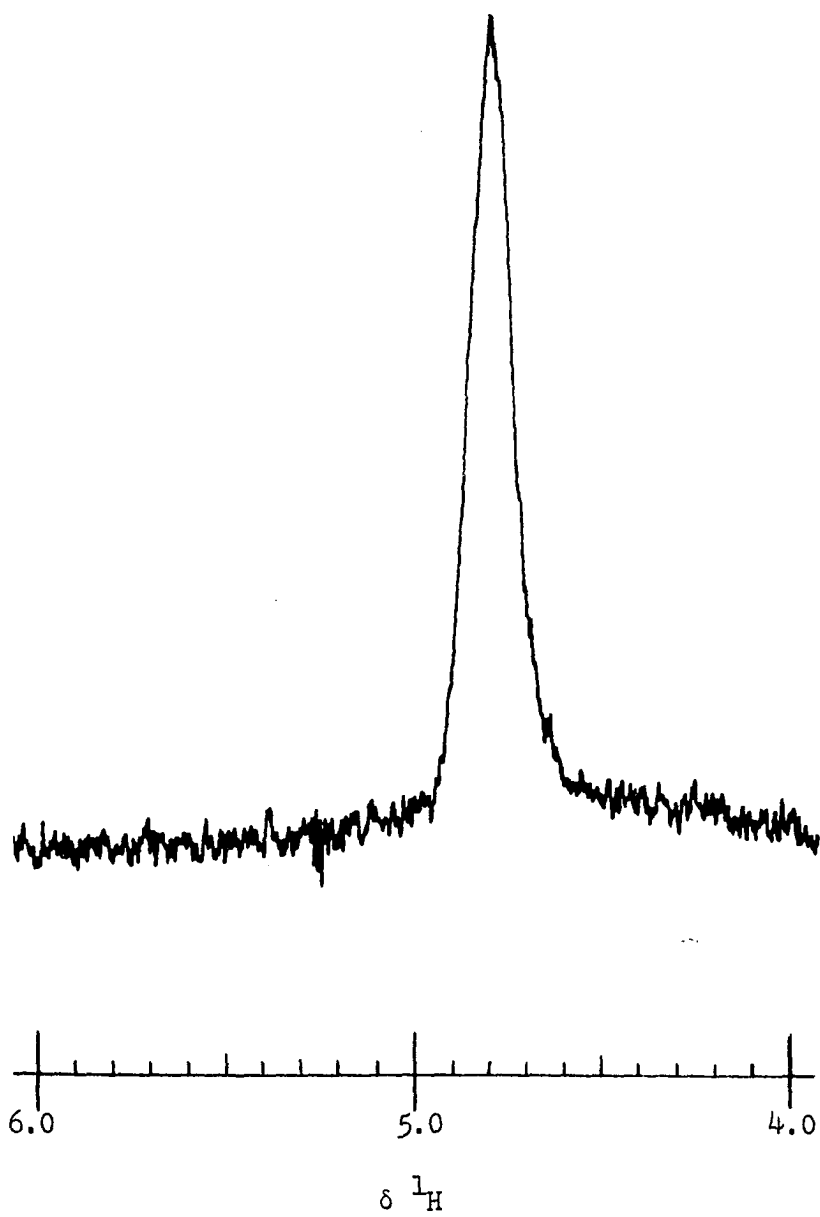
and ^{31}P NMR) cannot differentiate between a and b of Reaction 3.3 so that 81 was not used to make quadramers.

The quadramers 83-87 each have two metals coordinated to phosphite ends of 1 and two metals coordinated to the phosphine ends. Two sets of CO bands might be expected in the IR spectrum. In 84 there are two distinct A_1^2 peaks but this is the only instance where more than one set of carbonyl peaks was observed. This is not too surprising since complexes of the type $(\text{OC})_5\text{MP}(\text{CH}_2\text{O})_3\text{PM}(\text{CO})_5$ also exhibit only one set of IR bands (1).

The ^1H NMR spectra of the quadramers exhibit a single broad, symmetric resonance. Figure 3.3 shows the spectrum of 85 as an example. There is undoubtedly a great deal of complex spin-spin splitting present in these systems so the absence of fine structure on these peaks is not entirely unexpected. The symmetry of the peaks is consistent with the symmetry of the molecular structure.

The peaks of the ^{31}P NMR spectrum were also broadened by the complex splitting. The ^{31}P chemical shifts in Table 3.2 provide the most supportive evidence for quadramer formation. The chemical shifts of the phosphite atoms in the quadramers agree well with the values for the coordinated phosphites of 79-82. The chemical shift values for 86 and 87 show that the phosphine atoms in both molecules are coordinated to molybdenum while the phosphite atoms are coordinated to either chromium or tungsten.

Figure 3.3. ^1H NMR spectrum of 85



Attempts to obtain high resolution mass spectra for the quadramers proved fruitless since the nonvolatile quadramers decompose in the conventional mass spectrometer. A sample of 84 has been submitted to the Midwest NSF Mass Spectrometry Center for analysis using molecular desorption mass spectrometry.

Single crystals for X-ray diffraction of 84 were grown in an acetone/ether mixture. However, the compound apparently traps solvent molecules which diffuse out of the crystal when the crystal is mounted in a glass capillary, thus destroying the crystal lattice.

CONCLUSIONS

The new cage compounds $P(CH_2NR)_3P$ with $R = Me, Et, \text{ or } Ph$ have been prepared by transamination of the appropriate triamine $P(CH_2N(H)R)_3$ with $P(NMe_2)_3$. The reactivity and NMR parameters of these compounds have been investigated. The crystal structure determination of $P(CH_2NPh)_3P$ reveals the planar geometry of the nitrogen atoms typical of aminophosphines. The 3.12 \AA separation of the phosphorus atoms is less than the sum of the van der Waals radii but greater than a P-P single bond.

The ^{31}P NMR chemical shifts of trivalent phosphorus cage compounds are generally found upfield of analogous acyclic compounds. This observation can be rationalized on the basis of the interaction of the phosphorus lone pair orbital with orbitals on the second bridgehead atom as well as on the atoms of the bridging groups.

The diphospha cage compound $P(CH_2O)_3P$ was used as a bridging ligand to form cyclic transition metal complexes consisting of four $M(CO)_4$ centers ($M = Cr, Mo, \text{ or } W$) at the corners of a square, with four $P(CH_2O)_3P$ ligands acting as the sides of the square. The synthetic process produces high yields of the quadramers, and it also allows preparation of complexes incorporating two different metals.

SUGGESTIONS FOR FUTURE RESEARCH

The ligand properties of the new cage compounds 12, 13, and 14 were only briefly studied in this work. The two phosphorus atoms would allow these compounds to behave as bridging ligands such as 1. The lone pairs on nitrogen offer further reaction sites for Lewis acids. The phosphorus atom and one of the nitrogens of 6 form BH_3 adducts whereas only the phosphorus atoms of 3 form similar adducts. The basicity of the nitrogen atoms of 12, 13, and 14 should be investigated.

A study of the ^{14}N or ^{15}N NMR parameters for the new cages with phosphorus in both the +3 and +5 oxidation states would be useful to determine why the quadrupolar effects are smaller in the compounds in which phosphorus is in the +5 state. To further probe the quadrupole effect, a crystal structure of one of the compounds having +5 phosphorus atoms would help decide whether or not a change in the geometry of the nitrogen atoms may be associated with the quadrupolar interaction.

The results of ab initio calculations of some of these cage compounds should clarify the type and extent of intramolecular orbital interactions which affect the ^{31}P NMR chemical shifts in the bicyclic systems. The same interactions affecting ^{31}P NMR chemical shifts may contribute to the spin-spin coupling of the systems. Preparation of compounds of the type $\text{P}(\text{OCH}_2\text{PR}_2)_3$ would yield $^3J_{\text{PP}}$ values which have only one pathway for through-bond transfer of the coupling information. Comparing these $^3J_{\text{PP}}$ values to the $^3J_{\text{PP}}$ values of the cage 1 may be helpful in determining the presence or absence of through-space coupling.

REFERENCES

1. Verkade, J. G. Coord. Chem. Rev. 1972, 98, 1.
2. Vande Griend, L. J. Ph.D. Dissertation, Iowa State University, Ames, Iowa, 1973.
3. Allison, D. A. Ph.D. Dissertation, Iowa State University, Ames, Iowa, 1971.
4. Bertrand, R. D.; Allison, D. A.; Verkade, J. G. J. Am. Chem. Soc. 1970, 92, 71.
5. Bertrand, R. D. Ph.D. Dissertation, Iowa State University, Ames, Iowa, 1969.
6. Payne, D. S.; Nöth, H.; Henniger, G. J. Chem. Soc., Chem. Commun. 1965, 327.
7. Laube, B. L.; Bertrand, R. D.; Casedy, G. A.; Compton, R. D.; Verkade, J. G. Inorg. Chem. 1967, 6, 173.
8. Van Doorne, W.; Hunt, G. W.; Parry, R. W.; Cordes, A. W. Inorg. Chem. 1971, 10, 2591.
9. Gilje, J. W.; Seff, K. Inorg. Chem. 1972, 11, 1643.
10. Cordes, A. W.; Fair, C. K.; Bermann, M.; Van Wazer, J. R. J. Cryst. Mol. Struct. 1975, 5, 279.
11. Clardy, J. C.; Kolpa, R. L.; Verkade, J. G. Phosphorus 1974, 4, 133.
12. Trusdell, D. MASP: A computer program for mass spectrometry, Iowa State University, Ames, Iowa, 1972.
13. Watkins, G. R.; Shutt, R. Inorg. Syn. 1946, 2, 186.
14. Connor, J. A.; Jones, E. M.; McEwen, G. K. J. Organomet. Chem. 1972, 43, 357.
15. Coates, H.; Wilson, P. A. T. British Patent 842 592, 1960.
16. Frank, W. W.; Drake, G. L., Jr. J. Org. Chem. 1972, 37, 2752.
17. Field, F. H. "Ion-Molecule Reactions"; Franklin, J. L., Ed.; Plenum: New York, 1969.

18. Burgada, R. Ann. Chim. (Paris) 1963, 8, 347.
19. Mathis, F. Phosphorus and Sulfur 1976, 1, 109.
20. Hudson, R. F. "Structure and Mechanism in Organo-Phosphorus Chemistry"; Academic Press: New York, 1965.
21. Emsley, J.; Hall, D. "The Chemistry of Phosphorus"; John Wiley & Sons: New York, 1976.
22. Smith, N. L.; Sisler, H. H. J. Org. Chem. 1961, 26, 5145.
23. Kosolapoff, G. M.; Maier, L. "Organic Phosphorus Compounds"; John Wiley & Sons: New York, 1972, Vol. 4.
24. Abel, W. W.; Butler, I. S.; Reid, J. G. J. Chem. Soc. 1963, 2068.
25. Silverstein, R. M.; Bassler, G. C.; Morrill, T.C. "Spectrometric Identification of Organic Compounds", 3rd ed.; John Wiley & Sons: New York, 1974.
26. Pople, J. A.; Schneider, W. G.; Bernstein, H. J. "High Resolution Nuclear Magnetic Resonance"; McGraw-Hill: New York, 1959.
27. Kroshefsky, R. D. Ph.D. Dissertation, Iowa State University, Ames, Iowa, 1977.
28. Milbrath, D. S.; Springer, J. P.; Clardy, J. C.; Verkade, J. G. J. Am. Chem. Soc. 1976, 98, 5493.
29. ^{13}C spectrum obtained on a CDCl_3 solution using a Bruker HX-90 spectrometer operating at 22.63 MHz in the FT mode.
30. Clardy, J. C.; Dow, D. C.; Verkade, J. G. Phosphorus, 1975, 5, 85.
31. Bose, A. K.; Srinivasan, P. R. Tetrahedron, 1975, 31, 3025.
32. Crutchfield, M. M.; Dungan, C. H.; Letcher, J. H.; Mark, V.; Van Wazer, J. R. "Topics in Phosphorus Chemistry"; Interscience: New York, 1967, Vol. 5.
33. Grim, S. O.; McAllister, P. R.; Singer, R. M. J. Chem. Soc. D. 1968, 38.
34. Verkade, J. G. Phosphorus and Sulfur, 1976, 2, 251.

35. Hoffman, R. A.; Forsen, S. In "Progress in Nuclear Magnetic Resonance Spectroscopy"; Emsley, J. W.; Feeney, J.; Sutcliffe, L. H. Eds.; Pergamon: Oxford, 1966; Vol. 1, Chapter 2.
36. Buckingham, A. D.; Lovering, E. G. Trans. Faraday Soc. 1962, 58, 2077.
37. Friedman, E. F.; Gutowsky, H. S. J. Chem. Phys. 1966, 45, 3158.
38. Hilton, J.; Sutcliffe, L. H. In "Progress in Nuclear Magnetic Resonance Spectroscopy"; Emsley, J. W.; Feeney, J.; Sutcliffe, L. H., Eds.; Pergamon: Oxford, 1966; Vol. 10, Chapter 2.
39. McFarlane, W. M. Proc. Roy. Soc. A, 1968, 306, 185.
40. Mavel, G. In "Progress in Nuclear Magnetic Resonance Spectroscopy"; Emsley, J. W.; Feeney, J.; Sutcliffe, L. H., Eds.; Pergamon: Oxford, 1966; Vol. 1, Chapter 4.
41. Finer, E. G.; Harris, R. K. In "Progress in Nuclear Magnetic Resonance Spectroscopy"; Emsley, J. W.; Feeney, J.; Sutcliffe, L. H., Eds.; Pergamon: Oxford, 1971; Vol. 6, Chapter 4.
42. Yarbrough, L. W. III., Southern Arkansas University, personal communication, 1978.
43. Boros, E. J.; Verkade, J. G.; King, R. W.; Coskran, K. J. Chem. Eng. News 1965, 43(16), 42.
44. Boros, E. J.; Coskran, K. J.; King, R. W.; Verkade, J. G. J. Am. Chem. Soc. 1966, 88, 1140.
45. Witanowski, M.; Webb, G. A. "Nitrogen NMR", Plenum: New York, 1973.
46. Milbrath, D. S.; Verkade, J. G.; Kenyon, G. L.; Eargle, D. H., Jr. J. Am. Chem. Soc. 1978, 100, 3167.
47. Jacobson, R. A. J. Appl. Crystallogr. 1976, 9, 115.
48. Rohrbaugh, W. J.; Jacobson, R. A. Inorg. Chem. 1974, 13, 2535.
49. Lawton, S. L.; Jacobson, R. A. Inorg. Chem. 1968, 7, 2124.
50. Hubbard, C. A.; Quicksall, C. O.; Jacobson, R. A. "The Fast Fourier Algorithm and the Programs ALFF, ALFFDP, ALFFPROJ, ALFFT, and Friedel", U. S. Atomic Energy Commission Report IS-2625, Iowa State University and Institute for Atomic Research, Ames, Iowa, 1971.

51. Hanson, H. P.; Herman, F.; Lea, J. D.; Skillman, S. Acta Cryst. 1960, 17, 1040.
52. Stewart, R. F.; Davidson, E. R.; Simpson, W. T. J. Chem. Phys. 1965, 42, 3175.
53. Johnson, C. A. "Ortep II: A Fortran Thermal-Ellipsoid Plot Program for Crystal Structure Illustrations", U. S. Atomic Energy Commission Report ORNL-3794 (Second Revision with Supplemental Instructions), Oak Ridge National Laboratory, Oak Ridge, Tennessee, 1971.
54. Pauling, L. "The Nature of the Chemical Bond", 3rd ed.; Cornell University Press: Ithaca, New York, 1960.
55. Corbridge, D.E.C. "The Structural Chemistry of Phosphorus"; Elsevier-Verlag: London, 1974.
56. Nimrod, D. M.; Fitzwater, D. R.; Verkade, J. G. J. Am. Chem. Soc. 1968, 90, 2700.
57. Ramsey, N. F. Phys. Rev. 1950, 78, 699.
58. Saika, A.; Slichter, C. P. J. Chem. Phys. 1954, 22, 26.
59. Yarbrough, L. W. II Ph.D. Dissertation, Iowa State University, Ames, Iowa, 1978.
60. Pople, J. A. J. Chem. Phys. 1962, 37, 53.
61. Coulson, C. A. "Valence", 2nd ed.; Oxford University Press: London, 1963.
62. Dailey, B. P.; Shoolery, J. N. J. Am. Chem. Soc. 1955, 77, 3977.
63. Mark, V.; Van Wazer, J. R. J. Org. Chem. 1967, 32, 1187.
64. Haemers, M.; Ottinger, R.; Zimmermann, D.; Reisse, J. Tetrahedron 1973, 29, 3539.
65. Hilbrand, J.; Kaufman, G. Bull. Soc. Chim. Fr. 1970, 876.
66. Mann, B. E. J. Chem. Soc. Perkin II 1972, 30.
67. Oberhammer, H.; Schmutzler, R.; Stelzer, O. Inorg. Chem. 1978, 17, 1254.

68. Grim, S. O.; McFarlane, W.; Davidoff, E. F. J. Org. Chem. 1967, 32, 781 and references therein.
69. Cheney, V. B.; Grant, D. M. J. Am. Chem. Soc. 1967, 89, 5319.
70. Quin, L. D.; Gordon, M. D.; Lee, S. O. Org. Magn. Reson. 1975, 6, 503.
71. Lichter, R. L.; Roberts, J. D. J. Am. Chem. Soc. 1972, 94, 2495.
72. Quin, L. D.; Breen, J. J. Org. Magn. Reson. 1973, 5, 17.
73. Verkade, J. G.; Piper, T. S. "Advances in the Chemistry of the Coordination Compounds", Kirshner, S. Ed.; Macmillan Company: New York, New York, 1961.
74. Heilbronner, E.; Schmelzer, A. Helv. Chim. Acta 1975, 58, 936.
75. Hoffmann, R. Acc. Chem. Res. 1971, 4, 1.
76. Heilbronner, E.; Muszkat, K. A. J. Am. Chem. Soc. 1970, 92, 3818.
77. Hoffmann, R.; Imamura, A.; Hehre, W. J. J. Am. Chem. Soc. 1968, 90, 1499.
78. Nimmo, J. K.; Lucas, B. W. Acta Cryst. 1976, B32, 348.
79. Grutzner, J. B.; Jautelet, M.; Dence, J. B.; Smith, R. A.; Roberts, J. D. J. Am. Chem. Soc. 1970, 92, 7107.
80. Anderson, G. L.; Stock, L. M. J. Am. Chem. Soc. 1968, 90, 212.
81. Eliel, E. L.; Bailey, W. F.; Kopp, L. D.; Willer, R. L.; Grant, D. M.; Bertrand, R. D.; Christensen, K. A.; Dalling, D. K.; Duch, M. W.; Wenkert, E.; Shell, F. M.; Cochran, D. W. J. Am. Chem. Soc. 1975, 97, 322.
82. White, D. W.; Bertrand, R. D.; McEwen, G. K.; Verkade, J. G. J. Am. Chem. Soc. 1970, 92, 7125.
83. Hutchins, R. O.; Maryanoff, B. E.; Albrand, J. P.; Cogne, A.; Gagnaire, D.; Roberts, J. D. J. Am. Chem. Soc. 1972, 94, 9151.
84. Huheey, J. E. J. Phys. Chem. 1965, 69, 3284.
85. Hinze, J.; Jaffé, H. H. J. Am. Chem. Soc. 1962, 84, 540.

86. Mulliken, R. S. J. Chem. Phys. 1935, 3, 573.
87. Iczkowski, R. P.; Margrave, J. L. J. Am. Chem. Soc. 1961, 83, 3547.
88. Sanderson, R. T. J. Chem. Educ. 1945, 31, 2.
89. Levy, G. C.; Cargioli, J. D.; Juliano, P. C.; Mitchell, T. D. J. Am. Chem. Soc. 1973, 95, 3445.
90. Rathke, J. W.; Guyer, J. W.; Verkade, J. G. J. Org. Chem. 1970, 35, 2311.
91. Daigle, D. J.; Reeves, W. A.; Donaldson, D. J. Textile Res. J. 1969, 39, 363.
92. Gordon, I. U. S. Patent 3 076 034, 1963; Chem. Abstr. 1963, 59, 2860.
93. Petrov, K. A.; Parshima, V. A.; Luzanova, M. B. J. Gen. Chem. USSR (Engl. Transl.) 1962, 32, 449; Zh. Obshch. Khim. 1962, 32, 553.
94. Hooker Chemical Company U. S. Patent 3 257 460, 1966; Chem. Abstr. 1966, 65, 8962.
95. Stockel, B. U. S. Patent 3 704 325, 1973.
96. Reuter, M.; Orthner, L. Ger. Offen. 1 035 135, 1958; U. S. Patent 3 030 421, 1962; Chem. Abstr. 1960, 54, 14125.
97. Grinshtein, E. I. Doklady Akad. Nauk S.S.S.R. 1961, 139, 1359; Chem. Abstr. 1961, 55, 1059.
98. Grinshtein, E. I.; Bruker, A. B.; Soborovski, L. Z. J. Gen. Chem. USSR (Engl. Transl.) 1966, 36, 252; Zh. Obshch. Khim. 1966, 36, 302.
99. Vullo, W. J. J. Org. Chem. 1968, 33, 3665.
100. Kozlov, E. S.; Selov, A. I. J. Gen. Chem. USSR (Engl. Transl.) 1968, 38, 1881.
101. Daigle, D. J.; Pepperman, A. B., Jr. J. Chem. Eng. Data 1975, 20, 448.
102. Daigle, D. J.; Pepperman, A. B., Jr. J. Heterocycl. Chem. 1975, 12, 579.

103. Bertrand, R. D.; Compton, R. D.; Verkade, J. G. J. Am. Chem. Soc. 1970, 92, 2702.
104. Pimentel, G. C.; Spratley, R. D. "Chemical Bonding Clarified Through Quantum Mechanics", Holden-Day, Inc.: San Francisco, California, 1970.
105. Yarbrough, L. W. II; Hall, M. B. Inorg. Chem. 1978, 17, 2269.
106. Cowley, A. H.; Lattman, M.; Montag, R. A.; Verkade, J. G. Inorg. Chim. Acta 1977, 25, L151.
107. Ogata, H.; Onizuka, H.; Nihei, Y.; Kamada, H. Bull. Chem. Soc. Jap. 1973, 46, 3036.
108. Murrell, J. N.; Schmidt, W. J. Chem. Soc. Farad. Trans. 2 1972, 68, 1709.
109. Fridh, C.; Asbrink, L.; Lindholm, E. Chem. Phys. Lett. 1972, 15, 282.
110. Perry, W. B.; Jolly, W. L. J. Electron. Spectrosc. Relat. 1974, 4, 219.
111. Debies, T. P.; Rabalais, J. W. Inorg. Chem. 1974, 13, 308.
112. Cowley, A. H.; Goodman, D. W.; Kuebler, N. A.; Sanchez, M.; Verkade, J. G. Inorg. Chem. 1977, 16, 854.
113. Scholl, R. L.; Maciel, G. E.; Musker, W. K. J. Am. Chem. Soc. 1972, 94, 6376.
114. Dewar, M. J. S.; Worley, S. D. J. Chem. Phys. 1969, 50, 654.
115. Becka, L. N.; Cruickshank, D. W. J. Proc. Roy. Soc. A 1963, 273, 435.
116. Fluck, E.; Förster, J.; Weidlein, J.; Hadicke, E. Z. Naturforsch. 1977, 32b, 499.
117. White, D. W.; Karcher, B. A.; Jacobson, R. A.; Verkade, J. G. J. Am. Chem. Soc., in press.
118. Allison, D. A.; Clardy, J. C.; Verkade, J. G. Inorg. Chem. 1972, 11, 2804.

119. King, R. B. In "Organometallic Synthesis", Eisch, J.J.; King, R. B. Eds.; Academic Press: New York, 1965; Vol. I.
120. King, R. B.; Fronzaglia, A. Inorg. Chem. 1966, 5, 1837.
121. Dobson, G. R.; Faber, G. C. Inorg. Chim. Acta 1970, 4, 87.
122. Plummer, P. D.; Verkade, J. G., unpublished results, Iowa State University.
123. "Webster's Third New International Dictionary"; Phillip Babcock Gove, Ed.; G. & C. Merriam Corp.: Springfield, Massachusetts, 1976.
124. Grim, S. O.; Wheatland, D. A.; McFarlane, W. J. Am. Chem. Soc. 1967, 89, 5573.
125. Harris, R. K. Can. J. Chem. 1964, 42, 2275.
126. Bertrand, R. D.; Ogilvie, F. B.; Verkade, J. G. J. Chem. Soc., Chem. Commun. 1969, 756.

ACKNOWLEDGEMENTS

I would like to thank Dr. Verkade for his guidance and encouragement through this research effort and especially for the freedom to explore new ideas.

I am grateful to the National Science Foundation for financial support of much of this work.

My thanks also goes to the members of the instrumental services group for maintaining and instructing me in the use of the instruments necessary for this research, and to Dr. Jacobson's group for help in solving the crystal structure.

A special thanks goes to past and present members of the Verkade group for stimulating and helpful discussions.

I also wish to thank my daughter, Sarah Beth, and my dogs, Wolf and Scamp, for many hours of needed diversion and relaxation.

It is impossible for me to adequately express my thanks to my wife, Mary, for being an endless source of support and encouragement and for tolerating the numerous hours I have spent in the lab. Her help in preparing and typing this dissertation was invaluable.

APPENDIX 1. CALCULATED AND OBSERVED STRUCTURE FACTORS FOR 14

7	10	16	43	13	9	11	22	1	6	3	12	7	5	11	14	13	5	23	31	0	11	4	-23	6	10	31	19		
8	11	2	-4	14	1	13	11	1	7	12	12	7	6	15	15	13	6	7	29	1	1	60	66	6	11	9	-13		
9	12	4	4	14	3	17	-19	1	8	30	-61	7	7	7	-13	13	7	1	7	1	2	29	31	7	1	17	-23		
10	13	5	1	14	4	13	27	1	9	5	1	8	49	-88	-31	13	9	4	-24	1	3	2	0	7	2	60	50		
11	14	24	25	14	5	14	14	1	10	6	-14	7	10	13	-31	13	9	4	13	1	4	12	17	7	3	60	-65		
12	15	-14	-14	14	6	5	-7	1	11	9	-15	7	11	2	-4	14	1	24	45	1	5	73	-87	7	4	27	-43		
13	16	5	-4	14	7	14	43	1	12	12	-36	6	1	51	53	14	2	13	-15	1	6	5	-16	7	5	5	-1		
14	17	10	10	14	8	14	-29	2	1	63	-66	6	2	23	-25	14	3	15	24	1	7	4	0	7	9	21	-37		
15	18	20	-24	15	1	1	-1	2	2	2	5	8	3	47	-54	14	4	3	5	1	8	26	-44	7	7	12	-4		
16	19	7	16	15	2	10	-18	2	3	56	50	6	4	26	-40	14	5	1	1	1	1	-2	-44	7	9	13	-25		
17	20	7	-17	15	3	10	-36	2	4	39	-43	6	6	10	18	14	6	20	-50	1	1	4	4	7	10	17	-18		
18	21	12	-23	15	4	17	-36	2	5	10	3	8	7	10	18	14	7	2	-5	1	1	1	1	1	1	1	-17		
19	22	11	7	-10	15	5	6	1	6	7	-26	8	8	2	-19	14	8	13	-24	2	1	61	-72	6	2	21	15		
20	23	31	39	15	6	6	7	7	7	11	-22	8	9	18	62	14	9	4	24	2	3	38	-30	6	1	41	-65		
21	24	13	15	7	4	14	-18	2	8	12	-22	8	10	7	-12	15	1	30	-70	2	4	0	-3	6	4	10	12		
22	25	-27	-27	15	6	14	-34	2	9	32	45	8	11	7	16	15	2	25	-46	2	5	0	-50	9	5	28	-43		
23	26	-34	15	9	5	-15	-15	2	10	4	19	9	1	26	24	15	3	12	-20	2	6	4	0	12	10	8	6	1	0
24	27	-15	16	1	4	-14	3	1	29	-34	9	2	53	-66	15	4	12	-20	2	8	48	51	8	7	22	32			
25	28	5	18	16	5	16	34	3	2	36	-39	9	3	26	35	15	5	5	0	2	9	8	-21	8	6	10	-11		
26	29	21	-66	16	6	18	43	3	3	16	19	9	4	21	-31	15	7	4	0	2	10	6	24	8	9	17	-40		
27	30	18	17	16	7	1	3	3	4	35	37	9	5	26	-36	15	8	3	-12	2	11	8	14	8	10	15	23		
28	31	5	-13	17	1	23	39	3	5	20	-31	9	6	6	0	15	9	4	11	3	1	18	16	8	11	11	43		
29	32	1	-6	17	2	27	60	3	6	15	25	9	7	40	69	16	1	34	75	3	2	39	-45	9	1	70	-92		
30	33	4	-3	17	4	5	10	3	7	42	65	9	8	15	-32	16	2	3	-5	3	3	92	89	9	2	4	3		
31	34	13	-17	5	3	17	4	3	8	25	31	9	10	5	-9	16	3	7	30	3	4	45	51	9	3	27	-34		
32	35	6	17	6	16	-46	6	3	9	20	35	9	11	4	-11	16	4	13	23	3	5	44	-49	4	4	11	-5		
33	36	27	29	17	7	13	51	3	10	3	-1	10	1	32	47	16	7	4	3	3	6	47	53	9	5	23	27		
34	37	24	31	18	1	5	-4	4	1	14	15	10	2	11	10	16	8	1	0	3	7	5	-5	9	6	24	23		
35	38	10	-7	18	3	9	18	4	2	31	35	10	3	3	-6	17	1	17	41	3	8	14	30	9	7	17	33		
36	39	10	6	22	35	18	4	23	-59	4	36	44	10	4	13	-13	17	2	8	24	3	10	1	8	9	9	4	11	
37	40	10	-26	18	5	3	-3	4	5	10	9	10	5	4	7	17	3	14	-8	3	11	7	-9	9	10	9	-11		
38	41	4	-8	18	6	2	-10	4	6	8	-14	10	6	26	48	17	4	4	-2	4	1	51	-53	10	1	17	16		
39	42	20	46	18	7	3	-12	4	8	50	-75	10	7	15	-30	17	5	12	-26	4	2	4	-10	10	2	10	8		
40	43	3	2	19	1	2	13	4	9	28	-57	10	8	1	-3	17	6	8	16	4	4	29	36	10	3	1	7		
41	44	22	-24	19	2	2	-5	4	10	4	39	10	9	9	-33	17	7	5	-20	4	5	38	-49	10	5	9	12		
42	45	11	9	19	3	1	-5	4	11	20	-53	10	10	3	5	18	1	20	-58	4	6	19	-25	10	6	16	-18		
43	46	3	13	19	4	8	29	5	1	8	-4	11	1	27	39	18	2	1	-7	4	7	24	-29	10	8	9	-19		
44	47	11	5	7	19	4	6	29	5	1	13	11	2	1	1	18	3	23	-51	4	8	23	-42	10	9	4	0		
45	48	10	-11	20	4	13	37	5	2	13	13	11	3	24	-42	18	4	11	-25	4	9	8	3	10	10	5	-6		
46	49	11	15	-19	20	5	3	-4	5	4	-9	11	4	19	21	18	5	5	5	4	10	23	-67	11	1	44	65		
47	50	8	3	0	21	1	9	-16	5	5	29	34	11	5	13	-14	18	6	2	-4	4	11	9	-20	11	2	9	9	
48	51	10	10	24	21	2	5	-17	5	6	-14	11	6	8	3	19	1	7	17	5	1	86	94	11	3	15	16		
49	52	12	-19	21	3	4	-18	5	7	47	-57	11	7	20	-48	19	2	10	38	5	2	24	-27	11	4	24	-33		
50	53	7	-10	21	3	4	-18	5	8	57	109	11	8	18	39	19	3	12	26	5	3	7	-6	11	5	18	-16		
51	54	28	-36	2	-2	2	5	10	-29	10	-29	11	9	5	-6	19	5	6	27	5	4	6	-17	11	6	18	-12		
52	55	12	3	2	-2	2	5	11	4	1	11	10	6	1	21	20	3	6	16	5	5	17	24	11	7	6	0		
53	56	12	6	0	2	21	-32	6	1	33	-38	12	1	48	-60	20	4	12	-35	5	6	41	-50	11	8	6	-19		
54	57	13	-32	0	3	3	0	6	2	20	24	12	2	4	-4	21	2	9	-38	5	7	8	4	11	9	15	39		
55	58	28	-46	0	4	42	40	6	3	36	-42	12	3	5	-20	21	3	1	1	5	8	7	4	11	10	6	22		
56	59	2	4	0	5	0	0	6	4	30	28	12	4	2	-4	21	4	2	0	5	9	12	22	12	1	5	-11		
57	60	8	-13	0	6	38	47	6	5	14	10	12	5	22	-31	22	1	1	10	5	10	27	57	12	2	11	-27		
58	61	1	-3	0	6	47	74	6	6	29	43	12	6	19	41	1	1	1	1	5	11	1	-20	12	3	4	13		
59	62	7	8	0	10	10	0	6	7	4	1	12	7	16	-40	1	1	6	1	26	6	1	24	-23	12	4	21	-38	
60	63	20	-34	0	12	2	1	6	8	4	10	12	8	12	35	0	1	7	FC	6	2	14	-31	12	5	18	32		
61	64	13	18	1	1	2	1	6	11	15	35	12	9	14	14	0	1	68	71	6	3	55	49	11	6	28	62		
62	65	3	10	1	2	105	97	7	1	32	-36	13	1	22	-36	0	3	108	117	6	4	25	28	12	7	6	15		
63	66	4	22	37	1	3	33	-35	7	2	48	13	2	16	24	0	5	35	49	6	5	0	3	12	8	14	12		
64	67	5	4	1	4	42	42	7	3	55	64	13	3	12	30	0	7	50	73	6	6	24	30	12	9	1	1		
65	68	4	21	1	5	38	-39	7	4	8	-12	13	4	15	21	0	9	1	14	6	8	15	-22	13	1	14	26		

13	2	11	19	1	0	0	6	5	28	34	11	9	1	4	18	6	11	18	3	9	7	-12	9	4	11	10		
13	3	13	12	1	1	44	6	6	14	-18	11	10	9	-28	19	1	16	3	3	9	10	-33	9	5	17	18		
13	4	30	44	1	2	110	6	7	12	18	12	1	55	83	19	2	10	-30	3	10	14	-33	9	8	17	-22		
13	5	19	-30	1	3	43	6	6	14	18	12	1	12	21	19	3	1	10	3	11	6	11	9	9	10	-33		
13	6	7	-15	1	4	35	6	9	8	20	12	2	13	21	19	4	1	8	4	2	55	68	10	0	48	59		
13	7	7	-20	1	5	14	6	10	19	-36	12	3	4	6	19	5	3	-4	4	2	55	-62	10	1	32	-36		
14	1	17	-16	1	6	10	6	11	8	25	12	4	15	21	20	6	-19	4	3	32	36	10	2	29	-40			
14	2	16	31	1	7	14	7	0	6	0	12	5	4	1	84	6	6	4	4	4	0	2	10	3	12	25		
14	3	3	-12	1	8	14	7	1	52	-56	12	6	7	-16	20	1	1	-5	4	5	4	-3	10	4	13	-12		
14	4	16	-29	1	10	8	7	2	81	-81	12	7	22	38	20	2	1	7	4	6	11	12	10	5	9	3		
14	5	8	-17	1	11	16	7	3	12	13	12	8	10	-28	20	3	3	-10	4	7	23	29	10	7	22	-37		
14	6	7	0	2	0	59	7	4	12	13	12	9	6	-9	20	4	5	-16	4	8	2	-5	10	9	14	-49		
14	7	3	-10	2	1	57	7	5	10	-12	13	0	4	0	20	5	8	-23	4	9	4	-7	11	0	9	-13		
15	1	23	-50	2	2	0	7	6	28	-36	13	1	5	-9	21	1	1	-4	4	10	12	26	11	1	18	18		
15	2	13	-28	2	3	63	7	7	7	-9	13	2	2	-2	21	2	3	0	4	11	5	23	11	2	28	-35		
15	3	14	-28	2	4	1	7	8	7	8	13	3	39	55	21	3	4	-12	5	0	24	-28	11	3	21	-36		
15	4	16	21	2	5	2	0	7	9	6	-9	4	22	-29	22	1	1	-8	5	1	8	-7	11	4	37	56		
15	5	11	13	2	6	9	-16	7	10	19	48	5	14	-17	22	2	2	1	5	2	20	18	11	5	13	-35		
15	6	15	54	2	7	56	61	7	11	5	19	6	12	-27	22	2	2	1	5	3	28	31	11	6	5	8		
15	7	14	5	2	8	1	5	8	0	64	-67	13	7	21	-53				5	4	9	19	11	6	5	12		
16	1	1	7	2	9	4	-1	8	2	29	-33	13	8	9	-26				5	5	19	-22	11	9	10	-22		
16	2	4	16	2	10	17	34	0	8	3	11	14	13	9	1	11	0	0	5	6	10	9	12	0	39	45		
16	3	20	33	3	0	3	0	8	4	3	0	14	0	31	-36	0	1	48	-55	5	7	1	7	12	1	25	41	
16	4	3	5	3	1	87	89	8	5	8	6	14	1	4	0	3	69	-76	5	8	28	46	12	2	50	90		
16	5	4	6	3	2	15	14	6	18	25	14	2	9	-26	0	5	32	37	5	9	3	-6	12	3	10	-24		
16	6	8	-28	3	3	78	83	8	7	12	-12	14	3	15	-23	0	7	81	-102	5	10	16	-29	12	4	8	22	
16	7	9	-8	3	4	43	-66	8	6	7	31	14	6	6	-7	0	9	9	-21	6	0	8	-6	12	5	13	-23	
17	2	23	-50	3	5	14	20	5	9	3	-10	14	5	14	-28	0	11	5	15	6	1	71	81	12	7	5	-8	
17	3	10	-20	3	6	3	-2	8	10	15	38	14	6	12	16	1	1	0	1	6	2	12	15	12	8	11	-15	
17	4	9	-22	3	7	7	-12	9	0	2	0	15	0	2	0	1	1	67	-72	6	3	17	-16	13	0	5	-8	
18	1	7	1	3	8	3	5	9	1	34	50	15	1	21	48	1	105	-116	6	4	16	22	13	1	2	5	-8	
18	2	11	-25	3	9	22	-50	9	2	35	44	15	2	11	27	1	3	11	-11	6	5	34	-40	13	2	9	12	
18	3	7	10	3	10	16	-19	9	3	26	-27	15	3	6	-2	1	4	30	31	6	6	2	6	13	3	36	-49	
18	4	4	-12	3	11	12	-19	9	4	20	26	15	4	18	31	1	5	28	32	6	7	1	-2	13	4	33	-52	
18	5	11	34	4	1	77	-77	9	5	23	24	15	6	11	24	1	6	1	0	6	10	2	-5	13	5	4	-14	
18	6	6	7	4	2	6	-8	9	6	12	25	15	7	1	-21	1	7	12	-26	7	0	23	-23	13	6	15	-31	
19	1	1	-6	4	3	18	-24	9	7	6	14	15	8	3	17	1	8	11	27	7	1	41	-39	13	7	9	20	
19	2	14	31	4	4	19	-12	9	8	14	31	16	0	15	-27	1	9	16	42	7	2	10	-15	13	8	1	-9	
19	3	4	14	4	5	66	-78	9	9	11	-17	16	1	35	-60	1	10	15	23	7	3	29	33	13	9	3	-8	
19	4	7	9	4	6	19	-20	9	10	5	14	16	2	1	-7	1	11	13	27	7	4	31	41	14	0	7	-15	
20	1	7	19	4	7	1	-3	10	0	5	-4	16	3	2	-4	2	0	77	94	7	5	3	9	14	1	7	11	
20	2	9	24	4	8	24	31	10	1	13	-20	16	4	9	23	2	1	13	13	7	6	13	-23	14	2	6	-9	
20	3	6	-11	4	9	2	17	13	2	5	11	16	5	6	-30	2	2	7	14	7	7	12	-15	14	3	7	-15	
20	4	2	-5	4	11	6	14	10	3	8	9	16	6	6	-19	2	3	4	0	7	8	1	-1	14	4	21	-53	
21	1	3	-16	5	0	5	0	10	4	3	6	16	7	11	-14	2	4	18	-17	7	9	10	14	6	4	0	0	
21	2	5	-24	5	1	79	-82	10	5	31	-45	16	8	3	-18	2	5	11	15	8	0	50	-54	14	7	23	41	
22	1	4	20	5	2	9	13	10	6	5	-19	17	0	1	0	2	8	22	21	8	2	9	-12	15	0	1	13	
22	2	9	31	5	3	46	49	10	7	12	31	17	1	6	-13	2	7	6	6	3	14	25	15	1	13	-20		
22	3	6	-11	5	4	25	27	10	8	13	-7	17	2	0	14	2	8	10	-2	9	4	17	-31	15	2	5	-3	
22	4	9	31	5	5	32	-35	10	9	4	-25	17	3	8	-15	2	9	5	0	8	5	21	24	15	3	28	49	
22	5	16	-29	5	6	3	2	11	0	4	0	17	4	1	-17	2	10	8	-11	8	6	11	-9	15	4	7	-10	
22	6	8	-17	5	7	22	37	11	1	13	-23	17	5	5	-8	3	0	86	92	8	7	2	4	15	5	15	34	
22	7	3	0	5	8	11	-25	11	2	36	55	17	6	10	-25	3	1	48	-49	8	8	22	38	15	6	1	2	
22	8	29	-29	5	9	17	23	11	3	48	-57	17	7	10	33	2	3	40	40	8	9	12	27	15	8	1	-6	
22	9	1	0	6	10	25	20	15	4	27	-32	18	0	14	28	3	3	38	-35	6	10	6	-16	16	0	9	0	
22	10	7	1	0	11	12	-14	11	5	5	6	18	2	3	2	3	4	78	-87	9	0	35	47	16	1	3	-9	
22	11	32	-81	6	12	9	-11	11	6	3	16	3	16	4	1	3	5	35	45	9	1	3	-4	16	2	22	-52	
22	12	24	-61	6	13	11	7	31	69	18	4	18	4	3	-11	3	6	7	-6	9	2	19	-14	16	3	4	-8	
22	13	1	0	6	14	19	29	11	6	6	-29	18	5	13	36	3	7	8	11	9	3	53	69	16	4	7	16	

M = I
K L FO FC

3	3	9	4	0	20	2	5	2	7	0	23	33	16	1	5	24	5	3	9	-21	14	3	6	25	
4	1	50	72	10	7	4	-15	16	3	11	29	5	3	5	3	24	5	4	32	61	14	5	7	38	
4	4	75	-84	10	9	9	12	7	3	2	36	2	16	3	17	-36	16	5	16	-19	15	0	2	-13	
4	4	40	49	11	0	27	-34	0	1	25	43	11	10	17	0	-21	6	6	7	12	15	1	5	-17	
4	4	6	0	11	1	11	18	0	7	53	84	7	17	1	1	4	6	0	7	17	15	2	1	12	
4	4	13	27	11	3	15	-26	0	9	12	-41	8	17	2	6	-24	6	2	26	-38	15	4	6	6	
4	4	7	1	0	11	4	13	14	1	0	60	1	18	0	10	41	6	3	13	60	16	0	10	31	
4	4	10	-16	11	5	19	-38	1	1	53	60	8	18	2	10	-41	6	5	18	35	16	1	18	-22	
4	4	9	4	8	11	6	10	-8	1	2	7	18	16	2	10	-13	6	5	9	15	16	3	1	-8	
5	0	67	-78	11	7	2	-17	7	6	4	7	36	18	3	4	-15	6	4	2	5	17	0	2	-12	
5	2	12	-18	12	0	2	0	1	4	32	-60	5	19	0	10	34	7	0	5	-6	17	1	7	-23	
5	3	6	-8	12	2	21	46	1	6	11	11	6	3	3	19	31	7	2	14	-16	17	3	7	-18	
5	4	2	3	12	3	5	-2	1	8	1	0	6	20	0	5	27	7	3	6	-4	18	0	1	-17	
5	5	4	7	2	12	5	18	-34	1	9	2	-8	0	1	-4	-4	7	4	21	-61	18	2	5	37	
5	6	2	9	12	6	1	5	2	0	76	-77	9	19	2	7	18	7	5	4	-5	19	0	1	-6	
5	7	21	-25	12	7	1	0	2	2	41	47	6	14	12	14	-14	7	6	14	-24	19	0	1	-6	
5	8	9	-29	13	0	19	41	0	2	3	20	-14	0	14	12	0	0	0	1	4	19	0	7	7	
5	9	9	-50	13	2	16	20	2	4	6	15	9	0	2	4	53	8	1	24	-34	14	5	3	FC	
6	0	50	-50	13	3	8	23	0	6	3	-6	14	0	0	43	10	8	2	42	-69	14	3	3	-7	
6	1	12	12	13	4	6	14	2	8	19	32	9	0	6	10	-21	6	3	20	43	0	5	15	30	
6	2	1	11	13	5	18	33	2	9	4	-17	10	0	8	2	33	8	4	3	2	0	7	10	-1	
6	3	18	-19	13	7	3	20	3	0	27	-26	10	1	0	7	7	8	5	21	48	1	0	10	-24	
6	4	3	-3	14	0	3	-11	3	1	34	-44	10	1	0	3	-1	7	8	10	22	1	1	16	-31	
6	5	8	4	10	14	2	25	-37	3	2	17	16	1	2	23	-28	9	0	6	-7	1	3	1	27	
6	6	4	10	14	3	10	-31	3	4	26	22	10	6	1	4	70	11	2	8	36	1	4	16	35	
6	7	10	18	14	4	4	-3	3	5	17	-30	10	7	1	5	-117	9	2	8	19	1	6	9	23	
6	8	-12	14	4	4	9	-20	3	6	4	-4	11	0	1	6	2	9	3	19	58	1	7	1	-4	
7	0	58	59	14	5	9	-20	4	11	0	8	21	1	6	4	13	9	4	6	0	2	0	21	19	
7	1	4	-9	14	6	11	-34	3	7	8	9	11	1	7	3	-15	9	5	10	7	2	1	8	-7	
7	2	27	41	15	0	18	-45	4	10	11	10	17	1	8	11	-4	10	0	10	12	2	2	7	-15	
7	3	6	6	15	1	15	-28	4	0	32	40	11	2	1	5	-23	10	0	20	19	2	3	2	7	
7	4	10	46	15	2	2	-1	4	2	19	-20	12	2	2	52	-76	10	1	3	8	2	4	13	42	
7	5	10	20	15	3	5	20	4	3	18	47	11	5	6	2	47	10	2	8	-6	2	5	1	-3	
7	6	20	17	15	4	16	-35	4	4	17	23	11	6	7	18	39	10	3	13	-26	2	6	13	13	
7	7	1	-1	15	5	8	19	4	5	10	-26	12	2	6	1	-1	10	4	11	-25	2	7	2	14	
7	8	18	-10	16	6	18	-48	4	6	17	25	12	2	6	1	57	10	5	19	-45	3	0	15	22	
8	0	19	22	16	1	17	36	4	6	5	-6	12	3	0	14	-23	10	6	5	8	3	1	32	40	
8	1	5	1	16	2	16	-33	4	7	10	-8	13	0	1	27	30	11	1	11	33	3	2	34	45	
8	2	23	30	16	3	3	3	4	8	14	-49	13	3	3	48	80	11	0	2	0	3	3	5	35	
8	3	35	-50	16	4	4	0	5	0	13	-10	13	4	8	12	-28	11	1	6	8	3	4	1	19	
8	4	14	-17	16	5	10	28	5	1	10	16	13	5	1	21	11	3	10	-12	3	5	11	27	41	
8	5	8	11	16	6	9	48	5	2	19	-22	13	6	2	10	14	0	9	24	9	3	6	17	-41	
8	6	26	-55	17	0	7	6	6	3	2	7	14	0	5	-8	39	12	0	21	31	4	0	5	-12	
8	7	4	-22	17	1	7	15	5	4	2	-7	14	1	22	0	-2	12	2	5	9	4	1	13	24	
9	0	19	-35	17	2	4	10	5	5	16	-18	14	3	1	9	0	12	3	6	-14	4	2	11	-4	
9	1	1	-2	17	3	2	2	5	6	16	16	14	4	4	20	23	12	4	6	11	4	3	13	-26	
9	2	14	-10	17	4	1	5	7	7	16	14	5	4	3	29	-43	12	6	1	-13	4	4	25	-42	
9	3	1	-10	17	5	18	-66	5	8	4	-18	14	5	15	-46	4	13	0	3	9	4	5	10	-20	
9	4	15	-21	18	1	1	-5	6	0	18	18	15	0	23	-49	-48	13	0	3	9	4	4	6	2	-14
9	5	7	1	18	3	14	-31	6	1	17	-21	15	1	11	-26	4	9	13	1	-21	4	4	6	2	-14
9	6	14	9	18	4	6	-8	6	2	20	-38	15	2	9	28	4	7	9	-21	10	4	7	6	3	3
9	7	14	9	18	4	6	15	6	3	27	33	15	2	7	3	9	13	4	21	-46	5	0	20	-22	
10	0	24	44	19	1	1	0	6	4	3	-13	15	4	4	7	21	14	0	12	-3	5	2	12	12	
10	1	30	41	20	1	1	14	6	5	0	17	15	5	4	1	-37	14	0	13	-15	5	2	12	12	
10	2	17	21	21	0	1	-12	5	2	7	-12	15	5	2	9	9	12	1	12	-40	5	3	5	9	

M =

M =

M =

5	5	11	17	17	1	14	-43	10	0	4	-3	9	4	9	-12	3	2	2	11
5	5	14	35	18	0	3	20	10	1	14	-37	9	0	21	-41	4	0	4	22
5	7	5	-19					10	2	6	-4	9	1	14	47	4	1	7	-10
6	0	6	-2					10	3	2	4	9	2	2	-9	5	0	3	0
6	1	21	32					10	4	4	4	9	3	3	-8	6	0	6	25
6	2	27	51					11	1	4	-5	10	0	1	6	6	1	2	-5
6	3	16	37					11	2	11	-21	11	0	6	-11	7	0		
6	5	10	-24					11	3	17	43	11	1	9	-15				
6	6	2	6					12	1	17	54	11	2	14	33				
7	0	12	24					13	1	15	10	12	0	7	17				
7	1	34	-54					13	2	10	-22	13	0	1	1				
7	2	18	-31					13	3	11	-32	13	1	11	-20				
7	4	9	-15					14	0	1	3	14	0	8	-27				
7	5	19	-46					14	1	4	-2								
7	6	1	-14					14	2	10	25								
8	0	3	22					15	0	10	43								
8	1	10	-15					15	1	8	17								
8	2	3	-19					16	0	5	17								
8	3	4	13																
8	4	19	32																
8	5	7	0																
9	0	17	32																
9	1	18	15																
9	2	1	13																
9	3	8	10																
9	4	12	24																
9	5	2	-6																
9	6	0	-31																
10	1	8	-8																
10	2	9	-24																
10	3	16	-36																
10	4	17	-48																
10	5	4	1																
11	0	1	-6																
11	1	2	7																
11	2	7	-10																
11	3	2	-13																
11	4	2	-17																
11	5	6	13																
12	0	7	4																
12	1	1	0																
12	2	3	4																
12	3	10	32																
13	0	5	-8																
13	1	4	6																
13	2	0	-20																
13	3	4	11																
13	4	5	-15																
14	0	6	16																
14	1	15	-41																
14	2	9	12																
14	3	6	12																
15	1	9	30																
15	2	4	7																
15	3	14	43																
16	0	2	1																
16	1	3	6																
17	0	1	-3																

H=10

H=11

APPENDIX 2. SAMPLE CALCULATION OF GROUP ELECTRONEGATIVITY

The equation for the general group $-W \begin{matrix} \diagup X \\ - Y \\ \diagdown Z \end{matrix}$ developed by Huheey (84) was used to calculate the electronegativity of carbon next to phosphorus for the group $-\text{CH}_2\text{NR}_1\text{R}_2$.

Eq A-1

$$\chi_{\text{WXYZ}} = \frac{a_W b_X b_Y b_Z + a_X b_W b_Y b_Z + a_Y b_W b_X b_Z + a_Z b_W b_X b_Y + b_W b_X b_Y b_Z \delta_{\text{WXYZ}}}{b_X b_Y b_W + b_X b_Z b_W + b_X b_Y b_Z + b_Y b_Z b_W}$$

The quantity \underline{a} of equation A-1 is the inherent electronegativity of the atom or group and \underline{b} is the charge coefficient which describes the polarity of the bond. The $-\text{CH}_2\text{N}(\text{CH}_3)_2$ group will be used as an example. First, the group EN of $-\text{N}(\text{CH}_3)_2$ must be determined. The general equation of Huheey (84) for $W \begin{matrix} \diagup X \\ - Y \\ \diagdown \end{matrix}$ is used:

$$\chi_{\text{WXY}} = \frac{a_W b_X b_Y + a_X b_W b_Y + a_Y b_W b_X + b_W b_X b_Y \delta_{\text{WXY}}}{b_X b_Y + b_W b_X + b_W b_Y}$$

For $-\text{N}(\text{CH}_3)_2$, $W = \text{N}$, $X = Y = \text{CH}_3$. Values of \underline{a} and \underline{b} for the CH_3 group and a nitrogen atom (which is hybridized such that the bonding orbitals contain 23% s character) are taken from tables provided by Huheey (84).

$$\begin{aligned} a_W &= 11.21 & b_W &= 14.64 \\ a_X &= a_Y = 7.37 & b_X &= b_Y = 3.24 \end{aligned}$$

$$\begin{aligned}
 \chi_{\text{N(CH}_3)_2} &= \frac{117.68 + 349.59 + 349.59 + 153.68 \delta_{\text{N(CH}_3)_2}}{10.50 + 47.43 + 47.43} \\
 &= \frac{816.86 + 153.68 \delta_{\text{N(CH}_3)_2}}{105.37} \\
 &= 7.73 + 1.46 \delta_{\text{N(CH}_3)_2} \\
 7.73 &= a_{\text{N(CH}_3)_2} \quad \text{and} \quad 1.46 = b_{\text{N(CH}_3)_2}
 \end{aligned}$$

These values of a and b are substituted into equation A-1 along with the values for two hydrogen atoms and a tetrahedral carbon atom to calculate the group EN for $-\text{CH}_2\text{N(CH}_3)_2$.

The butyl radical was not tabulated by Huheey so the parameters for butyl were derived by using the ethyl values to calculate parameters for propyl which could then be used to calculate the butyl parameters.

The group EN for morpholino $-\text{N} \begin{array}{c} \diagup \text{CH}_2\text{-CH}_3 \\ \diagdown \text{CH}_2\text{-CH}_2\text{-O-CH}_2\text{-CH}_3 \end{array}$ was estimated by calculating parameters for $-\text{N} \begin{array}{c} \diagup \text{CH}_2\text{-CH}_3 \\ \diagdown \text{CH}_2\text{-CH}_2\text{-O-CH}_2\text{-CH}_3 \end{array}$.